Financial crisis forecasts and applications to systematic trading strategies

Antoine Kornprobst

UNIVERSITÉ PARIS I PANTHÉON-SORBONNE

ÉCOLE DOCTORALE ED-465

CENTRE D'ÉCONOMIE DE LA SORBONNE

Thèse

pour obtenir le grade de

DOCTEUR DE L'UNIVERSITÉ PARIS I PANTHÉON-SORBONNE

Spécialité : Mathématiques Appliquées

présentée et soutenue par

Antoine Kornprobst

le 23 Octobre 2017

Financial Crisis Forecasts and Applications to Systematic Trading Strategies

Thèse dirigée par Raphael Douady

JURY :

Michele Benzi	Professor, Emory University	Rapporteur
Roy Cerqueti	Associate Professor, University of Macerata	Rapporteur
Christophe Chorro	Maitre de Conférences HDR, Université Paris I	Examinateur
Raphael Douady	Chercheur CNRS HDR, Centre d'Economie de la Sorbonne	Directeur de thèse
Hayette Gatfaoui	Associate Professor HDR, IESEG School of Management	Examinateur
Olivier Guéant	Professeur des Universités, Université Paris I	Examinateur
Stefano Marmi	Professor, Scuola Normale Superiore di Pisa	Examinateur
Philippe de Peretti	Maitre de Conférences HDR, Université Paris I	Examinateur

Acknowledgements

Dear Professors and friends,

I first would like to thank my Research Director, Raphael Douady for his support and teachings during my years as a PhD student. I am very grateful to him for the time he has spent guiding my research, for all the fascinating people he introduced me to and for the many places I visited worldwide thanks to him. Those many travels, which are so important in the formative years of a researcher, would not have been possible without funding from the EDUCO Educational Consortium, our Doctoral School as well as the Labex ReFi. I express my warmest thanks to all of them.

I wish to thank all the members of my Jury for the interest they have shown to my research, in particular Philippe de Peretti who has always given me honest and benevolent advice since my first day at the Doctoral School and Olivier Guéant, whose support has been so important to me during my last months as a PhD student. I am of course especially grateful to my two referees: Michele Benzi with whom I had the privilege to work for four month during my stay at Emory University and Roy Cerqueti from the University of Macerata.

My journey into mathematical finance started five years ago at the Paris I Panthéon-Sorbonne University MMMEF Master Program. I had just graduated from the algebraic topology Master Program at Paris VII Denis Diderot University and I will never forget my first day when Christophe Chorro welcomed me. His courses in theoretical economics and econometrics made me discover my true calling as an applied mathematician specialized in finance. I will also never forget the kindness that Dominique Guégan showed me during my audition in front of the selection committee, which she was presiding in June 2013, and where I won my Doctoral Grant. I am very grateful to Paris I Panthéon-Sorbonne University for granting me this funding and the Maison des Sciences Economiques will forever be my academic home. I would like to express my gratitude as well to all the Professors of UFR27 and UFR02 who have entrusted me with teaching duties, especially Philippe Bich at the QEM Master Program, where I had the privilege to work as a teaching assistant for his course in optimization.

I also wish to thank Simone Scotti of Paris VII Denis Diderot University and Guillaume Bernis of Natixis Asset Management, who are my co-authors in one of the three papers constituting my thesis. I learned a lot from them and I am very grateful for the many work meetings we had over the course of the past year. Our common work on the dynamic evolution of distributions applied to CDS indices offered me the possibility to see the forecasting of market events from another, completely different, point of view than the one I had on this question and it opened for me many new research paths, which I am still exploring. I also feel very privileged to have met during this journey my friends Michel Perez at the Labex ReFi as well Michel Cojean and Edouard-François de Lencquesaing at the EIFR. They have given me many great opportunities to meet and interact with professionals in the finance industry, both in Paris and in New York. This was an essential part of my education and will be an essential part of my future career.

Finally I would like to thank my father, Emmanuel Kornprobst for his support during all these years and especially during my years as a PhD student. Back when I was a kid growing up in Cagnes sur Mer, I remember being at school and learning how to write on blank official exam papers that he used to bring me back from Paris Sorbonne University. Many decades later, I am very happy and proud that he is here today to witness the end of my life as a student and the beginning of my new life as a researcher in applied mathematics◆

Antoine Kornprobst, Paris, October 23rd 2017

Introduction

The research work presented in my thesis has been articulated around the goal of building financial crisis indicators with the ability to forecast as accurately as possible future market events and then use that information to devise systematic trading strategies. Those financial crisis indicators work from multiple points of view that complement one another. They rely on the correlation and the volatility inside a basked of asset or the components of an equity index, like the SP500 and, in one part of the thesis, we also develop indicators based on the distribution of the spreads of the components of a CDS index, like the Itraxx Europe 125. Those financial crisis indicators are then applied to many different datasets, large and small, and the signal that they provide is used as the basis for the construction of an active trading signal.

This thesis is made of three research papers constituting its three chapters. Each of those three papers is, at the date of my defence, about to be independently submitted or already undergoing review at a peer reviewed publication, albeit sometimes in a shortened form.

The first chapter deals with the construction of two kinds of financial crisis indicators. The first kind of financial crisis indicators is based on the comparison of the empirical spectrum of a rolling covariance matrix to a distribution of reference that may represent either a calm or an agitated market reference. The second kind of financial crisis indicators is based on the computation of the trace or of the spectral radius of the covariance matrix, the correlation matrix or a weighted version of the correlation matrix. The weights that we use in this first chapter are the market capitalization and the volume traded. After defining a total of nine financial crisis indicators, of both kinds, we then proceed to demonstrate out-of-sample predictive power for one of them, which we choose to be the spectral radius of the correlation matrix weighted by volume traded applied on our best and most detailed dataset that contains the SP500 index and its stock components. The most interesting aspect of the demonstration of the prediction power of our financial crisis indicator is the implementation of a successful protective put systematic trading strategy based on its signal. While the worth of our approach is demonstrated and the prediction power of our financial crisis indicators clearly established, we also underline the limitations of our approach, which in particular may take the form of a significant number of false positive errors in the signal provided by our financial crisis indicators.

The second chapter is constituted of a paper that builds upon the framework and financial crisis indicators constructed in the first chapter. In this second paper, we expands the use of our financial crisis indicators by combining the signals provided by 29 of them and create a decision process designed to govern a portfolio constituted of a mix of cash and ETF shares. Since the main limitation of our financial crisis indicators, while considered individually, is the presence of false positives in their predictions, we aim in this paper at combining the signals provided by many of them and make a systematic trading strategy act on the composition of the portfolio, selling the shares when the risk of a crisis is high and converting the cash into shares when the risk of a crisis is low, only when the indicators reach some kind of consensus in their forecasts. We then apply this approach to five datasets containing the stock components of five major

equity indices. The success of the systematic trading strategies based on our financial crisis indicators is demonstrated by comparing their performances to a buy and hold strategy as well as to a large number of paths of a strategy where the choices to convert the cash into shares or the shares into cash is random. The main result in this chapter is the validation of our framework and the demonstration of the usefulness and prediction power of our financial crisis indicators through the production of winning investment strategies based on those financial crisis indicators. The added value of our systematic active strategies, both in comparison to the static buy and hold references and to the random paths is clear in terms of Sharpe ratio, reduced volatility, increased overall performance and Calmar ratio.

The third and final chapter talks about another and novel approach to financial crisis indicators, this time by using the dynamic evolution of the distribution of the spreads of the components of a CDS index, like the Itraxx Europe 125. After establishing some results that allow us to work with dynamic distributions on solid theoretical ground, we fit the empirical distribution of the spreads of the components of the index with a mixture of two lognormal distributions. From the study of the dynamics of the coefficients of the decomposition of the empirical distribution of the spreads on the basis constituted of the two chosen lognormal distributions, we then build a lower and an upper boundary around the fitted empirical cumulative distribution function of the spreads of the components of the CDS index. This approach defines a Bollinger band around the fitted empirical cumulative distribution function and the crossing of either boundary defining by that band is interpreted in terms of risk and therefore translated into a trading signal. While the establishment of a complete and fully functional active trading strategy using that Bollinger band upper and lower boundary crossing signal is going to be presented in a mature form only in future revisions of this work, the results obtained are still attractive enough to be considered by the asset management industry, to which we believe this work can be extremely useful in order to navigate through a globally uncertain environment.

Chapter 1

An Empirical Approach to Financial Crisis Indicators Based on Random Matrices

An Empirical Approach to Financial Crisis Indicators Based on Random Matrices

Raphael Douady[1] and Antoine Kornprobst [*2]

[1] *Stony Brook University, Université Paris 1 Panthéon-Sorbonne*
[2] *Université Paris 1 Panthéon Sorbonne, Labex ReFi*

September 5th 2017

Abstract

The aim of this work is to build financial crisis indicators based on spectral properties of the dynamics of market data. After choosing an optimal size for a rolling window, the historical market data in this window is seen every trading day as a random matrix from which a covariance and a correlation matrix are obtained. The financial crisis indicators that we have built deal with the spectral properties of these covariance and correlation matrices and they are of two kinds. The first one is based on the Hellinger distance, computed between the distribution of the eigenvalues of the empirical covariance matrix and the distribution of the eigenvalues of a reference covariance matrix representing either a calm or agitated market. The idea behind this first type of indicators is that when the empirical distribution of the spectrum of the covariance matrix is deviating from the reference in the sense of Hellinger, then a crisis may be forthcoming. The second type of indicators is based on the study of the spectral radius and the trace of the covariance and correlation matrices as a mean to directly study the volatility and correlations inside the market. The idea behind the second type of indicators is the fact that large eigenvalues are a sign of dynamic instability. The predictive power of the financial crisis indicators in this framework is then demonstrated, in particular by using them as decision-making tools in a protective-put strategy.

Keywords: Quantitative Finance, Econometrics, Simulation Methods, Forecasting, Large Data Sets, Financial Crises, Random Matrix Theory

[*]Corresponding author: antoinekor9042@gmail.com

1 Introduction

The objective of this paper is to build financial crisis indicators capable of producing a useful forecast of future market events. The goal that we set for this study is *not* to predict the actual occurrence of financial crises. What we aim to achieve is rather to be able to evaluate at a given date whether the probability of a financial crisis happening at the given time horizon is getting higher, because the market conditions are ripe for a random adverse event from inside or even outside the market, to trigger a destructive chain reaction. Examples of random events capable of triggering a financial crisis are many. It may take the form of the sudden failure of a critical company, the publishing of new macro-economic data, a sovereign state defaulting on its debt, a major political event or even a terrorist attack. To use an analogy, we do not pretend to be able to predict the exact moment when a random spark will ignite the gas in the room, but we can measure whether the gas concentration in the room is just right for a random spark to cause a disaster. Since random adverse events happen all the time, measuring whether the conditions are just right in the market for one such event to trigger a crisis should be statistically equivalent to forecasting the actual occurrence of financial crises.

We build nine original financial crisis indicators which are divided into two kinds: those that study the distribution of the whole spectrum of the covariance matrix and compare it to a reference distribution and those that compute a specific spectral property (namely the trace and the spectral radius) of the covariance, correlation and weighted correlation matrix. Both kinds of indicators rely on the study of the underlying correlation and volatility signals inside the market. This is a novel approach because, while many different kinds of financial crisis indicators do exist in the literature, we are not aware of any that use reference distributions to compare the empirical spectrum of the covariance matrix to, nor any that use a modified version of the correlation matrix where the assets have been weighted with respect to the market capitalization of the corresponding companies or the daily traded volume. This approach enables us to maximize the amount of information coming from the market that is used by the financial crisis indicators, with the goal of boosting their predictive power. We work with seven datasets, each one designed with its own unique composition characteristics. This provides us with original results about many different financial markets from North America to emerging countries.

There is a large literature on financial crisis forecasting, especially works by Sornette (2009), Sornette and Johansen (2010) , Jiang et al. (2010) and Maltritz (2010) , which aim at producing a comprehensive model comprising the genesis,

dynamics and eventual prediction of financial crises, especially using the powerful tools of time-series analysis. Network theory has also been successfully applied to financial crisis forecasting and the building of financial crisis indicators as in Celik and Karatepe (2007) or Niemira and Saaty (2004). A machine learning approach, based on K-means clustering, to forecasting financial turmoil, and especially sovereign debt crises, has been developed in Fuertes and Kalotychou (2007) who also demonstrated that combining multiple forecasting methods improves the quality of the predictions, as Clemen (1989) had underlined in a review and annotated bibliography about combining forecasts. Cross sectional time series analysis in a panel data framework was studied in Van den Berg et al. (2008) to predict financial crises while Bussiere and Fratzscher (2006) chose to develop early warning systems of financial crises based on a multinomial logit model. Demyanyk and Hasan (2010) summarized the results provided by several prediction methods of financial crises, and especially bank failures, based on economic analysis, operations research and decision theory, while Drehmann and Juselius (2014) proposed detailed evaluation criteria of the performance of early warning indicators of banking crises. Financial crisis forecasts can also be based on the quantitative study of any kind of qualitative macro-economic data like the FOMC [1] minutes, or any other qualitative forecasts. That approach was developed by Stekler and Symington (2016) as well as Ericsson (2016). Its main limitation resides in the quality of the qualitative forecasts and the FOMC for example did not predict the 2007-2008 financial crisis in advance nor did it identify it quickly as a major systemic event. From another point of view, Guégan (2008) used chaos theory and data filtering techniques to make market forecasts. The approach that we adopt is more modest in the sense that we do not pretend to explain the precise macro-economic mechanism that creates the many different kinds of financial crises and to predict the precise date of the next crisis. The ambition of this work is merely to detect a heightened risk of a crisis happening, not to predict its actual occurrence. The approach we adopt is closer to the work of Sandoval Junior and De Paula Franca (2012) who proved in their paper, using random matrix theory techniques, that high volatility in financial markets is intimately linked to strong correlations between those financial markets.

Nonetheless, Sandoval Junior and De Paula Franca only used the Marchenko Pastur distribution in their work, while we intend to build and use additional distributions in the framework of random matrix theory. We also address internal correlations within the financial markets and not just the correlations between market indices. Those new distributions are numerically computed as closed form

[1] Federal Open Market Committee, which is the branch of the Federal Reserve Board that determines the direction of monetary policy

formulas for them do not exist to our knowledge. They are introduced in order to escape the restrictive framework of Marchenko-Pastur's theorem, which assumes uncorrelated Gaussian components. Indeed, the empirical covariance matrix of assets inside a market in turmoil is dominated by strong correlation and a non-Gaussian distribution of the log-returns. Of course, the objectives of this study are also very different, since we attempt to build empirical financial crisis indicators, which are almost ready for use by practitioners, while Sandoval Junior and De Paula Franca were concerned with proving a result about volatility and correlation reinforcing their effects during a financial crisis.

The approach and methods used in this study are also close to the work of Bouchaud, Potters and Laloux (2005 and 2009). Indeed, in their 2005 physics paper and 2009 review, they apply random matrix theory and principal component analysis to the financial context in order to anticipate market events and produce optimal portfolio allocations as well as risk estimations. Their idea to use, like Sandoval Junior and De Paula Franca, the Marchenko Pastur distribution as a reference distribution to which they compare empirical spectra is similar to the framework that we have developed but they use an exponentially weighted moving averages in place of the rolling matrix that we work with. The work of Singh and Xu (2013) and of Snarska (2007) about the dynamics of the covariance matrix in a random matrix theory framework was also inspirational to us. Indeed, the approach we select uses as well rolling windows for dynamic correlation and covariance matrices. Exploiting the spectra of those matrices forms the very foundation of the framework of this study.

We can also see the financial crisis indicators that we build as *market instability indicators*. Indeed, they are able to say at a given date whether the probability of occurrence of a financial crisis within a given time horizon has increased, while it is still possible that the probability of nothing happening remains very high. In particular, one possible limitation of our approach is the relatively high ratio of false positives. There is still usually a high probability that nothing will happen, even when the indicators return red flags. From a practitioner's point of view, the information that the probability of a crisis occurring in the near future has risen from, say, 0.1% to 10% has tremendous value, even though there is still a 90% chance of nothing happening. For us, a financial crisis indicator is a tool that makes use of publicly available data to determine whether the market conditions, measured by taking into account both correlation and volatility, are ripe in the market for a crisis event to happen.

The robust methods used in this paper are applied to an intuitive principle of

financial economics: when correlations between asset returns increase and develop abnormal patterns, when volatility goes up, then something is not right inside the market and a financial crisis event might be around the corner. Any kind of market data can be used within the framework that we created. Depending on the order of magnitude and scope of the financial crises that we intend to forecast, we have the freedom to choose the geographical characteristics of the data. Indeed, we can use prices time series restricted to assets located in one given country, one region or the whole world. The nature of the data can also be freely defined depending on the nature of the crisis events that we plan on forecasting. Stock prices and equity index prices, as well as sector indices may be used to forecast stock market crashes. Foreign exchange (FX) spreads may be used to forecast primarily monetary crises, and the methods that we develop provide a complementary point of view to the work of Guégan and Ielpo (2011) who used time-series models to forecast monetary policy. However, we are not limited to any asset class. We may also use bond yields, commodity prices or credit default swaps (CDS) spreads. Finally, it is possible to choose the frequency of the data and adapt it to reflect the kind and scope of the financial crises that we aim at forecasting, the only limitation being data availability.

In this paper, we chose to mainly focus on global financial crises, most of which are well known to the general public and the he data [2] has been selected accordingly. The code has been written using Matlab and its various optional toolboxes . The reader is very much encouraged to apply the methods developed in this paper to their own datasets and to verify the reproducibility of their forecasting power to various kinds and scopes of financial crises using data from many different kinds of asset classes and of various frequencies. We look forward to feedback and comments.

We propose in this paper a new approach regarding early warning financial crisis indicators that we then illustrate using many different datasets of market data. We also demonstrate the ability of the methods that we develop to make out-of-sample predictions. From our point of view, it seems that no such work has been published before with the same objectives and methodology. Therefore, we cannot compare quantitatively in terms of accuracy and predictive power the results that we have obtained to other existing studies. The work of Bouchaud, Potters and Laloux (2005 and 2009) uses a methodology that is similar to the one we chose, however we did not find detailed empirical results for their work, that would have been suitable for comparison in a robust way with the numerical results that we have obtained in this study.

[2] The data we use in this paper has been collected from Bloomberg and Yahoo Finance.

Besides the present introduction and a general conclusion, the paper is divided into four parts. We first describe how we built, collected and processed the databases. Indeed, their quality and diversity constitutes a major part of the interest of the study we conducted. In a second part, we detail the methodology and then we build the financial crisis indicators. The third part is dedicated to the qualitative analysis of the results provided by the financial crisis indicators over the whole length of the datasets. Finally, in the fourth part, we demonstrate the predictive power of the approach we developed by selecting two of the best performing financial crisis indicators applied to the largest and most detailed dataset that we possess. After dividing the data between an in-sample and an out-of-sample period, we study in details the forecasting possibilities they provide, firstly by using fixed dates of known financial crises and then by quantitatively defining a financial crisis in terms of the crossing of a chosen maximum draw down threshold.

2 The Data

The data is constituted at each date of the log-returns with respect to the previous trading day, computed from open or close prices. The prices have been adjusted for dividends and splits beforehand. We have chosen daily data for this study because of easy access and faster numerical handling. Further studies may explore higher frequency data. The model that we develop requires the choice of a rolling window in order to compute the financial crisis indicators. In order to limit averaging effects and to have financial crisis indicators with enough responsiveness to provide useful information to a practitioner, we chose the size of the rolling window to be 150 days in the past. This represents roughly six months of trading since we only take trading days into account. Using a relatively large rolling window means that the covariance matrix will be degenerate sometimes since there will be more observations than assets. This fact however is not going to be a problem because for the first type of indicators, the distance between the empirical distribution and the reference will be computed after truncating the empirical distribution around zero and making it stick to the reference in order to eliminate the contribution of the small eigenvalues. The motivations for this operation will be explained in the next section where the methodology that we use is explained in detail. For the second type of indicators, the presence of zeros, even quite a lot of them, in the spectrum will not change anything for the computation of the trace and spectral radius.

Seven datasets, each designed with its own unique properties and composition are considered in this study :

- The first dataset (Dataset 1) is constituted of eleven stock indices representative of the Asian, European and American financial markets in order to obtain a picture of the global financial system. It is a pure equity dataset that is designed to capture contagion between major financial markets as a way to forecast financial crises. It contains the Nikkei225 (NKY, Japan), Hang Seng (HSI, Hong-Kong/China), Taiwan Stock Exchange Weighted Index (TWSE, Taiwan) for the Asian market, the DAX30 (DAX, Germany), FTSE100 (UKX, U.K), IBEX35 (IBX, Spain) for the European market, the SP500 (SPX, U.S.A), Russel3000 (RAY, U.S.A), NASDAQ (CCMP, U.S.A), Dow Jones Industrial Average (INDU, U.S.A), SP/TSX Composite Index (SPTSX, Canada) for the North American market. Dataset 1 spans from January 7th 1987 to February 5th 2015. In order to avoid contaminating the data with time differences which might create bias and spurious correlations, we matched at a same date t the close price in Asia at t, the close price in Europe at t and the open price in America (East Coast) at t. In the absence of intraday data, this appeared to be a reasonable choice. We considered only the trading days and because of the different holidays specific to each of the three markets considered (Asian, European and North American) and the requirement to keep only the trading days that were common to all the markets, the 252 trading days a year have been reduced to around 200 dates. Comparison with the other datasets (particularly Dataset 3 and Dataset 4 below which do have around 250 entries a year since they are exclusively American and European, respectively) shows that this is not a major issue in practice.

- The second dataset (Dataset 2) is constituted of sixteen assets. It contains all of the indices of Dataset 1, some commodity indices and some safe haven or cash equivalent securities toward which investors tend to turn in a time of crisis or impending crisis. It spans the same period as Dataset 1, from January 7th 1987 to February 5th 2015. The treatment of the data with regard to time differences between geographical regions and non-trading days is the same. On top of the content of Dataset 1, Dataset 2 includes: The London Gold Market Fixing Index (GOLDLNPM, U.K), the Philadelphia Stock Exchange Gold and Silver Index (XAU, U.S.A), Oppenheimer Limited-Term Government Fund Class A (OPGVX, U.S.A), Sugar Generic Future Contract (SB1, U.S.A), generic First Crude Oil WTI (CL1, U.S.A). The inclusion of precious metal indices, cash equivalent short-government monetary funds, representative agricultural as well as energy commodities (in the form of investable futures) is supposed to provide a longer fuse to the financial crisis indicators. As a matter of fact, when the market starts to overheat, investors may liquidate some of their equity positions but they will have to re-invest

the cash somewhere and those cash equivalent securities are here to account for that. Since those safer, cash equivalent securities are in Dataset 2, we anticipate that the risk of a crisis happening will be detected sooner. Moreover, when the market is becoming unstable, one typically witnesses an increase in the correlations between commodity and energy securities (typically large oil companies stocks included in the indices). Since we included some investable commodity futures (like oil futures) in Dataset 2, we expect to capture that effect which is indicative of the appearance inside the financial market of the right conditions for a crisis to happen.

- The third dataset (Dataset 3) contains twelve assets which are the SP500 index and its ten sector sub-indices (consumer discretionary, consumer staples, energy, financials, health care, industrials, information technology, materials, telecommunication services, utilities) plus a small capitalization index, the Russel 2000. This dataset should provide information about the inner workings of the SP500 and enable us to detect "American" crises (for example the Sub-Prime Crisis of 2007) sooner and with a higher precision than Dataset 1 or Dataset 2 which are global by design and include information about the contagion between the three largest financial markets (Asia, Europe, North America). However, since the North American market still leads the world of finance, it is to be expected that the actual crises anticipated by the use of either three of Dataset 1, Dataset 2 or Dataset 3 will be roughly the same. The inclusion in the mix of a small capitalization index is to try to take advantage of the fact that in the times leading up to a financial crisis, the small caps tend to overheat and form speculative bubbles while they become more and more correlated between themselves and stocks with larger market capitalization. Dataset 3 spans from September 13th 1989 to December 27th 2013.

- The fourth dataset (Dataset 4) is the European counterpart of Dataset 3. It contains eleven assets : the Bloomberg European 500 Index (BE500) and its ten sector sub-indices, which are the same as for the SP500 (consumer discretionary, consumer staples, energy, financials, health care, industrials, information technology, materials, telecommunication services, utilities). As we did not find any European-wide equivalent to the Russel 2000, it does not include small caps however. It should enable us to better and sooner detect "European" crises like the E.U Sovereign Debt Crisis of 2010 while still containing enough information to detect all the other global financial crises. It spans from January 1st 1987 to December 27th 2013.

- The fifth dataset (Dataset 5) is designed with the financial concept of *flight to quality* in mind. Indeed, in the times preceding a financial crisis, the

anxiety of market agents is building up and they tend to abandon equity positions in favor of safer investment grade treasury or corporate bonds. In that regard, the usual observed phenomenon is a positive correlation between equity and bonds in a bull market and a negative correlation between equity and bonds in a bear market. When the correlation between equity and bonds is becoming too high, this may be a sign that the bull market is about to burn itself out, that a bubble is about to burst, heralding the start of a financial crisis. Dataset 5 is built with the detection of that phenomenon in mind. It contains all of the data of Dataset 3 (SP500 index, its 10 sector indices and the Russel 2000 as a small capitalization index) plus a number of funds based on investment grade sovereign or corporate bonds. Much like Dataset 3, Dataset 5 is U.S market oriented and is therefore more suited to anticipate crises that originate from or directly affect the North American market. For the long government bonds we have : Wasatch-Hoisington U.S. Treasury Fund (WHOSX) and Thornburg Limited Term U.S. Government Fund Class A (LTUCX). For the corporate bonds we have selected Lord Abbett Bond Debenture Fund Class A (LBNDX) and Vanguard Long-Term Investment-Grade Fund Investor Shares (VWESX) which have both enough AUM (Assets Under Management) to be systemically significant and have existed for a long enough time to be historically relevant. Dataset 5 contains therefore 16 assets and spans from September 13th 1989 to December 27th 2013.

- The sixth dataset (Dataset 6) is constituted of 226 individual components of the SP500 index. Because of the evolution over time in the composition of the index, a balance had to be found between keeping a sufficient number of components and having enough historical data. It spans from January 17th 1990 to May 15th 2015. The Apple Inc (AAPL) stock was chosen as the reference with regard to filtering out non-trading days and whenever another element of data was unavailable (on rare seemingly random days it appears that some individual stocks were not traded or the data was unavailable) we carried over the last previously available value. We assumed that this manipulation would not compromise the overall quality of the data. Besides those considerations, a few stocks like for example Range Resources Corporation (RRC UN) and The Charles Schwab Corporation (SHCW UN) presented significant data gaps and were removed from the dataset. Since building a dataset with exactly 500 components of the SP500, taking in account the evolution in the composition of the index over time, proved an impossible task due to its complexity and the availability of the data (mergers, corporate spin-offs and private equity acquisitions would have had to be taken into considerations as well), we are aware of the fact that Dataset 6, especially

when used in conjunction with financial crises indicators might suffer from survivorship bias. As a matter of fact, especially in the times leading up to a crisis, the failing companies drop below the capitalization threshold or are acquired by others while new healthier firms enter the index. We built Dataset 6 because, as we are going to see in the empirical section, working with whole indices and/or limited number of individual securities like in all the previous datasets we created (especially Dataset 3 which resembles a scaled down version of Dataset 6), tends to have an averaging effect on the correlations and renders the correlation signal too noisy and blurred to be useful as a crisis detection method. For reference, the Bloomberg tickers of all the stocks inside Dataset 6 are provided in appendix. Besides the daily close price, from which we derive the log-returns, that is contained in all the other datasets, Dataset 6 also includes daily volumes and market capitalization. Those extra variables will enable us later to add appropriate weights to the individual stocks in order to refine the computation of the indicators.

- The seventh dataset (Dataset 7) is constituted of the SP500, the Russel 2000 index and ten indices from emerging markets : Buenos Aires Stock Exchange Merval Index (MERVAL, Argentina), Ibovespa Brasil Sao Paulo Stock Exchange Index (IBOV, Brasil), Mexican Stock Exchange Index (MEXBOL, Mexico), Moscow Exchange Composite Index (MICEX, Russia), Hong Kong Hang Seng Index (HSI, Hong Kong/China), Shanghai Stock Exchange Composite Index (SHCOMP, China), Jakarta Stock Exchange Composite Index (JCI, Indonesia), National Stock Exchange CNX Nifty Index (NIFTY, India), FTSE/JSE Africa All Share Index (JALSH, South Africa), Borsa Istanbul 100 Index (XU100, Turkey). It spans from September 22nd 1997 to May 12th 2015. The relatively shallow depth of this dataset, which in particular may render the study of the Asian crisis of the late 1990' more difficult, is due to gaps in data availability, especially for the Russian index that we decided to keep anyway due to its importance for the global commodity and energy markets. All those emerging indices were expressed in the local currency on Bloomberg and were therefore converted into U.S dollars. This conversion was very important when dealing with emerging economies where the exchange rate of the local currency against the U.S dollar can fluctuate wildly and violently especially in the times leading up to, and during a financial crisis. Unlike in advanced economies (we did not convert the European and Japanese indices into U.S dollars in Dataset 1 for example), the position of the currency of an emerging country against the U.S dollar is also highly correlated to the health of the local real economy. This idea was developed by Hawkins and Klau (2000) when they were working with the Bank of International Settlements: in emerging markets, financial crises are

often preceded by overvalued exchange rates and inadequate international monetary reserves.

Regarding the selection of the financial crisis events on a global scale (for use mainly with Dataset 1 and Dataset 2) or at least a regional scale (for use mainly with Dataset 3, Dataset 4, Dataset 5, Dataset 6 and Dataset 7) of the last 30 years, we compiled Table 1 below, which has no ambition of being exhaustive. Succinct historical context will be discussed in the empirical results section when needed. While categorizing the various kinds of financial crises goes far beyond the scope of this paper, we strove to consider a wide selection in the kinds of crises. There are stock market crashes like Black Monday in 1987 and the NASDAQ Crash in 2000. There are financial crises that are rooted into a deep structural fragility of some parts of the real economy, like the real estate sector in the case of the Japanese Asset Price Bubble of the early 1990' and the Sub-prime Crisis that started in America during the summer of 2007 or the automobile industry in the case of the bankruptcy of General Motors in June 2009, four years after Delphi Corporation, which was General Motors' main supplier of automotive parts. There are financial crises for which the main trigger was a sovereign debt default like the Russian crisis in 1998, the Argentine crisis in 2001 or the Eurozone crisis, triggered by the Greek haircut in 2010. There are monetary crises as well, like Black Wednesday in 1992 when the British government was forced to withdraw the Pound Sterling from the European Exchange Rate Mechanism (ERM) or the Mexican crisis triggered by the devaluation of the peso against the U.S Dollar. Since none of the datasets include foreign exchange data, we do not expect that any of the indicators will perform well when it comes to anticipating monetary crises, however. There are banking crises as well such as the S&L crisis in America that spanned from the mid-1980' to the mid-1990' and during which almost one third of all American savings and loans associations (financial institutions that are allowed to accept savings deposits and to make loans) failed, including hundreds of banks of all sizes and systemic significance. The dates chosen may sometimes seem a little arbitrary but choices had to be made, especially for crises that, unlike Black Monday that played out mostly within a few days of extreme market distress, took place over many months or even years of sustained drop like the NASDAQ in early 2000, which took nearly four months to lose almost two fifth of its March 10th peak. Most financial crises do not happen in one day and instead result from a long process of instability buildup inside the market, the kind of which the indicators that we have built are detecting. When a crisis is best described by a clear explosion, then the date of that event was chosen (Black Monday, the day Lehman Brothers failed, etc...). When a date for a crisis spanning months or years had to be chosen for this study, we considered either the date of the most marking event (the day the NASDAQ peaked, the day General Motors filled for Chapter 11

bankruptcy [3], the day the Greek haircut was announced, etc...) or a date roughly situated in the middle of the crisis process like January 1st 1990 for the S&L crisis.

Date (Y/M/D)	Name
1987-10-19	Crisis 1 : Black Monday
1990-01-01	Crisis 2 : S&L Crisis
1990-08-01	Crisis 3 : Japanese Asset Prices Bubble Burst
1991-09-19	Crisis 4 : Scandinavian Banking Crisis
1992-09-16	Crisis 5 : Black Wednesday
1994-12-20	Crisis 6 : Mexican Crisis
1997-07-25	Crisis 7 : Asian Crisis
1998-08-17	Crisis 8 : Russian Crisis
2000-03-10	Crisis 9 : NASDAQ Crash (dot-com Bubble)
2001-02-19	Crisis 10 : Turkish Crisis
2001-09-11	Crisis 11 : 911 Attacks
2001-12-27	Crisis 12 : Argentine Default
2005-10-08	Crisis 13 : Delphi (G.M) Bankruptcy
2007-07-01	Crisis 14 : Sub-prime Crisis
2008-09-15	Crisis 15 : Lehman Brothers Collapse
2009-06-01	Crisis 16 : General Motors Bankruptcy
2010-04-23	Crisis 17 : European Sovereign Crisis
2011-08-05	Crisis 18 : US Sovereign Credit Degradation
2014-12-16	Crisis 19 : Russian Financial Crisis

(Table 1: Selection of Financial Crisis Events in the past 30 years)

3 Methodology

Using the seven datasets that we have built, the methodology is based on the use of the spectrum of the covariance matrix, the correlation matrix and a weighted version of the correlation matrix. At each date, for a sequence of rolling windows, we either compare the whole spectrum to three reference distributions detailed below (two of the reference distributions characterize a calm market and a third one represents a market in turmoil), which gives us the indicators of the first kind, or we merely compute the spectral radius and the trace, which gives us the indicators of the second kind. We now details this methodology using Matlab's formalism and vector indexing conventions.

[3]Chapter 11 of Title 11 of the United States Code (also known as the United States Bankruptcy Code) which permits reorganization. In contrast, Chapter 7 provides a legal framework for liquidation.

3.1 Framework

We decided to consider a rolling window T of 150 days in the past at each date and for all datasets, irrespective of the number N of assets they contain. This choice provides us with a good balance between the readability of the signals, favored by a longer rolling window because of the averaging effect, and the responsiveness of the indicators, favored by a shorter rolling window.

For each of the seven datasets, we build at each date t a rolling window $ROL(t)$ of length T. Then, we compute the rolling covariance matrix $CV(t)$ and the rolling correlation matrix $CR(t)$ by using the following formulas written for every row (i.e asset) $j \in [\![1, N]\!]$:

$$ROL^*(t)(j,:) = ROL(t)(j,:) - mean(ROL(t)(j,:)) \quad (1)$$

$$CV(t) = \frac{1}{T}.ROL^*(t) \times (ROL^*(t))' \quad (2)$$

$$CR(t)(j,:) = \frac{ROL^*(t)(j,:)}{\sqrt{var(ROL(t)(j,:))}} \quad (3)$$

While working with a covariance matrix instead of a correlation matrix, we of course have to rescale the eigenvalues of $CV(t)$. We perform this either by noticing that the standard deviation of financial log-returns is typically in the order of magnitude of a few percents ($a \in [0.01, 0.03]$) and therefore multiplying the eigenvalues by $\frac{1}{a^2}$, or by computing the mean of the variances of all the complete time-series in advance and multiplying by the inverse of that value (for example, we find a rescaling factor of 3410 for Dataset 2). This is what we decided to do but it should not be considered as a violation of the measurability of the indicators with respect to the natural time filtration (i.e knowledge of the future). It is just a practical way of rescaling by choosing the most appropriate value and it could just as well have been obtained from historical data predating the sample.

With regard to the reference distributions we use for the first type of indicators, we have built three of them :

- $\Theta 1$: the theoretical Marchenko Pastur distribution. It is derived from Marchenko Pastur's theorem presented in the work of Marchenko and Pastur (1967). Let X be a $N \times T$ random matrix of i.i.d normal $\mathcal{N}(0, \sigma^2)$ coefficients (in this study, each row represents an asset and each column represents an observation at a date t), then when $N, T \longrightarrow \infty$ and the aspect ratio of the matrix, $N/T \longrightarrow \gamma < \infty$, then the distribution of the eigenvalues of the covariance matrix $Y = \frac{1}{c}(XX')$ is the Marchenko Pastur distribution with the density

below. This formula (6) below is supposed to be valid for $0 < \gamma < 1$, otherwise in the degenerate case, an atom at zero has to be added, but since we intend to truncate the computation of the Hellinger distance to exclude the very small eigenvalues, as we will explain in the next section, this is the formula we are going to use anyway for simplicity.

$$\lambda^+ = \sigma^2(1+\sqrt{\gamma})^2 \quad (4)$$

$$\lambda^- = \sigma^2(1-\sqrt{\gamma})^2 \quad (5)$$

$$f(x) = \frac{1}{2\pi\sigma^2\gamma}\frac{\sqrt{(\lambda^+ - x)(x-\lambda^-)}}{x}1_{[\lambda^-,\lambda^+]} \quad (6)$$

The Marchenko Pastur distribution also provides thresholds λ^+ and λ^- that we use even while working with other simulated reference distributions. Because of the stringent theoretical requirements of Marchenko Pastur's theorem, that will never be even remotely satisfied by real financial data, the Marchenko Pastur distribution has no vocation to be the best distribution fulfilling the role of a calm market reference, but it is still going to be useful in this study.

- $\Theta 2$: the distribution of the eigenvalues of the covariance matrix of a simulated random matrix made of Gaussian $\mathscr{N}(0,1)$ coefficients where the assets, materialized as the rows, present some correlation to one another. Let us consider a rolling matrix $(Z_{i,j})_{(i,j)\in[\![0,N]\!]\times[\![0,T]\!]}$, containing T observations (columns) and N assets (rows) and constituted of i.i.d Gaussian $\mathscr{N}(0,1)$ coefficients. We introduce correlation between the assets by adding the same Gaussian coefficient to each of the assets at a given time. $\forall j \in [\![0,T]\!]$, Z_0^j is following a Gaussian $\mathscr{N}(0,1)$ law. With those notations, $\forall i \in [\![0,N]\!]$ and $\forall j \in [\![0,T]\!]$, each of the coefficients $X_{i,j}$ of the rolling random matrix from which we obtain the covariance matrix, is computed in the following manner:

$$X_{i,j} = \rho Z_0^j + \sqrt{(1-\rho^2)}Z_{i,j} \quad (7)$$

$$Z_{i,j} \sim \mathscr{N}(0,1),\ Z_0^j \sim \mathscr{N}(0,1) \quad (8)$$

The coefficient ρ is chosen as the mean of the long term correlation coefficients between all the assets of the whole sample contained in the chosen dataset. Like when we had to decide on a rescaling coefficient for the spectrum, this choice of ρ should not be considered as knowledge from the future, as it could just as well have been obtained from historical data. As a matter of fact, we find something very close to 50 % for all the datasets, which is what we had expected. $\Theta 2$ is going to be the second, more realistic, calm market reference distribution.

- $\Theta 3$: the distribution obtained using the same blueprint as $\Theta 2$ but where all the Gaussian $\mathcal{N}(0,1)$ distribution have been replaced by Student (t=3) distributions. This will be the reference distribution characterizing a market in turmoil.

As an illustration, Figure 1 below contains the three reference distributions $\Theta 1$, $\Theta 2$ and $\Theta 3$ for the number of assets contained inside Dataset 1 (eleven assets) and a rolling window of 150 days. We also included in appendix the three reference distributions computed for all the other datasets and the same rolling window of 150 days.

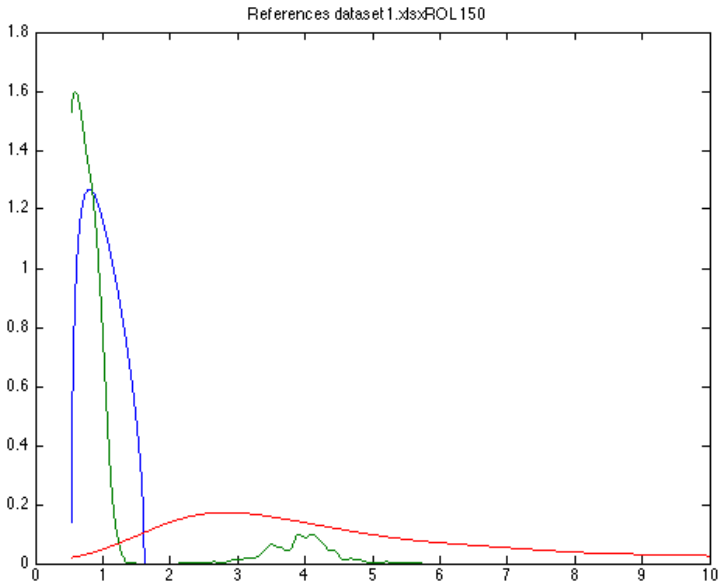

Figure 1: Reference distributions for Dataset 1. Blue: Marchenko Pastur ($\Theta 1$), Green: $\Theta 2$, Red: $\Theta 3$

3.2 Financial Crisis Indicators

Using the tools described above, we build two kinds of financial crisis indicators: the indicators of the A-series and the indicators of the B-series.

The indicators of the A-series compare at each date the empirical distribution of the spectrum of the covariance matrix to the references that we introduced in the previous subsection. We chose to use the Hellinger distance in its discrete form as introduced by Hellinger (1909). We decided to use this metric on the space of distribution instead of the Kullback–Leibler divergence introduced in Kullback and

Leibler (1951), which is also of very common use in probability theory, because we wanted a true metric, which the Kullback–Leibler divergence is not since it does not satisfy the triangle inequality. The Kullback–Leibler divergence is also not symmetric with respect to the two distributions considered. Moreover, since we chose an empirical approach with a strong focus on the intuitive aspect of the study, we felt that the Hellinger distance, which is plainly the Euclidean distance of the square root of the components, was easier to see when drawing two distributions on the same graphic than the Kullback–Leibler divergence which is defined as the expectation of the logarithmic difference between the two distributions.

We recall that the Hellinger distance $\mathbb{D}$ between two probability distributions with densities $P(x)$ and $Q(x)$, which are both known at a number of points X_i, $(i \in [\![1, K]\!])$, is computed using the formula below :

$$\mathbb{D}^2 = \sum_{i=1}^{K} (\sqrt{P(X_i)} - \sqrt{Q(X_i)})^2 \quad (9)$$

Considering any of the three reference distributions, we compute at each date its Hellinger distance to the empirical distribution of the eigenvalues of the covariance matrix. Our assumption is that the further away in the sense of the Hellinger distance the empirical distribution drifts away from the calm market reference, and the closer in the sense of the Hellinger distance the empirical distribution comes to the market in turmoil reference, then the more likely it becomes that the market is about to experience a crisis. Indeed, such movements tend to indicate a build-up of correlation and volatility inside the market. There is however no way to study those two effects, volatility and correlation, separately in the Hellinger distance approach and the indicators of the A-series always lump those two instability factors together in their forecasts of financial crises.

Since all datasets except Dataset 6 only have a small number N of assets and will therefore give us only a small number of eigenvalues at each date, we combine at each date t the spectra obtained from the previous 20 days in order to have $20.N$ eigenvalues, which is enough observations, to derive a distribution by using a normalized histogram. We then compute the Hellinger distance to the reference distribution on a sufficiently large support in order to capture all of the spectral distribution. In empirical studies such as Stanley and al. (2000), eigenvalues of the covariance matrix have been observed to grow as large as twenty five times the critical value λ^+ of Marchenko Pastur's distribution (4). In consequence, we decided to consider 25 times the support $[\lambda^-, \lambda^+]$ in order to account for all of the empirical spectrum.

The indicators of the first type are the following. There are three of them, corresponding to the three reference distribution that we have introduced before:

- Indicator A1: It is the Hellinger distance between a modified version $\mathscr{E}_1^*(x)$, detailed below, of the empirical distribution $\mathscr{E}(x)$ of the eigenvalues of the covariance matrix and the theoretical distribution of Marchenko Pastur $\Theta 1$. Indeed, Indicator A1, as well as all the indicators based on the Hellinger distance, needed to be adapted to filter out the effects of a parasitic phenomenon consisting of an accumulation of small eigenvalues close to zero, which deforms the unmodified empirical distribution and distorts the computation of its Hellinger distance with respect to the reference distribution. We illustrate this in Figure 2 and Figure 3:

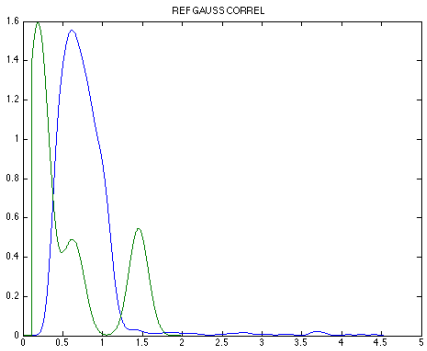

Figure 2
Accumulation of Small Eigenvalues for $\Theta 2$

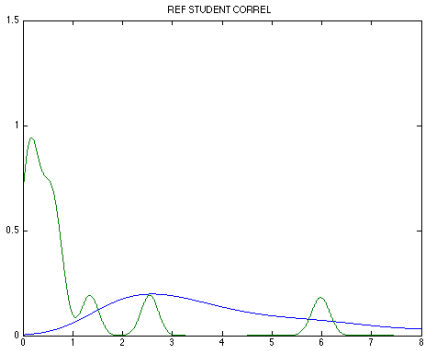

Figure 3
Accumulation of Small Eigenvalues for $\Theta 3$

In those two examples, which are very typical of the situations that we encounter in practice for a given date t while using all the datasets, we see the

reference distribution (in blue) and we see the empirical distribution of the eigenvalues of the covariance matrix (in green). The empirical distribution can differ from the reference distribution in two ways. It can overflow to the right toward the higher eigenvalues: that's the kind of behavior that we are looking for in order to detect a financial crisis. It can also unfortunately accumulate itself, sometimes most of the mass is even there, closer to zero toward the very small eigenvalues. Such a behavior of the distribution of the eigenvalues of the covariance matrix is more indicative of the prevalence of risk free combinations of assets which equates to a very calm and diversified market.

The solution was to define A1 and the A-series indicators in the following way : instead of computing the Hellinger distance between the unmodified empirical distribution $\mathscr{E}$ and the Marchenko Pastur reference $\Theta 1$, we compute the Hellinger distance between $\Theta 1$ and the distribution $\mathscr{E}_1^*$ defined in the following way :

$$\mathscr{E}_1^*(x) = min(\mathscr{E}(x), \Theta 1(x)),\ x < \frac{\lambda^+}{10} \quad (10)$$

$$\mathscr{E}_1^*(x) = \mathscr{E}(x),\ x > \frac{\lambda^+}{10} \quad (11)$$

Therefore :

$$A1 = \mathbb{D}\{\mathscr{E}_1^*, \Theta 1\} \quad (12)$$

For a given dataset, this indicator measures at each date by how much the assumptions of Marchenko Pastur's theorem (normal i.i.d coefficients of variance equal to 1) are violated. Since the finite size of the rolling covariance matrix does not change over time, it will not be responsible for any dynamical variations of the Hellinger distance although it does certainly account for part of the distance between the theoretical asymptotic distribution of Marchenko Pastur and the empirical distribution. This indicator lumps together the apparition of non-normality, correlations and volatility in the log-return time series, it cannot differentiate between all those effects but it is still very useful. As a matter of fact, the apparition of any of those phenomena, whose effects are not expected to compensate one another, can be interpreted as a warning that a crisis might be around the corner. Therefore our assumption is going to be that the further away the modified empirical distribution $\mathscr{E}^*(x)$ becomes from the reference Marchenko Pastur distribution in the sense of the Hellinger distance, the more likely a crisis is going to happen in the near future.

Like we said earlier, using the Marchenko Pastur distribution for a given aspect ratio as a reference distribution might not be optimal because it is an asymptotic result and we deal with finite size matrices and because even a perfectly calm financial market might be better modeled by random matrices of coefficients with some natural correlations.

- Indicator A2: It is the Hellinger distance between the modified version $\mathscr{E}_2^*(x)$, detailed below, of the empirical distribution of the eigenvalues of the covariance matrix $\mathscr{E}(x)$ and the simulated reference distribution $\Theta 2$. Since correlated Gaussian coefficients are supposed to better model the market situation, we expect $\Theta 2$ to provide a better calm market reference from which to measure a drift of the empirical distribution of the eigenvalues of the covariance matrix in the times leading up to a financial crisis. Like with Indicator A1, we decided to work on 25 times the support of the corresponding theoretical Marchenko Pastur distribution and the same issues of accumulation of the empirical distribution toward the small eigenvalues in time of market calm presented itself. There is no closed form formula for the reference $\Theta 2$ and we cannot assume that its support is bounded like the support of Marchenko Pastur's distribution is bounded by λ^- and λ^+ so we decided to keep $\lambda^* = \frac{\lambda^+}{10}$ as a threshold, such that an abundance of very small eigenvalues would not make the Hellinger distance explode. Therefore, we compute the Hellinger distance between $\Theta 2$ and $\mathscr{E}^*$ in the following manner :

$$\mathscr{E}_2^*(x) = min(\mathscr{E}(x), \Theta 2),\ x < \lambda^* \quad (13)$$

$$\mathscr{E}_2^*(x) = \mathscr{E}(x),\ x \geq \lambda^* \quad (14)$$

Therefore :

$$A2 = \mathbb{D}\{\mathscr{E}_2^*, \Theta 2\} \quad (15)$$

- Indicator A3: It is the Hellinger distance between the modified version $\mathscr{E}_3^*(x)$, detailed below, of the empirical distribution of the eigenvalues of the covariance matrix $\mathscr{E}(x)$ and the simulated reference distribution $\Theta 3$. We included very fat tails (coefficients that follow a Student (t=3) distribution) as a way to model crisis conditions, therefore Indicator A3 is an inverted indicator. Indeed, it produces red flags when it is getting small, which means that the empirical distribution of the eigenvalues of the covariance matrix is getting very close to $\Theta 3$, with is extremely heavy tailed and represents a spectrum entirely shifted toward the large eigenvalues, characterizing a market in deep turmoil. When the market goes from a calm state to a crisis state, the modeling that we make of the log-returns goes from a Gaussian to a Student

(t=3) distribution. As a remark, we did not include skewness in the random coefficients from which we derive the reference distributions because financial log-returns do not typically present persistent skewness, especially over the time periods considered for the rolling window, as demonstrated in the work of Singleton and Wingender (1986). We retain for A3 the same method of computation as in the other ones of the A-series. We compute it over 25 times the support of the corresponding theoretical Marchenko Pastur distribution and the threshold $\lambda^* = \frac{\lambda^+}{10}$ is used to filter out the very small eigenvalues. Indicator A3 then computes at each date t the Hellinger distance between $\Theta 3$ and $\mathscr{E}^*$ such that :

$$\mathscr{E}_3^*(x) = min(\mathscr{E}(x), \Theta 3),\ x < \lambda^* \quad (16)$$

$$\mathscr{E}_3^*(x) = \mathscr{E}(x),\ x \geq \lambda^* \quad (17)$$

Therefore :

$$A3 = \mathbb{D}\{\mathscr{E}_3^*, \Theta 3\} \quad (18)$$

We therefore have three indicators of the first type, called A1, A2 and A3. Each possesses its own characteristics and looks at specific market conditions that may be indicative of an impending financial crisis. We do expect the three indicators of the first kind to be coherent with one another, especially since they are of similar origin, but they also complement one another and the financial crisis forecasts that we make need to take all three into consideration to be effective.

We now shift to the indicators of the B-series. At each date t, the centered rolling matrix $ROL^*(t)$ in formula (1) contains two components: a volatility component and a correlation component. The indicators of the B-series are based on those two components. As we are going to see, both components are important, but the relative strength of their signal will greatly depend on the choice of the dataset we use. We build at each date t the three indicators of the second type in the following way :

- Indicator B1: It is defined as the spectral radius of the covariance matrix $CV(t)$ in formula (2). It measures a mixed signal depending on both volatility and correlations in the market. A larger value for the spectral radius is indicative of dynamical instability and increased correlations in the system but it also takes the volatility effect into account since we are working with a covariance instead of a correlation matrix. This indicator takes the effects of both volatility and correlations into account and those two effects are not supposed to compensate each other, on the contrary they are expected to evolve in the same direction in the times leading up to a financial crisis as it was demonstrated by Sandoval Junior and De Paula Franca (2012).

- Indicator B2: It is defined as the trace of the covariance matrix $CV(t)$. It measures the volatility signal alone. While it may seem at first that B2 lacks a very important aspect of what is happening inside the market, we will see while discussing experimental results that it is still a very good financial crisis indicator. It is also very easy and fast to compute. As a matter of fact it is not even needed to compute the whole spectrum of the covariance matrix to compute its trace.

- Indicator B3: It is defined as the spectral radius of the correlation matrix $CR(t)$ in formula (3). It measures the correlation signal alone. The usefulness of Indicator B3 greatly depends on the choice of the dataset. We will discuss more about this in the section discussing the numerical results. Only when used on Dataset 6, which contains a large number of assets, which are individual stocks components of an index, does indicator B3 realize its full potential. Indeed, there is a lot averaging effect inside an index and when we use the value of the index itself as opposed to its individual components, the correlation signal is generally smothered. The potential of Indicator B3 is great however, because unlike with the study of volatility alone, the study of correlation may be the only way to give the indicators that we have built real predictive power. Since Dataset 6 also features daily volume and daily market capitalization data, we also build the following variations of indicator B3, to be used on Dataset 6 exclusively:

  - Indicator B3A: the spectral radius of the matrix $CR_1(t)$. Its coefficients are those of $CR(t)$ which have been weighted at each date t by the market capitalization ($cap(t)$) expressed in dollars, in the following way for a dataset containing F assets. $\forall (i,j) \in [1,F]^2$:

$$CR_1(t)(i,j) = CR(t)(i,j).\frac{cap(t)(i).cap(t)(j)}{\sum_{k=1}^{F} cap(t)(k)^2} \quad (19)$$

  - Indicator B3B: the spectral radius of the matrix $CR_2(t)$. Its coefficients are those of $CR(t)$ which have been weighted at each date t by the volume of stocks exchanged ($volu(t)$) expressed in dollars, in the following way for a dataset containing F assets. $\forall (i,j) \in [1,F]^2$:

$$CR_1(t)(i,j) = CR(t)(i,j).\frac{volu(t)(i).volu(t)(j)}{\sum_{k=1}^{F} volu(t)(k)^2} \quad (20)$$

  - Indicator B3C: Since indicator B3B will prove useful but will also usually produce a noisy signal, B3C is computed at each date t as a moving

average of B3B. We chose to average on 150 days, which is also the length T of the rolling window.

$$B3C(t) = \frac{\sum_{k=1}^{T} B3B(t-k)}{T} \quad (21)$$

To conclude this section, we have therefore built nine financial crisis indicators in all. There are three of the first kind (A1, A2, A3) and six of the second kind (B1, B3, B3, B3A, B3B, B3C). Now we are going to use those indicators on the seven datasets that we possess in order to detect the periods of crisis.

4 Empirical Results, Global Studies

In this section we look at the global profiles produced by the nine financial crisis indicators that we have built for the seven datasets that we have chosen, and study in a qualitative manner what happens around the crises that we presented in Table 1. A more quantitative approach will be taken in the next section. Starting with the indicators of the A-series, we obtain the following results, the crisis events in Table 1 have been added as vertical purple lines and A1 is in blue, A2 in green and A3 in red. As a general remark, we can say that although useful global structures do clearly appear, all the profiles also appear to be quite noisy. We cannot miss the collapse of Lehman Brothers (Crisis 15) for example and it is a fact that most other crises are accompanied by very noticeable patterns in the value of the Hellinger distance, but there are also many false positives that blur the message of the indicators of the A-series. A1 and A2 always produce profiles that are similar, which is explained by the close resemblance between the reference distribution $\Theta 1$ and $\Theta 2$ (as seen in Figure 1 and in appendix), while the inverted indicator A3 produces radically different profiles. Many times we see A1 and A2 climb just before a truly major crisis, while A3 plummets. Indeed, the distribution $\Theta 3$, which was derived from the covariance matrix obtained from a random matrix made of sums of very heavy tailed and correlated Student (t=3) coefficients is a good reference for a market that is in the process of dislocation, with the preeminence of very large eigenvalues in the covariance matrix that are indicative of dynamical instability. With that point of view, the correct way to read the profiles is: if A1 and A2 go up, then we are moving away in the sense of Hellinger from a distribution that is characteristic of a calm market, danger might be around the corner. If on top of that A3 is going down, then we are moving closer in the sense of Hellinger to a distribution of the eigenvalues of the covariance matrix that is characteristic of a market in distress. If those two effects are happening at the same time, then this pattern in the behavior of the indicators tends to indicate that the probability of a truly major market event is getting dangerously high.

- For Dataset 1, the pure international equity dataset, we get Figure 4 below. We observe elevated levels of A1 and A2 in the aftermath of Black Monday and during the build-up toward the S&L crisis and Japanese Asset Price Bubble of 1990. Then there is a relative period of calm in the early 1990'. Monetary crises like Black Wednesday are not going to be visible using a dataset that does not contain any foreign exchange (FX) data because, despite causing a lot of pain, especially in the U.K, its long lasting influence on the global financial system remained limited. Then there is a sharp increase of A1 and A2 accompanied by a sudden characteristic drop of A3 just before and during the terrible blow of the 1997 Asian Crisis (Crisis 7). The 2000 NASDAQ crash is not very visible on those profiles, even though the NASDAQ is part of Dataset 1. Maybe this is due to the fact that it remained primarily an "American crisis" that is not going to be very apparent in a dataset that focuses primarily on contagion between international markets. The bullish market period of the early 2000's is characterized by mostly flat profiles of A1, A2 and A3 indicating a globally stable market structure. Before the Lehman Brothers collapse of 2008, we see again that pattern of an increase in A1 and A2 accompanied by a drop of A3.

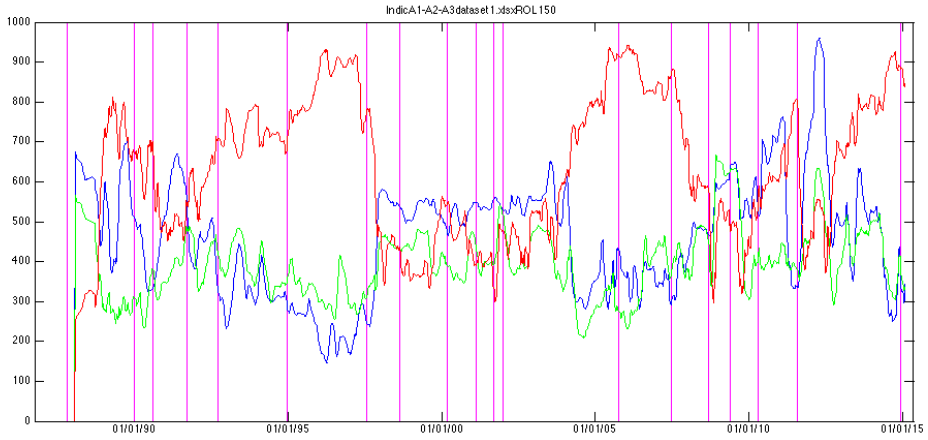

Figure 4: A1 blue, A2 green, A3 red

- For Dataset 2, which is Dataset 1 augmented with commodities and safe, cash equivalent securities, we obtain the profiles below (Figure 5). Those profiles structurally resemble those obtained from Dataset 1 but they are much tamer, probably because of the presence of safe haven securities inside the dataset which provide a way for market agents to re-invest their money as they liquidate equity positions in the times leading up to and during a

financial crisis. Since Dataset 2 includes commodities, we observe a very noticeable buildup in A1 and A2 leading up to the December 2014 Russian crisis (Crisis 19). It is again accompanied by an ominous drop in A3. The increased correlation between commodity and energy securities, which are represented in the equity indices by the major U.S oil companies, in the times leading up to a financial crisis, creates a strong build-up of market instability which provides valuable beforehand information that a crisis is becoming more likely.

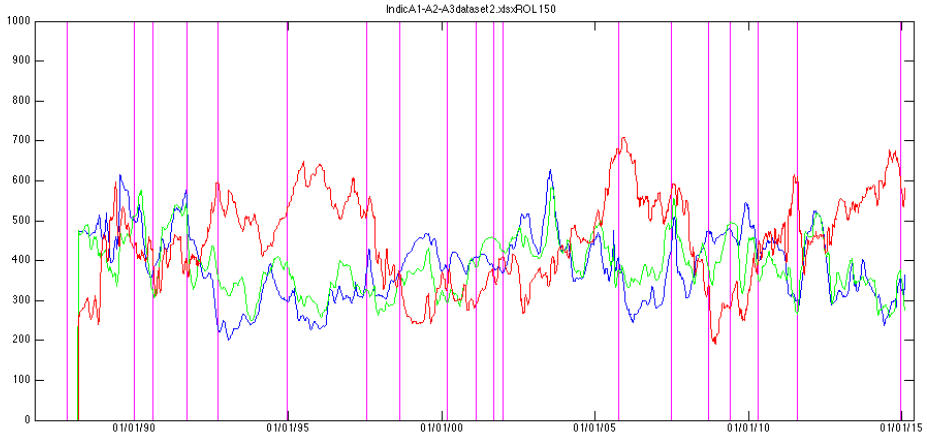

Figure 5: A1 blue, A2 green, A3 red

- For Dataset 3, which is the "American" dataset, we get the following profiles (Figure 6). Those profiles emphasize primarily, as anticipated, the events when the U.S market is overheating. The Savings and Loans crisis (Crisis 2) is anticipated a few months in advance by a sharp increase in A1 and A2. The indicators are mostly unresponsive during the Asian crisis of 1997 but the NASDAQ crash of March 2000 is this time accompanied by a spectacular spike of A1 and A2 accompanied by a depression in A3. This very good anticipation of the NASDAQ crash for this dataset which contains the sector components of the SP500 could be explained in part by the fact that the information technology sector component of the SP500 is correlated at over 90% with the NASDAQ. In the wake of the dot-com bubble, the same pattern reproduces itself around the 9-11 attacks. The same phenomenon happens again in the times leading up to the Sub-prime Crisis of August 2007 (although the drop in A3 is less noticeable) and on an even grander scale around the time of the Lehman Brothers collapse. The bankruptcy of General Motors on June 1st 2009 and the U.S sovereign credit degradation of

August 5th 2011, when Standard & Poor's reduced the country's rating from AAA (outstanding) to AA+ (excellent), are also anticipated by a spike in A1 and A2 while the behavior of A3 is less easy to interpret in those instances.

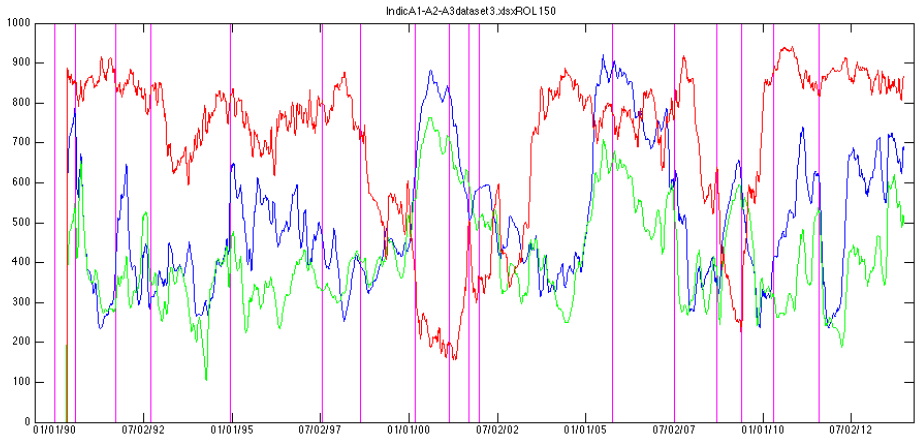

Figure 6: A1 blue, A2 green, A3 red

- For Dataset 4, which is the "European" dataset, we get the following profiles (Figure 7).

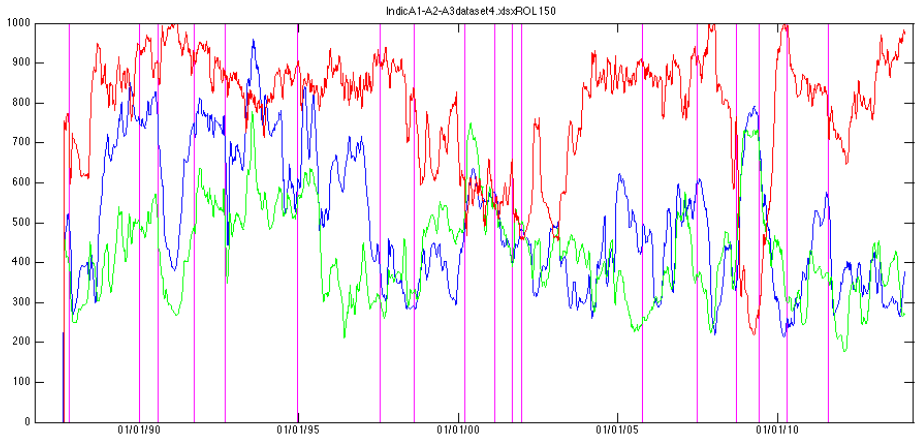

Figure 7: A1 blue, A2 green, A3 red

Since the U.S financial market still leads the world, the global structure of the profiles of A1, A2 and A3 is somewhat similar to the structure of the profiles

we had obtained for Dataset 1 and Dataset 3. There are however some very interesting specificities, which are characteristic of the European nature of Dataset 4. Events like the S&L crisis, the NASDAQ bubble burst and even the Sub-prime Crisis of 2007 that preceded the Lehman Brothers collapse of 2008 are much less visible while the European sovereign debt crisis of April 23rd 2010 (Crisis 17) is spectacularly well anticipated with a huge spike in A1 and A2 accompanied by the ominous drop in A3. The U.S sovereign credit degradation of 2011 is also very well anticipated. That could be explained by the fact that the sovereign credit degradation of several leading European countries (France was degraded as well from AAA to AA1 by Moody's on November 19th 2012) was also being discussed by the media and anticipated by the financial markets.

- For Dataset 5, the *flight to quality* dataset which exploits the increasing correlation between equity and bonds in the times leading up to a financial crisis, we obtain the A1, A2 and A3 profiles below (Figure 8). In a way they seem even tamer and noisier than those of Dataset 2 which included, besides the commodities, some safe haven securities adding elements of *flight to quality* to its design as well. In Dataset 5, the profiles of the indicators of A-series present few remarkable features, besides the obvious ones that all the others possess, like the spike in A1, A2 and the drop in A3 around the failure of Lehman Brothers in 2008. Unfortunately it seems that the inclusion of high quality sovereign and corporate bonds into the equity mix produced a dataset that is a little too resistant to most financial crises and is therefore, for the indicators of A-series at least, of limited interest as a way to anticipate crisis events.

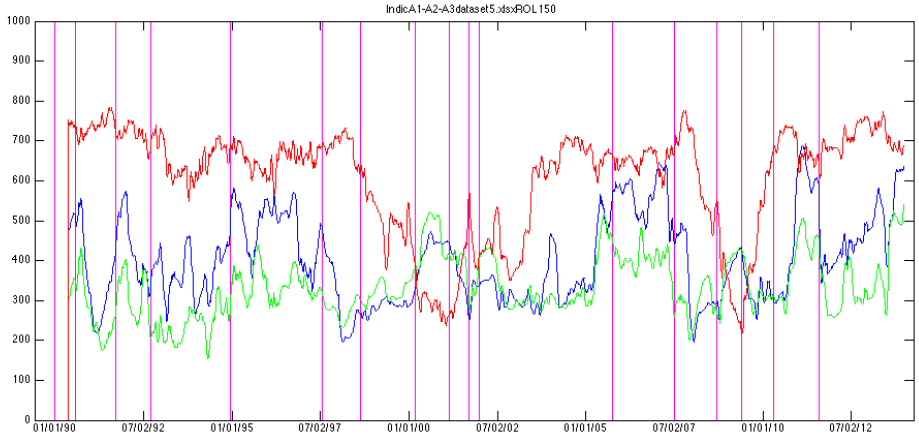

Figure 8: A1 blue, A2 green, A3 red

- Dataset 6, the largest dataset containing 226 individual components of the SP500 index, produces the following high quality profiles when used with the indicators of the A-series (Figure 9). Black Monday is outside of the span of Dataset 6 and the S&L crisis is surprisingly not visible (maybe it is because the affected companies dropped out of the index which, like all composite stock indices, shows some survivorship bias). The buildup to the 2000 NASDAQ crash is spectacular and characterized by the usual climb of A1 and A2 and fall of A3 as the correlations and volatility simmer inside the market and the spectrum of the covariance matrix is shifting to the right, toward the larger eigenvalues, away from $\Theta 1$ and $\Theta 2$ and toward $\Theta 3$. This pattern started well in advance of the actual crisis event, which we chose to place on March 10th 2000 when the NASDAQ started its sharp and sustained fall. The indicators did provide a valuable early warning in that instance. Then we observe the period of bullish market in the early 2000's and again a slow buildup of correlations and volatility inside the market characterized by an increase in A1 and A2 (but not a drop in A3 that seems to only accompany truly catastrophic events) culminating during the Subprime Crisis of August 2007 which sets into motion the pattern of A1 and A2 spiking while A3 plummets leading up to the collapse of Lehman Brothers. Then there is some recovery in the market before the 2011 U.S sovereign credit rating degradation, which is anticipated by an increase in A1 and A2. Finally the Russian financial crisis of December 2014, which hit very hard some of the largest firms inside the SP500 (energy companies), because of the fall in the price of crude and gas, is anticipated by an increase in A1 and A2 but we don't observe much on A3 at the same time.

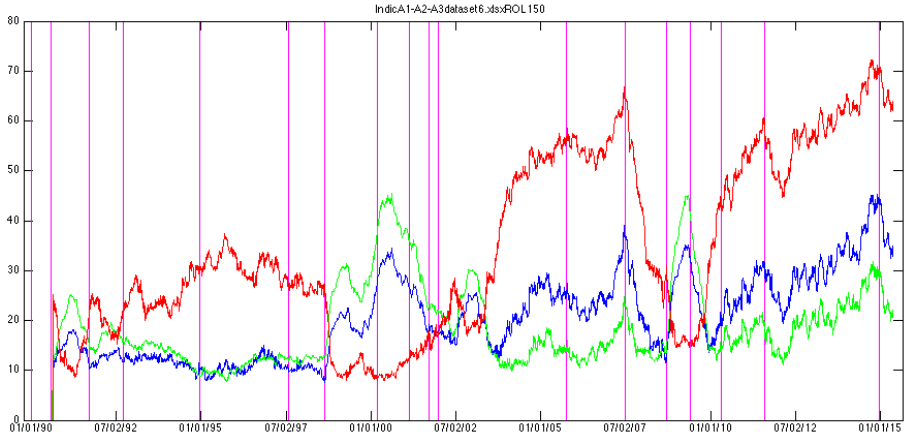

Figure 9: A1 blue, A2 green, A3 red

- The A-series profiles for Dataset 7 are represented below (Figure 10). This dataset contains international indices from emerging economies converted from the local currency into U.S dollars. The usual features that dominated all the other A-series profiles for all the other datasets look a bit diluted in the case of Dataset 7: the collapse of Lehman Brothers is one unremarkable bump among dozens of others and the NASDAQ crash is not visible, for example. The Delphi bankruptcy of late 2005 ("Red October") did trigger an economic crisis in many emerging countries due to the closure or expected closure of many of the overseas factories of the American automotive parts giant and this event is indeed anticipated by a rise in A1 and A2, but it is difficult to differentiate it from the many false positives. The Argentine sovereign default of late 2001 is surprisingly not visible although many South American indices (and the MERVAL itself) are included in Dataset 7. The Russian crisis of 2014 is however much more visible and better anticipated now than with the previous datasets and we observe a large spike in indicators A1 and A2 accompanied by a noticeable drop in indicator A3.

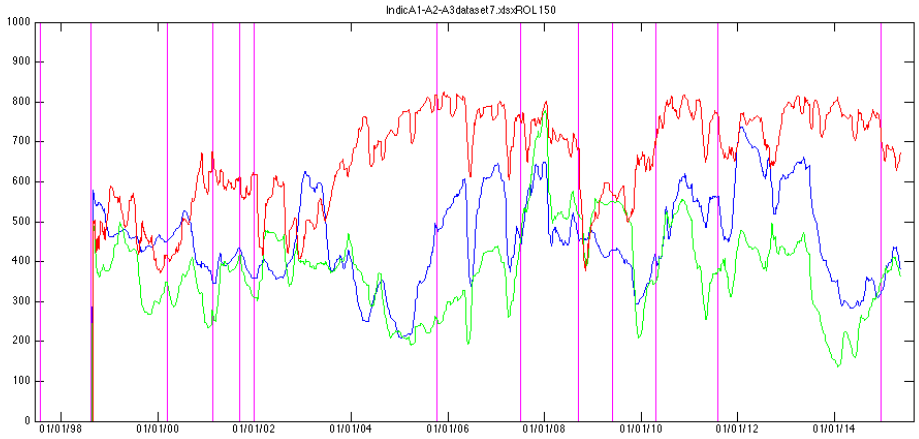

Figure 10: A1 blue, A2 green, A3 red

We now switch our attention to the indicators of the B-series. On all the profiles below, the crises of Table 1 are again represented as vertical purple lines. The spectral radius of the covariance matrix (mixed volatility and correlation signal), Indicator B1, is in green. The trace of the covariance matrix (volatility signal), Indicator B2, is in red. The spectral radius of the correlation matrix (correlation signal), Indicator B3, is in blue and is not represented on the same scale as the others for better readability (we multiplied it by 20). For Dataset 6, the correlation signal for the assets weighted by the market capitalization and volume traded, as

defined in the previous section, is also going to be studied. We first remark that all the profiles of the B-series feature many false positives, as those of the A-series and the spikes are located, with specificities depending on the dataset used, in the vicinity of the crisis events of Table 1 for B1 and B2. The structure of the B3 profiles is usually a little harder to interpret but it still holds valuable information.

For most datasets and most crises, B1 and B2 produce very similar profiles. When the profiles of B1 and B2 get closer to one another (ie. for the covariance matrix, the trace becomes close to the spectral radius) it means that correlations are increasing inside the financial market because one eigenvector's direction (the direction of the spectral radius) is becoming dominant over all the other ones. We do not however generally observe on the graphs that B3 is increasing when B1 and B2 are getting closer and that is due to the fact that B3 is only taking correlations into account while B1 is a mixed signal of volatility and correlation. The correlation component of B1 is at each date an average correlation weighted by the volatility of the assets constituting the dataset. In order to compare the relative position of B1 and B2 to the behavior of B3, we could have weighted the coefficients of the correlation matrix by the volatility of the assets. However doing this would have defeated the goal to study the correlations alone. In other words, when the relative position of B1 and B2 is not compatible with the behavior of B3, then it means that the assets are becoming correlated or uncorrelated depending on their volatility. For example when B1 and B2 are getting closer (correlations are increasing) but B3 is not increasing in a clear manner, it means that the high volatility stocks are becoming uncorrelated while the low volatility stocks are becoming correlated.

- For Dataset 1, we obtain the following results (Figure 11). This international equity dataset produces profiles of B1 and B2 which are very similar, with spikes in the vicinity of the major international crises like the NASDAQ crash and the failure of Lehman Brothers. The relaxation in both volatility and correlations after a crisis event is also much more noticeable than with the profiles based on the Hellinger distance, especially after the NASDAQ crash and the onset of the bullish market period. The B1 and B2 signals are almost always co-monotonic, it is what we expected and it is coherent with the work of Sandoval Junior and De Paula Franca (2012) who proved, using data which was very different from the data that we used, that high volatility in financial markets usually accompany a high level of correlations.

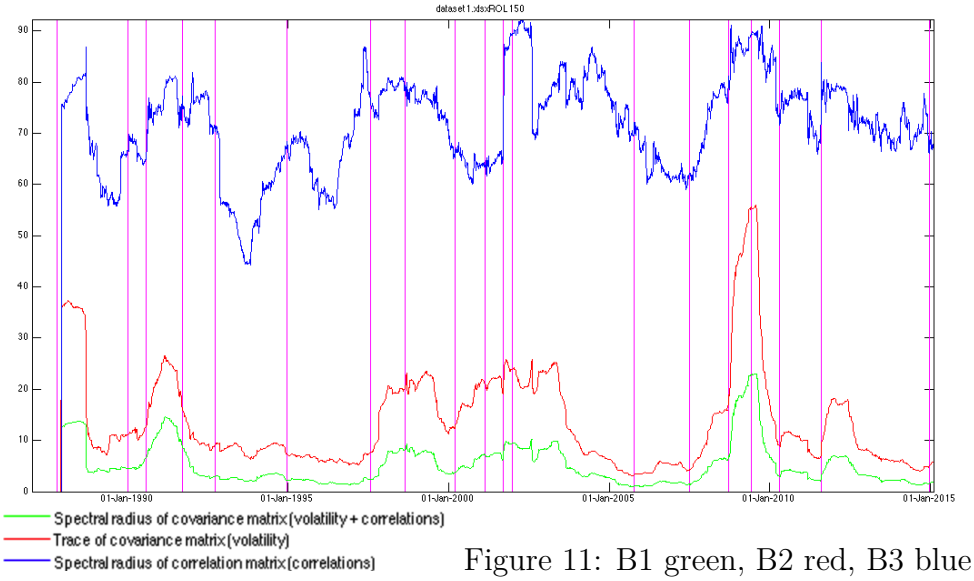

Figure 11: B1 green, B2 red, B3 blue (20x)

- For Dataset 2, we obtain the following results (Figure 12). The profiles are very similar to those of Dataset 1, with less prominent features because of the inclusion of safe haven securities in the dataset. The elevation in both volatility and correlations is a little more noticeable around the Russian sovereign crisis of 1998, which may result from the inclusion of energy related commodities in this dataset. It also highlights the typically increased correlations between energy (like oil companies stocks) and commodity securities in the times leading up to a financial crisis.

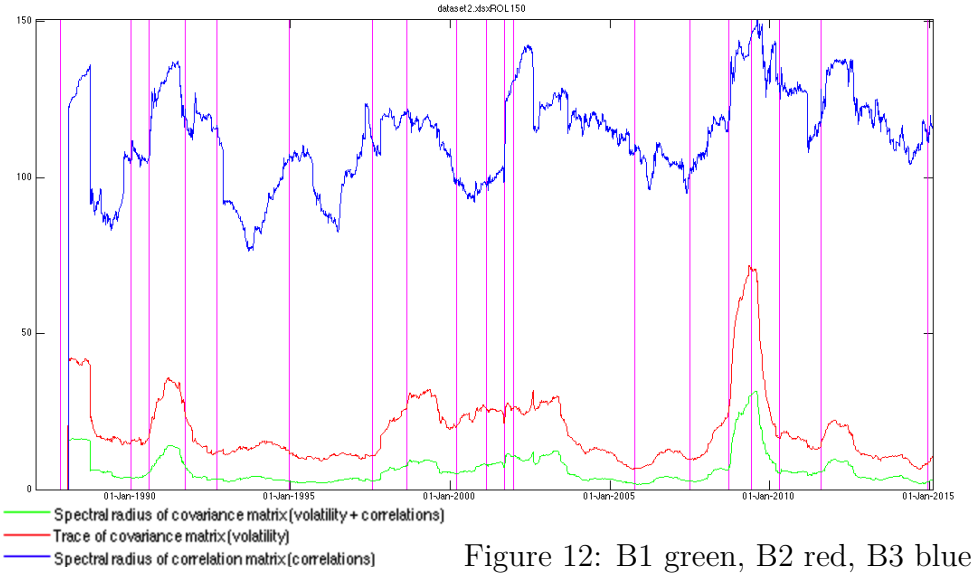

Figure 12: B1 green, B2 red, B3 blue (20x)

- For Dataset 3, we obtain the following results (Figure 13). The profiles of B1 and B2 highlight the American nature of Dataset 3. There are especially visible features for the NASDAQ crisis, the 2008 global financial crisis and the U.S sovereign credit degradation. The profile of B3 is again more difficult to interpret. In particular there is an apparent massive drop in correlations following the NASDAQ crisis that is not accompanied by a similar drop in volatility.

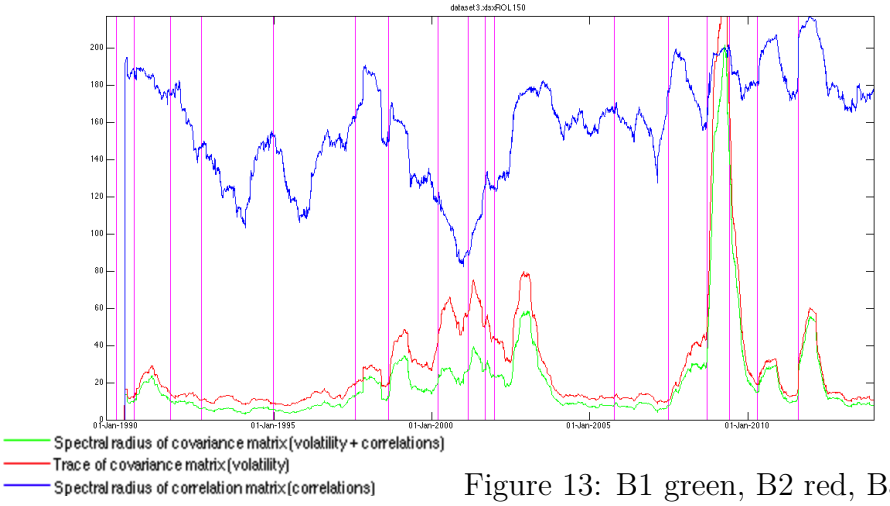

Figure 13: B1 green, B2 red, B3 blue (20x)

- For Dataset 4, we obtain the following results (Figure 14). It is the European counterpart of Dataset 3 and produces better detection of crises that are mostly or originally European in nature like the Eurozone sovereign debt crisis.

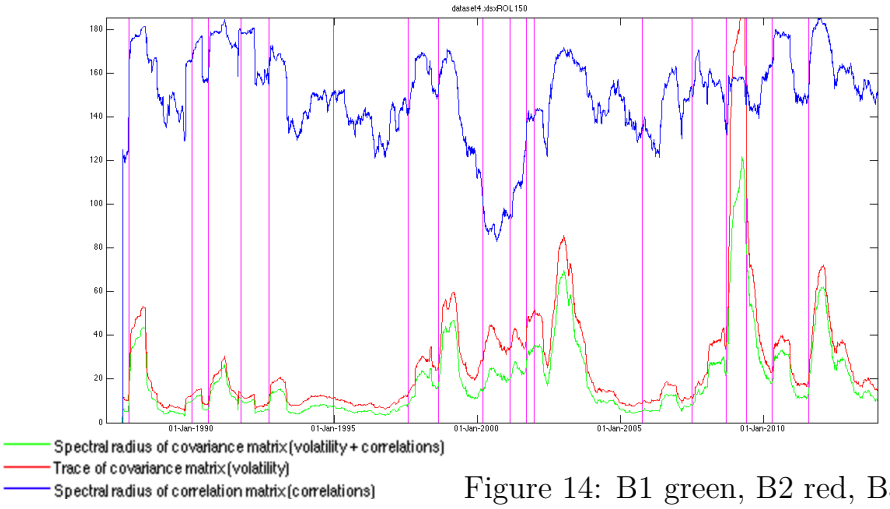

Figure 14: B1 green, B2 red, B3 blue (20x)

- For Dataset 5, we obtain the following results (Figure 15). The inclusion of high quality bonds to model the *flight to quality* effect in the times leading up to a financial crisis has the effect, like for the A-series indicators, to produce very tame profiles of B1 and B2. Only the truly momentous events like the NASDAQ crash and the 2008 crisis are visible but all the other events are difficult to see, even the Asian crisis of 1997 which is surprising. The volatility signal B3 is still very noisy but some structure is starting to emerge with big spikes in the vicinity of known crises and large drops afterwards when the market is entering a post-crisis relaxation phase.

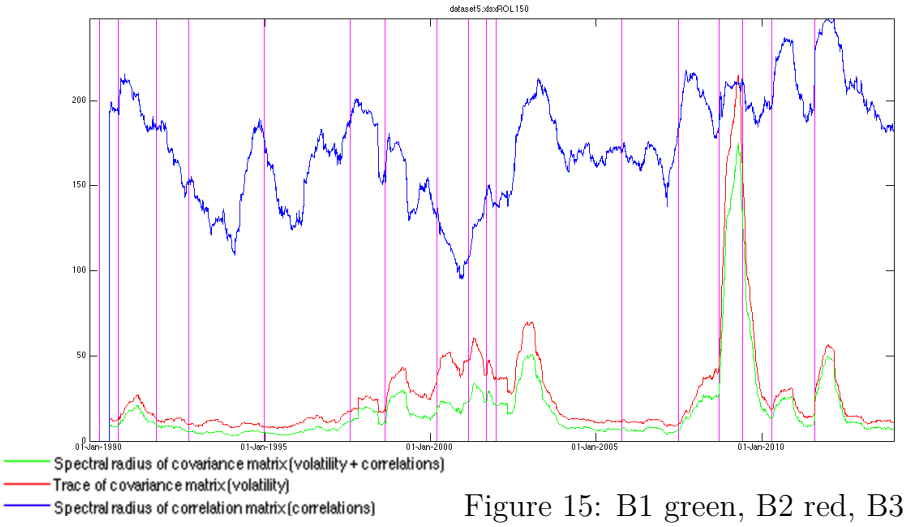

Figure 15: B1 green, B2 red, B3 blue (20x)

- For Dataset 6, we obtain the following results (Figure 16,17,18,19).

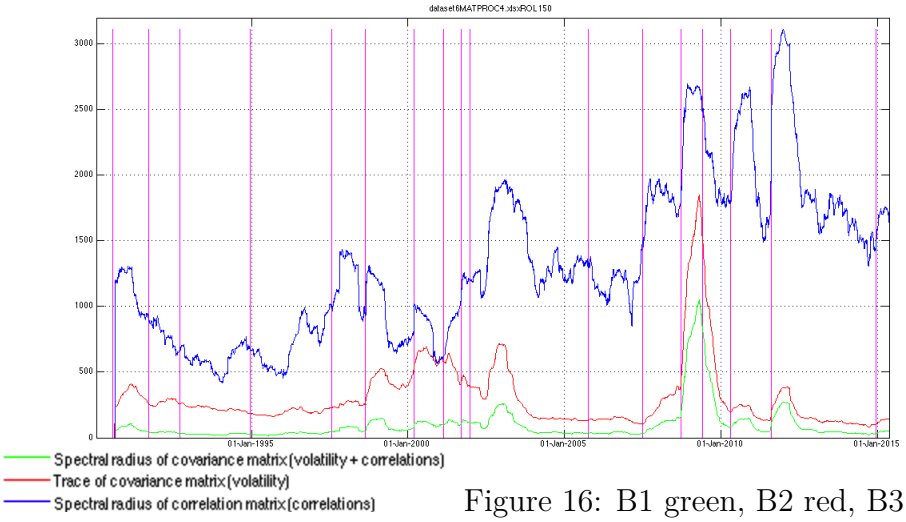

Figure 16: B1 green, B2 red, B3 blue (20x)

The profiles for B1 and B2 are globally similar to those that we obtained for Dataset 1 and Dataset 3. However, the buildup of leverage during the sub-prime crisis is much more clearly visible and this time the correlation signal B3 in blue is much more interesting and contains a lot of usable information about the detection and anticipation of many of the financial crises of Table 1. Indeed, this increased precision of the results that we obtain is not surprising because Dataset 6 is constituted of a large number of individual stocks instead of indices and there is no averaging effect on the correlations.

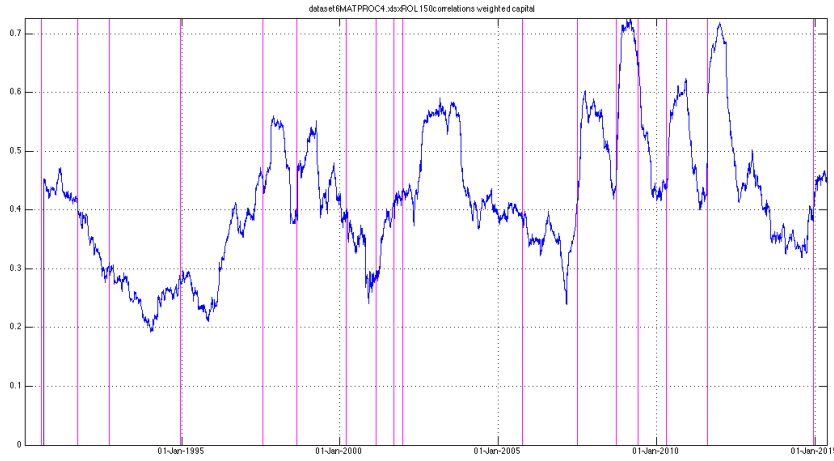

Figure 17
B3A : correlation signal B3 weighted by the capital of the companies corresponding to the stocks. We see new patterns emerge and a possible increase of the power of prediction for this indicator due to the weighting.

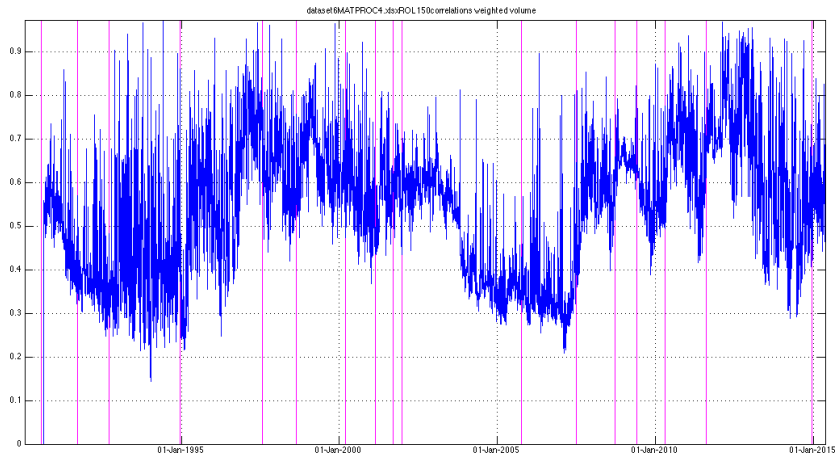

Figure 18
B3B : correlation signal B3 weighted by the volume traded. New patterns emerge and the power of this indicator to preempt rather than merely confirm the crises, as it was likely the case for most of the financial crisis indicators we have studied until now, appears to have increased.

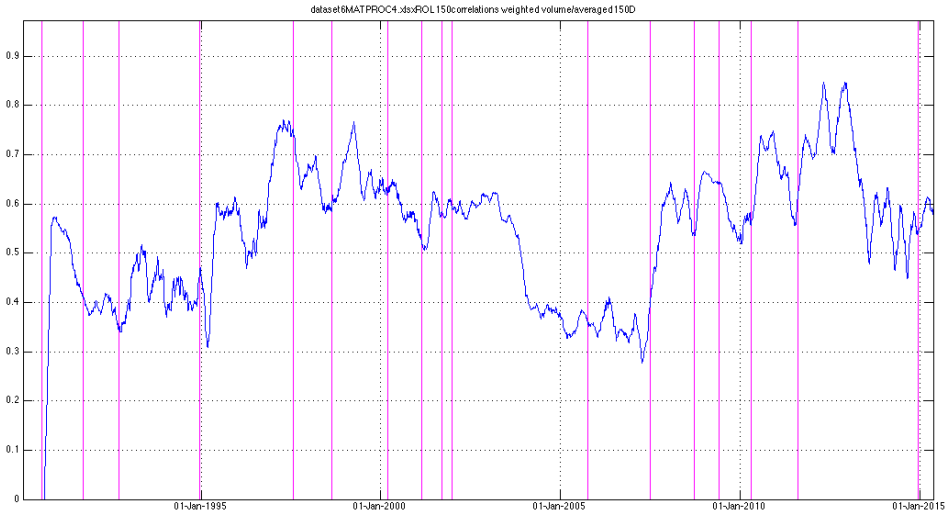

Figure 19
B3C : averaged version of B3B for better readability and noise reduction.

- For Dataset 7, we obtain the following results (Figure 20).

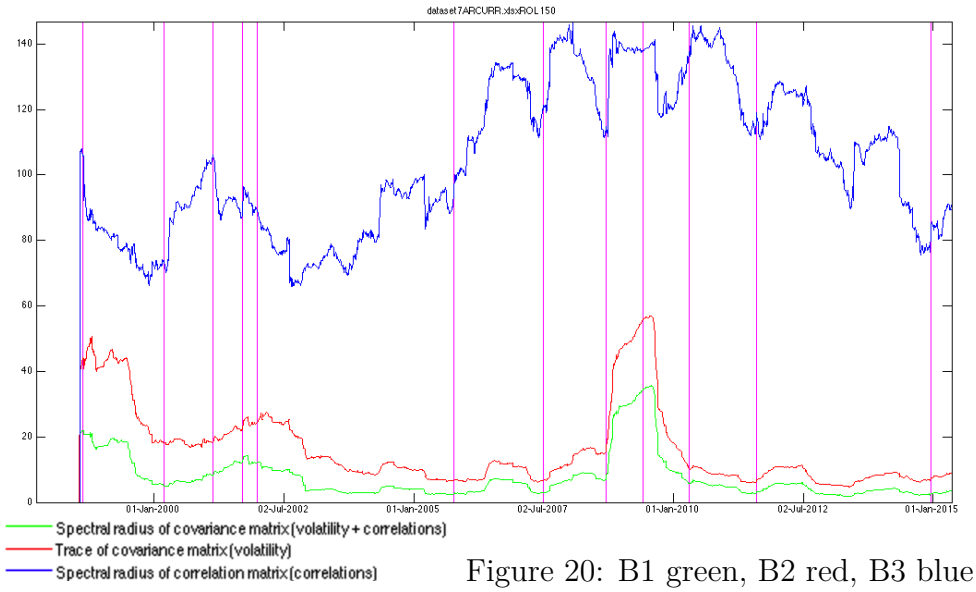

Figure 20: B1 green, B2 red, B3 blue (20x)

The profiles do not seem to possess much useful signal and few truly noticeable features appear besides the obvious ones for B1 and B2 as well as for B3. The Asian crisis of 1997 (located at the very edge of the dataset) seems to have been much more visible when using Dataset 7 than when using the other datasets. This is without any doubt due to the fact that Dataset 7 contains information about

emerging markets. Unfortunately in this study, we can only see the aftermath of the Asian crisis.

5 Predictive Power

In this section, we study in details the predictive power of indicators B3B and B3C, which are those that are based on the correlations weighted by daily traded volume of the assets. We decided to concentrate this study on those two indicators for simplicity. It is however clear that the same work could have been done using any of the nine indicators. We use Dataset 6, which contains the components of the SP500 index. The choice of this particular dataset is justified by the fact that it is the largest and most detailed of all the datasets we possess and therefore it is the one for which we expect to obtain the best quantitative results. We rely on the Maximum Draw Down (MDD) at horizon $H = 100$ days, which is commonly used by practitioners in the financial industry. The reference asset price A for which this quantity is computed at each date is the SP500 index.

$$MDD_H(t) = max_{t \leq x \leq y \leq t+H} \left(1 - \frac{A(y)}{A(x)}\right) \quad (22)$$

5.1 Historical Approach

We work with the scatter plots $[B3B(t), MDD_H(t)]$ and $[B3C(t), MDD_H(t)]$ for all dates t covering the span of Dataset 6. We notice that the structure of each of those two scatter plots is dominated by a double threshold. We are going to exploit that fact in order to build a trigger for the indicators. At a given time t, when the value of B3B (resp. B3C) is between those twin thresholds, we say that we are in the *danger zone*, which is where the probability of a crisis happening within 100 days is the highest. This makes also a lot of sense from a theoretical point of view. As a matter of fact, when the weighted correlations are low, then the probability of a crisis happening (i.e. experiencing a very high MDD over the next 100 days) is low, but when it is extremely high that means that we are already right in the middle of a crisis and the expected MDD at 100 days is low as well because the market would be likely out of the crisis and already in full recovery.

A crisis from Table 1 happening at time t_0 is (ex-post) considered to be predicted by B3B (resp. B3C) if at least 60% of the points $[B3B(t), MDD_H(t)]$ (resp. $[B3C(t), MDD_H(t)]$) such that $t \in [t_0 - 100, t_0]$ are in the danger zone of the indicator. The false positive ratio is defined as the number of points inside the danger zone that belong to one of the crisis of Table 1 over the total number of points

inside the danger zone.

To define the danger zone, we separate Dataset 6 into two periods: one in-sample calibration period between January 17th 1990 and December 31st 1999 and one out-of-sample forecast period where the power of prediction of B3B and B3C is going to be put to the test. For both indicators, the scatter plot restricted to the calibration period and the scatter plot covering the whole sample are represented below in Figure 21 and Figure 22. Both for B3B and B3C, the two scatter plots have roughly the same global structure. That fact is quite reassuring with regards to the validity of the approach that we have chosen. Indeed it means that whether we are considering the in-sample calibration period of the whole span of Dataset 6, the behavior of the indicators is the same and the danger zone is stable. This stationarity of the danger zone is crucial if we intend to make useful predictions in the out-of-sample forecast period.

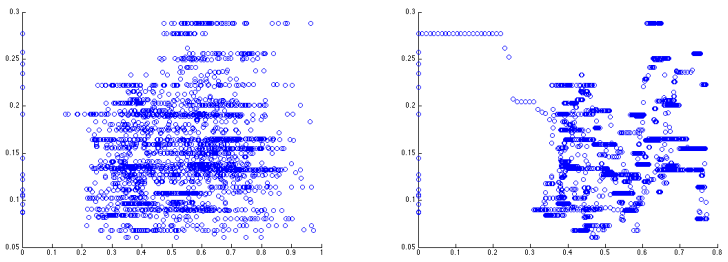

Figure 21: Calibration period / left: B3B, right: B3C

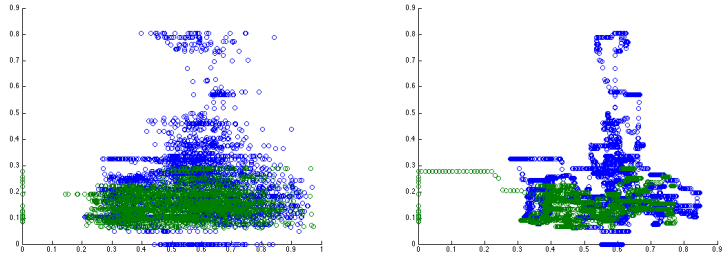

Figure 22: Calibration period: green, Whole sample: blue ; left: B3B, right: B3C

Using Figure 21, we set empirically the optimal values for the low and high thresholds that define the danger zones of the indicators. We obtained the intervals [0.41,0.8] for B3B and [0.50,0.70] for B3C. Using those values, we are now able to count for each crisis of Table 1 inside the out-of-sample forecast period the number of dates in a 100 days window preceding each crisis for which the value of

B3B (resp. B3C) was inside the danger zone as well as the global proportion of false positives.

We obtain the following results (Table 2) in which the crises inside the calibration period have been put in italic (Crisis 1 and Crisis 2 are located before the start of Dataset 6).

	B3B	B3C
Crisis 1	NA	NA
Crisis 2	NA	NA
Crisis 3	*0*	*0*
Crisis 4	*51*	*18*
Crisis 5	*22*	*0*
Crisis 6	*41*	*0*
Crisis 7	*74*	*0*
Crisis 8	*98*	*100*
Crisis 9	93	100
Crisis 10	94	100
Crisis 11	98	100
Crisis 12	100	100
Crisis 13	13	0
Crisis 14	15	0
Crisis 15	98	100
Crisis 16	99	100
Crisis 17	97	100
Crisis 18	96	100
Crisis 19	90	78
False Positive (%)	73.38	71.30

Table 2: Historical Crisis Prediction

We observe that using the indicators B3B and B3C properly calibrated would have enabled us to predict and anticipate almost all the crises of Table 1 inside the out-of-sample forecast period. Indeed there are very few false negatives. Only the Bankruptcy of Delphi (Crisis 13) and the Sub-prime Crisis (Crisis 14) are not properly forecasted. Those two events were however difficult to predict. Indeed, the effects of the Bankruptcy of Delphi were not instantaneous on the U.S economy in general and on the SP500 in particular and the Sub-prime Crisis was a months long process starting in August 2007 and on which we had to pin a date. The proportion of false positives, while still relatively high, is unlikely to represent an insurmountable obstacle for a practitioner as the information at a given date

t that there is around a 30% chance of a crisis happening (and a 70% chance of nothing happening) in the next 100 days is already an extremely valuable piece of information and a much more precise one than what we had expected initially. Indeed, in the introduction we where talking about a 10% chance of a crisis happening being already a very valuable piece of information from an investor's point of view.

5.2 Algorithmic Trading Approach

In this section we do not consider the historical financial crisis events of Table 1 anymore. Instead, we focus on the MDD at each date, computed ex-post using the market data for the 100 days horizon. A financial crisis is defined here as a market event where the MDD at 100 days exceeds a given threshold. We consider MDD thresholds from 10% for a mild crisis to 25 % for a serious downturn. This approach frees us of the sometimes arbitrary choice of a date for the financial crises of Table 1 and the signal given by the various indicators is now going to be made usable as the decision-making tool underlying an algorithmic trading strategy. In this study to showcase the predictive power of the indicators that we have built, we choose to consider Indicator B3B, but the same work could have be undertaken using any of the nine indicators of either the A-series or B-series. The complete construction of an optimal trading strategy based on those indicators will be the topic of an upcoming paper and in this section we merely intend to demonstrate that the red flags produced by B3B generate few false negatives, especially for higher MDD thresholds, and an acceptable proportion of false positives. The binary signal produced by one of the indicators (i.e. "red flag" & "no red flag") can afterwards interact with a set of predetermined rules to give at each date a "*buy*", "*sell*" or "*stay*" recommendation.

We separate Dataset 6 into two periods again: one in-sample calibration period and one out-of-sample period where the forecasting power of the financial crisis indicators that we have built is going to be tested. The period spanning from January 17th 1990 to December 29th 2000 is chosen this time for the calibration of the indicators. It is slightly larger than in the previous subsection and encompasses the 2000 NASDAQ crisis in order to boost the predictive power of the indicator by including a large market event in its calibration period (especially since the 1987 crash lies outside Dataset 6). We empirically chose the optimal interval [0.47,0.75] for the danger zone using Figure 23 below.

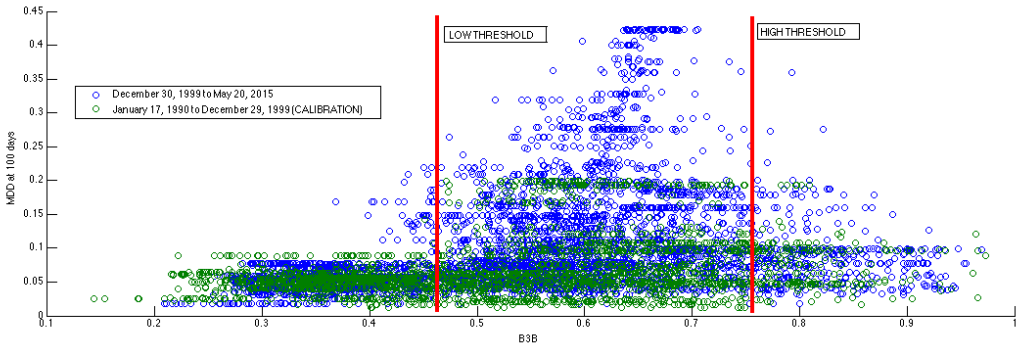

Figure 23 (Optimal danger zone for B3B / Green: calibration period, Blue: forecast period)

We kept the rule that states that a red flag is given at a date t_0 if at least 60% of the points $[B3B(t), MDD_H(t)]$ such that $t \in [t_0 - 100, t_0]$ are in the danger zone of the indicator and we obtain the following results (Table 3) for various thresholds of MDD at the horizon 100 days.

MDD Threshold	10%	15 %	20 %	25 %
Crises	1281	794	400	268
Predicted crises	1201	751	400	268
False positives	1083	1533	1884	2016
False negatives	80	43	0	0

(Table 3: Crisis Prediction)

The forecast period is constituted of 3770 trading days. For a MDD threshold of 10% there are 1281 crisis events in the forecast period and Indicator B3B predicts 1201 of them while missing 80 and giving 1083 false positives. When the MDD threshold is put at 25%, there are only 268 crisis events in the forecast period and Indicator B3B predicts all of them while giving 2016 false positives. The fact that Indicator B3B does not miss any crisis event characterized by the larger MDD threshold ($\geq 15\%$) is reassuring from a financial stability point of view: an investor using a trading strategy based on the indicator that we have built would not have been caught off guard by a serious market downturn. Of course there are a lot of false positives, especially for the larger crises and there is room for improvement but, as we said in the introduction, the information that there is only a 10% chance of a serious market event to happen within the next 100 days has tremendous value for market agents. False negatives can spell disaster while false positives might merely reduce profit and in that sense Indicator B3B is already very useful for a traditional risk averse investor or a regulator. However, if profit

maximization is the most important benchmark for a less risk averse investor, then we could say that Indicator B3B performs best for the medium intensity crises (15 % to 20 % MDD threshold) because it is there that the proportion of false positives remains smaller while the risk of a false negative is still acceptable.

The predictive power of the financial crisis indicators developed in this study can also be demonstrated by considering European put options used as a protection tool against market downturns. The use of listed options for portfolio structuring had indeed become the norm among portfolio managers and many techniques exist to use those derivatives in order to decrease risk or boost performance, as explained in Bookstaber (1985). Bookstaber and Clarke (1981) also explained how using different kinds of put and call options in a portfolio helps set the necessary balance between risk and maximization of return.

Our purpose in this study is not to detail an elaborate structured portfolio but rather to demonstrate the predictive power of our financial crisis indicators, therefore we will limit ourselves to a basic protective-put strategy where the purchase and sale of European put options are merely used as a risk and volatility decreasing techniques. The performance of the various test portfolios, while still evidently an important benchmark, is not necessarily optimized like it would have been by, for example, considering more elaborate strategies, like a covered call instead of a protective put.

We work again with Indicator B3B and Dataset 6 because it is experimentally the setup that works the best and produces the most useful results, but the same study could have been conducted with any of our financial crisis indicators of either the A-series or the B-series. The basic idea is to compare the performances of three demonstration portfolios, which are updated monthly:

- A static *buy and hold* portfolio (BAH) constituted only of shares of an Exchange Traded Fund (ETF) replicating the SP500 (SPX).
- A dynamic passive protective-put portfolio (PPP) constituted of a mix of equal proportions of SPX shares and SPX put options purchased every month as a protection.
- A dynamic active protective-put portfolio (PPA) constituted either of a mix of equal proportions of SPX shares and SPX put options, or of SPX shares only, depending on the risk signal generated by indicator B3B. In this portfolio, the put options are only purchased as a protection when our financial crisis indicator forecasts a higher risk of a financial crisis happening withing a given time horizon. In this study, the time horizon for the predictive power

of the financial crisis indicators is 100 days, corresponding to the 100 days horizon of the MDD that we consider and which was used to experimentally obtain the danger zone of the indicator, as we have detailed previously.

The decisions dates are chosen every month as the third Friday of the month between January 2000 and May 2015. Indeed, the third Friday of every month is the day that put options with a maturity of one month or more traditionally reach maturity. For accurate option quotes, we use a database of real historical option prices for the SPX [4].

The process of decision on whether or not to buy a protective put option in PPA is the following: at a given monthly decision date t_0, we count the number N_{t_0} of times when indicator B3B was inside its danger zone, as defined previously, in the 100 days preceding t_0.

The choice of an appropriate threshold $\mathscr{T}$ above which the value of N_{t_0} triggers the purchase of the put option is crucial. If $\mathscr{T}$ is too high, we will not buy the protection at dates when it would have been prudent, but on the other hand if $\mathscr{T}$ is too low, we will buy many very expensive put options at dates when the risk of a crisis was relatively low according to our indicator, thus destroying the anticipated performance gain of PPA with respect to PPP and BAH.

After careful considerations, we choose $\mathscr{T} = 80$. Such a value provides a good balance between the need to maximize the performance of PPA and the need to keep its risk withing reasonable bounds.

At t_0, if $N_{t_0} \geq 80$ we interpret this signal as an indication of a heightened probability of a crisis happening in the near future, thus triggering the purchase of a put option for protection. On the other hand, if $N_{t_0} < 80$, then we interpret this as a reassuring signal indicating that the probability of a crisis happening in the near future is relatively low and thus that the money needed to buy a put option for protection can be saved for increased performance of the portfolio.

The investors considered are *price takers*. Unlike a market maker, they have to accept the prices that the market is offering them. Therefore, at a given monthly decision date, any put option is bought at its *last ask price* and any put option is sold at its *last bid price*, as provided by our database of real historical SPX option quotes. The price of the underlying (the SPX shares) is always taken as the last price of the day.

[4] The date was purchased from the website *historicaloptiondata.com*

More precisely, once a strike S and a maturity M for the protective put option has been chosen, and we will discuss about that below, the execution of our three test strategies will be as follows:

- The investor holding BAH starts with a given number of SPX shares (normalized at 1 share in our computations) and holds on to it for the duration of the experience, which spans 185 months between January 2000 and May 2015.

- The investor who holds PPP starts with a given number of SPX shares and purchases every month an equal number of put options (normalized at 1 in our study), while selling the put option already present in the portfolio. All the purchased options are kept only for one month and then they are sold again to help cover the cost of the next option purchase. Therefore, every month, the investor who holds PPP buys a put option of strike S and maturity M and sell the option purchased the month before, which is also of strike S and maturity M.

  We do not include a cash allocation in our portfolios in order to boost performance and in order to be always entirely invested in the market. Besides, as explained in Harper (2003), the inclusion of cash in a portfolio is generally counterproductive and, regardless of performance consideration, a riskless security like U.S bonds is usually a better choice than plain cash anyway. Since there is no cash in our study, the SPX shares, which are very liquid, are used as cash-equivalent to purchase the options and the proceedings of the option sales is immediately converted into SPX shares as well. Disregarding the small technical detail of having to consider fractional SPX shares in the computations, we rebalance PPP at each decision date such that the proportions of SPX shares and put options remain equal (i.e there is always one unit of put option covering one unit of share).

- The investor who holds the dynamic active portfolio PPA adopts a strategy with rolling put options to protect the SPX shares, similar in nature the strategy governing the PPP portfolio, but with one fundamental difference: at a given decision date, the decision to buy, or not to buy, the protective put option is made according to the signal produced by indicator B3B. If at a given decision date the financial crisis indicator recommends not to buy the protective put option, then the investor sells the option purchased the month before, if it is present, does not buy any other option and reverts to a portfolio entirely made of SPX shares, like in the case of BAH.

After the choice of the threshold $\mathscr{T}$ that establishes the desired balance between performance and safety in the active strategy, the choice of the strike S and the maturity M of the rolling put options is the next important step that will determine whether the active strategy PPA is a success or not.

The maturity M has to be long enough so that when the put option is sold again after one month its value has not depreciated too much, but on the other hand, in order for our study to have meaning, we should not take the maturity so far away in the future that it goes beyond the horizon of prediction of the financial crisis indicator, which is fixed at 100 trading days and which represents, assuming 252 trading days per year, a little under five months. While taking this into consideration, we chose the maturity for the rolling put option equal to four months: $M = 4\ months$

The strike S is chosen at 100% of the price of the underlying SPX share (put option *at-the-money*). Our goal is to beat, both in terms of performance maximization and risk minimization, the static SPX portfolio BAH with our active, financial crisis indicator controlled, portfolio PPA. Therefore, it is best not to settle for a loss mitigation approach by choosing a strike $S < 100$. The risk has also to be kept between reasonable bounds, but choosing to use more expensive at-the-money options did not in practice increase the volatility of the portfolios, while it did maximize overall performance.

For every decision date $t \in [\![1, 185]\!]$, the riskless asset TB is chosen as the one month U.S Treasury Bond (US0001M). Considering an asset A, which can represent either BAH, PPP or PPA, we define the following benchmarks, Sharpe ratio and Calmar ratio, that we will use to compare the strategies to one another and demonstrate the predictive power of Indicator B3B. We also recall the Maximum Draw Down (MDD), that we have already defined in Equation (22). Here we consider MDD(A), which is the maximum draw down computed over the entire period of study and not anymore at a given time horizon.

- To compute the yearly Sharpe ratio, we proceed in the following manner. The Sharpe ratio measures the quotient of the excess performance with respect to a riskless asset over the volatility. To achieve the desired highest Sharpe possible, a strategy has to maximize return while at the same time minimize volatility, which represents risk.

  $$- \ \forall t \in [\![1, 185]\!] \ , \ ExcessReturn_A(t) = \frac{A(t)}{A(t-1)} - \frac{TB(t-1)}{12} - 1$$

- $Perf(A) = (\frac{A(185)}{A(1)})^{\frac{360}{5550}} - 1$ (Annualized performance, assuming 30 days per month and 185 months in our experience)

- $Vol(A) = stdev(ExcessReturn_A).\sqrt{12}$ (Annualized volatility)

$$Sharpe(A) = \frac{Perf(A) - mean(TB)}{Vol} \quad (23)$$

- We define the yearly Calmar ratio as the quotient of the performance by the maximum draw down (MDD).

$$Calmar(A) = \frac{Perf(A)}{MDD(A)} \quad (24)$$

In Figure 24, we draw the profiles of BAH, PPP and PPA as well the quantity $TR = \frac{PPA}{BAH}$, which represents the extra performance of the active strategy governing portfolio PPA with respect to the static portfolio BAH (the tracking error). The Performance, the Sharpe and the profile of TR are the main tools at our disposal to illustrate the benefit of using PPA instead of all the alternatives presented in this study and thus demonstrate the power of prediction of our financial crisis indicator B3B, and by extension the power of prediction of our original approach to financial crisis indicators as a whole.

We immediately notice that PPP is a complete failure. It has a negative Sharpe (anti performance with respect to the riskless asset) and while it does somewhat reduce volatility and MDD with respect to BAH, which is a good thing and which was expected given the very nature of the protective-put strategy, the complete collapse of its performance under the crippling cost of having to buy a new put option each and every month makes this strategy very unattractive. The cost of having to buy the protection every month is not to be underestimated. Indeed, as explained in Israelov and Nielsen (2015), the cost of buying the options in a protective-put setting is usually very high. It is also often much higher than it might seem, even during a calm market and low volatility period, unless the price and fundamental value of the underlying are properly taken into consideration.

The strategy PPA is a success, both in terms of maximization of the return and in terms of reduction of the risk. The performance of BAH was only 2.6% and is boosted to almost 6% in PPA, while the volatility goes down from 18% to 13% and the MDD goes down from almost 50% to 33%. These MDD values in particular show that the effects of the September 2008 financial crisis, with the failure of Lehman Brothers in particular, had been correctly anticipated by our

financial crisis indicator, allowing the strategy PPA to anticipate the fall by buying protective put options in advance while also anticipating the post crisis recovery and stop buying the protection to save money when it was no longer necessary. The Sharpe ratio of PPA is 0.323 while it was only 0.047 for BAH, demonstrating a tangible gain of performance for our dynamic active protective-put portfolio PPA and therefore demonstrating the power of prediction of our financial crisis indicator.

While a Sharpe in the order of magnitude of 0.3 would still be considered modest from the point of view of a hedge fund manager, it must be pointed out that it is the result of a single and simple protective-put strategy, without any diversification. In a real-world setting, diversification of the assets in the portfolio and of the strategies as well as the choosing of more elaborate and realistic rules for the purchase of options, which could also include call options to finance the purchase of the put in a covered call framework, might very well produce much more impressive Sharpe ratios. Also the Sharpe ratio that we have obtained for PPA is computed over a very long period of 15 years that includes long phases of market stagnation as well as several major financial crises, which reduce the overall annualized performance. If we had truncated our study to make it start from 2007, for example, the Sharpe ratio of PPA would have been much larger. The Calmar ratio for its part goes from 5.2% in BAH up to 18% in PPA and demonstrates that using our financial crisis indicator to pilot a protective-put strategy permits to both increase performance and at the same time reduce the MDD, which is a very desirable outcome for an asset manager.

The study of the profile of the TR coefficient is interesting as well. Like we have said it measures the extra performance of PPA with respect to BAH. Since the performance of TR is 3.3% it means that PPA is performing 3.3% above the SP500 ETF, which is already a very good result. The structure of the TR profile over time is remarkable as well. It features a sequence of increasing plateaux corresponding to the times of low market risk when Indicator B3B correctly recommends not buying the protective put option in the PPA strategy. Those plateaux, besides showing that our financial crisis indicator correctly anticipates most of the periods of low risk calm market, as well as anticipating the crises of course, shows that a correct selection of the threshold $\mathscr{T}$ at 80% instead of 60% enables us to limit the occurrences of false positives, without of course eliminating them and they still remain the main limitation in our framework. The Sharpe of TR, at around 0.278, while the Sharpe of BAH was only 0.047, demonstrates also the added value that the predictive power of our financial crisis indicator brings to portfolio PPA.

We now switch our attention to Figure 25 and Figure 26 which show the comparison between PPA and two kinds of random strategies. The basic idea between comparing PPA to random strategies is to show that the success of PPA compared to BAH and PPP is *not* just due a stroke of luck and that the added value and predictive power of our framework of financial crisis indicator is real. In the first kind of random strategy, the choice to buy, or not, the protective put option is random at each one of the 185 monthly decision dates in our study. We just flip a coin at each date and decide accordingly whether to buy the protection or not. We call those strategies *random at every date* (RED) strategies and they are shown in Figure 25. In the second kind of random strategies, that we call *random with the same proportion* (RSP), one random strategy is equivalent to performing a random permutation on the signal that Indicator B3B provides for PPA ('1' for *buy* and '0' for *don't buy*). Those strategies are compared to PPA in Figure 26.

We observe that indeed, both the RED and RSP strategies perform on average much worse than PPA, which is very reassuring. They have on average higher volatility, much lower performance and a significantly larger MDD. Visually, PPA performs better than most random strategies of both kinds because it is "above" most of them and it is located, most of the time, at the top of the area of the plane defined by the superposition of all the random paths. PPA is not in the middle, which would have suggested than on average the probability of doing better than PPA by adopting a random strategy would have been around 50%, which would have seriously damaged the credibility of our approach. PPA is not at the bottom of the area defined by the random paths either, which would have been even worse and implied that our active strategies, on average, would have been beaten by random ones. In fact, while considering the 2000 simulated random strategies, either RED or RSP, the strategy PPA beats them, in the sense that the final value of the PPA portfolio is above the final value of the portfolio governed by the random strategy, 1992 times for RED and 1989 times for RSP. That means that PPA is better in terms of global return than a random strategy around 99.5% of the time. Portfolio PPA perform even better when compared to a RED strategy than to a RSP strategy since the RSP strategy, while random, do contain a little information about the signal provided by Indicator B3B in the form of the global proportion of purchases over the course of all the 185 decision dates. Computing the average Sharpe ratio of the random strategies confirms that the good performance of PPA is due to skill rather than luck. Indeed, while the Sharpe of PPA is 0.323, the average Sharpe ratio of the 2000 paths of RED and RSP is very close to zero(-0.0101 and +0.0034, respectively), which is still better than the Sharpe of PPP, for which the cost of buying the protection every month destroys the performance of the portfolio.

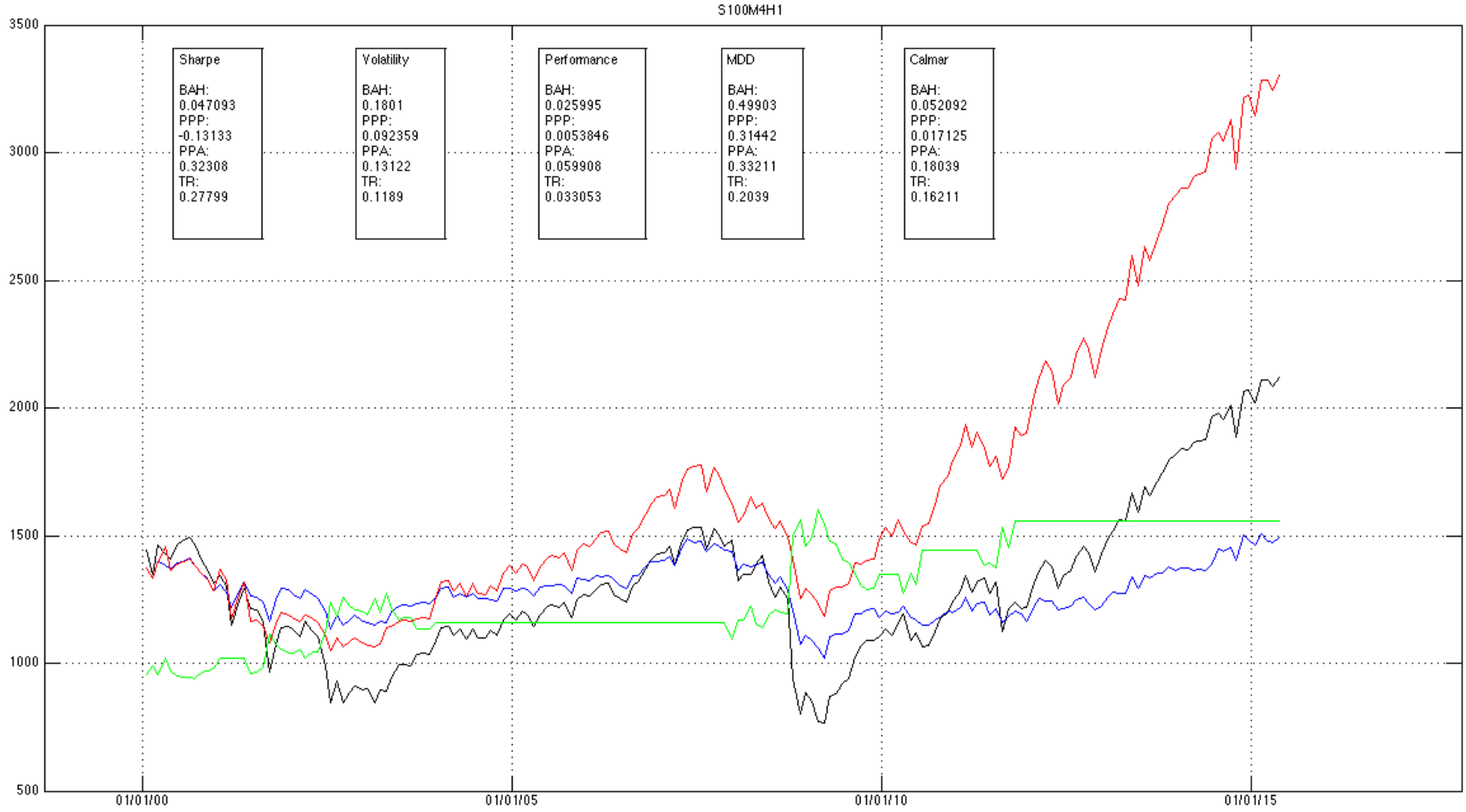

Figure 24 (Value of the portfolios BAH (black), PPP (blue) and PPA (red). The extra performance of PPA with respect to BAH (tracking error) is represented in green and is not on the same scale (x1000).)

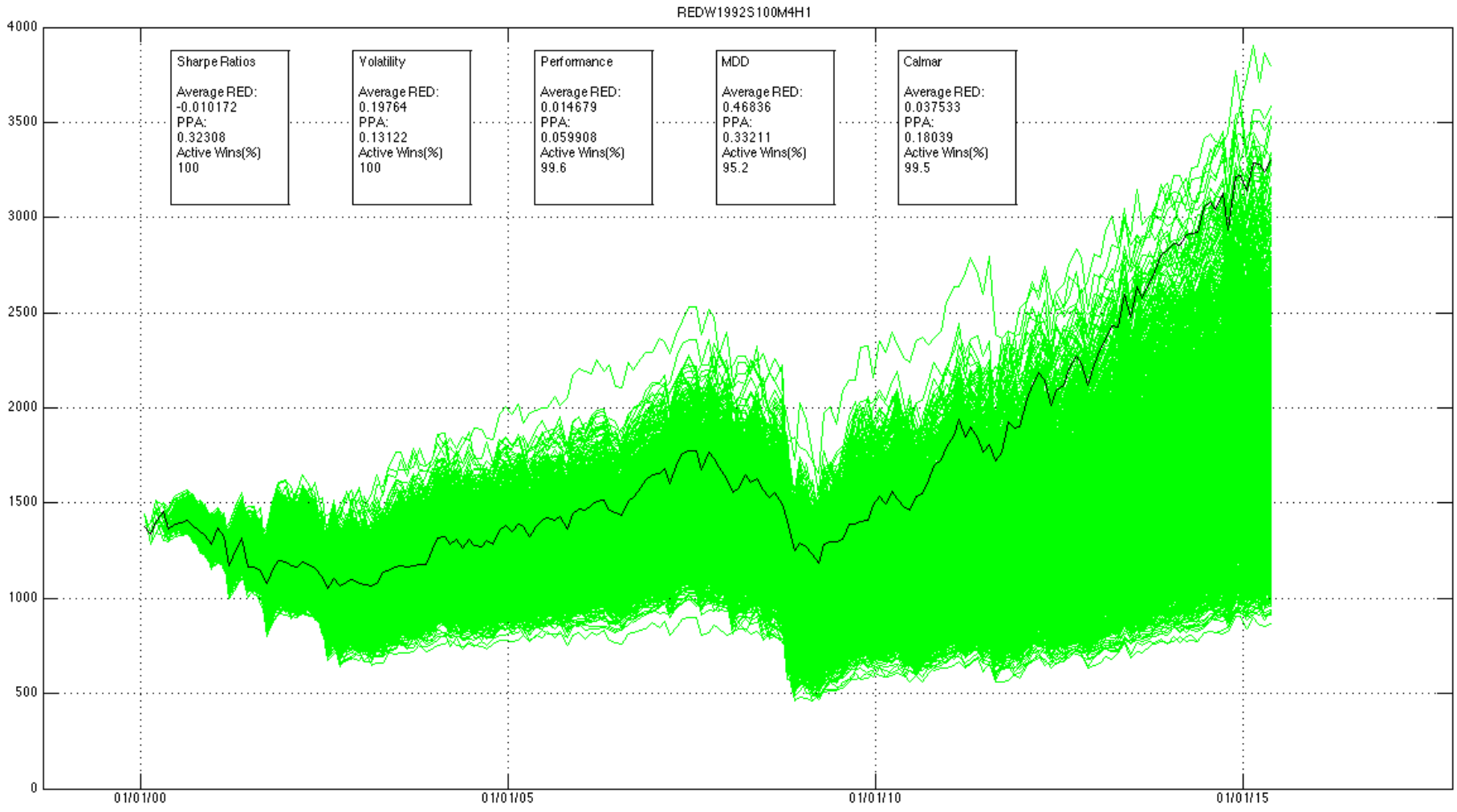

Figure 25 (Comparison between PPA (black) and 2000 random strategies (green) for which the choice of whether to buy, or not, the put option is random (coin flip) at every monthly decision date (random every date).)

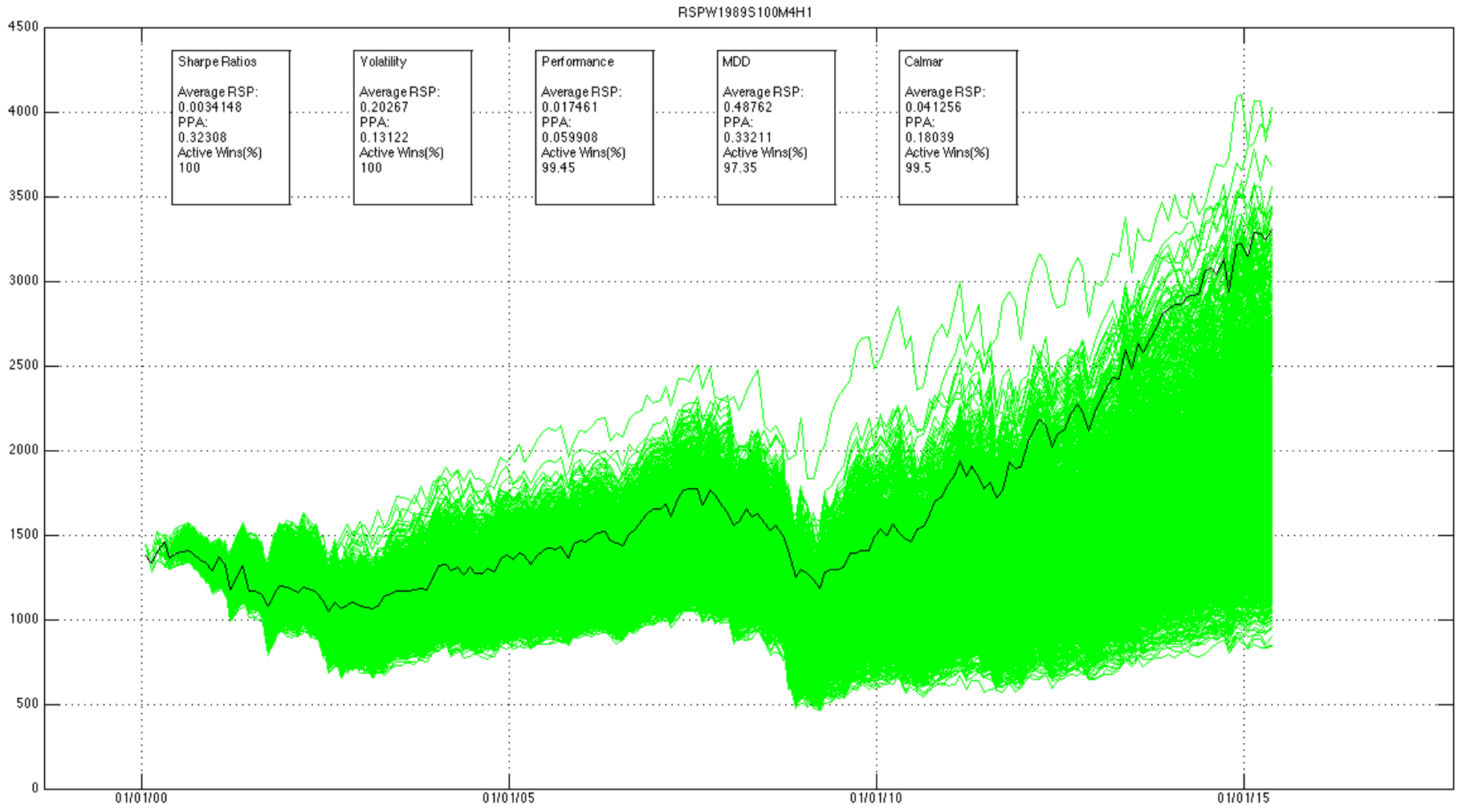

Figure 26 (Comparison between PPA (black) and 2000 random strategies (green) for which the choice of whether to buy, or not, the put option is random at every monthly decision date and the same global proportion of purchases as in PPA over the 185 decision is preserved (random same proportion).)

6 Conclusion

As a general conclusion, we could start by saying that the nine financial crisis indicators that we have built are all generally able to detect most of the financial crises that we have studied. In both the historical approach, where we made use of chosen dates for the crisis events, and the algorithmic trading approach, where we used a more quantitative definition of the financial crises based on the MDD, the indicators were indeed capable of confirming the occurrence of market turmoil. Moreover, we demonstrated an out-of-sample predictive power for several of those indicators, while using a dataset constituted of selected components of the SP500 index. We also demonstrated the predictive power of the indicators in our framework by using a signal produced by Indicator B3B in order to build a successful portfolio constituted of SPX shares and European put options and governed by an active protective-put strategy.

We recall that we have built two sets of financial crisis indicators and that we then applied them on seven datasets. The financial crisis indicators that we have built are all based of the study of the spectrum of a covariance matrix, a correlation matrix or a weighted correlation matrix. They measure the volatility and correlations between a number of assets in order to evaluate whether the conditions are right for adverse random events, which are happening all the time, to trigger financial crises.

The first kind of indicators, that we called the A-series, comprises three indicators. Indicator A1 and A2 are at each date the Hellinger distance between the empirical distribution of the spectrum of the covariance matrix and two different calm market reference distributions. Indicator A3 for its part is at each date the Hellinger distance between the empirical distribution of the spectrum of the covariance matrix and a reference distribution characterizing a market in turmoil. We found that one of the most useful patterns for financial crisis detection and forecast in the profiles of the indicators of the A-series is characterized by a spike in A1 and A2 accompanied by a drop in A3. Indeed, when this pattern occurs, it means that the market is in the process of moving away from a calm state and toward more turbulence.

We called the indicators of the second type the B-series. Indicator B1 is the spectral radius of the covariance matrix and bases its forecasts on a mixed signal of volatility and correlation. Indicator B2 is the trace of the covariance matrix and relies on volatility only to make its predictions. Indicator B3 is the spectral radius of the correlation matrix and relies on correlation only to make its predictions. We also have built three additional versions of B3. B3A is the spectral radius

of a correlation matrix where the assets have been weighted with regards to the market capitalization of the firms they represent. B3B is the spectral radius of a correlation matrix where the assets have been weighted with regards to their daily traded volume and B3C is an averaged version of B3B. We found that the indicators of the B-series, especially those that rely, in part or in whole, on correlation performed better while using the components of an index rather than a basket of indices. That probably has to do with the averaging effect that is a very strong influence in the computation of an index. Used on Dataset 6, which contains the components of the SP500, Indicator B3B is the one which gave us the best and the most reproducible results.

In the last part of the study, we demonstrated that Indicators B3B and B3C do possess, after proper calibration, a real out-of-sample power of prediction in estimating the probability of a financial crisis happening at a given time horizon in the future. While the approach that we adopted gave many false positives (a red flag is returned and no crisis happens in the market) as well, the low number of false negatives reinforced our conviction about the viability and usefulness of the financial crisis indicators that we have built. For indicator B3B, we also developed a quantitative approach relying on defining a financial crisis in terms of the crossing of an MDD threshold. Indicator B3B was also successfully used in order to build a signal governing a protective-put strategy in a portfolio constituted of a mix of options and ETF shares.

We are confident that our framework and the financial crisis indicators that we have built are able to bring new insight on the topic of financial crisis detection and prediction. In the future, one of the possible ways of applying these methods would be to use them in order to build more elaborate systematic trading strategies, which make use of all our nine indicators as well as new ones. Those strategies based on the aggregated signals coming from many different financial crisis indicators in our framework will be the topic of an upcoming paper.

References

[1] Bookstaber R. (1985) "The use of options in performance structuring", *Journal of Portfolio Management*, 11(4), pp. 36-50

[2] Bookstaber R. and R. Clarke (1981) "Options can alter portfolio return distributions", *Journal of Portfolio Management*, 7(3), pp. 63-70

[3] Bouchaud J.P. , M. Potters and L. Laloux (2005) "Financial Applications of Random Matrix Theory: Old Laces and New Pieces", *arxiv.org/abs/physics/0507111v1*

[4] Bouchaud J.P. and M. Potters (2009) "Financial Applications of Random Matrix Theory, A Short Review", *arxiv.org/abs/0910.1205*

[5] Bussiere M. and M. Fratzscher (2006) "Towards a New Early Warning System of Financial Crises", *Journal of International Money and Finance*, 25(6), pp. 953-973

[6] Celik A.E. and Y. Karatepe (2007) "Evaluating and Forecasting Banking Crises Through Neural Network Models: An Application for Turkish Banking Sector", *Expert Systems with Applications*, 33(4), pp. 809-815

[7] Clemen R.T. (1989) "Combining Forecasts: A Review and Annotated Bibliography", *International Journal of Forecasting*, 5(4), pp. 559-583

[8] Demyanyk Y. and I. Hasan (2010) "Financial Crises and Bank Failures: A Review of Prediction Methods", *Omega*, 38(5), pp. 315-324

[9] Drehmann M. and M. Juselius (2014) "Evaluating early Warning Indicators of Banking Crises: Satisfying Policy Requirements", *International Journal of Forecasting*, 30(3), pp. 759-780

[10] Ericsson N.R. (2016) "Eliciting GDP Forecasts from the FOMC's Minutes Around the Financial Crises", *International Journal of Forecasting*, 32(2), pp. 571-583

[11] Fuertes A-M. and E. Kalotychou (2007) "Optimal Design of Early Warning Systems for Sovereign Debt Crises", *International Journal of Forecasting*, 23(1), pp. 85-100

[12] Guégan D. and F. Ielpo (2008) "Flexible Time Series Models for Subjective Distribution Estimation with Monetary Policy in View", *Brussels Economic Review*, 51(1), pp. 79-103

[13] Guégan D. (2011) "Effect of Noise Filtering on Predictions: on the Routes of Chaos", *Brussels Economic Review*, 53(2), pp. 255-272

[14] Harper R.B. (2003) "Asset Allocation, Decoupling, and the Opportunity Cost of Cash", *Journal of Portfolio Management*, 29(4), pp. 25-35

[15] Hawkins J. and M. Klau (2000) "Measuring Potential Vulnerabilities in Emerging Market Economies", *B.I.S Working Papers - SSRN-ID = 849258*

[16] Hellinger E. (1909) "Neue Begründung der Theorie quadratischer Formen von unendlichvielen Veränderlichen", Journal for Pure and Applied Mathematics, 136, pp. 210-271

[17] Israelov R. and L.N. Nielsen (2015) "Still Not Cheap: Portfolio Protection in Calm Markets", *Journal of Portfolio Management*, 41(4), pp. 108-120

[18] Jiang Z.Q. , W.X. Zhoua , D. Sornette , R. Woodard , K. Bastiaensen and P. Cauwels (2010) "Bubble Diagnosis and Prediction of the 2005–2007 and 2008–2009 Chinese Stock Market Bubbles", *Journal of Economic Behavior and Organization*, 74(3), pp. 149–162

[19] Kullback S. and R.A. Leibler (1951) "On Information and Sufficiency", *Annals of Mathematical Statistics*, 22(1), pp. 79–86

[20] Marchenko V. A. and L.A. Pastur (1967) "Distribution of Eigenvalues for Some Sets of Random Matrices", *Mathematics of the USSR-Sbornik*, 1(4), pp. 457–483

[21] Maltritz D. (2010) "Currency Crisis Prediction using ADR Market Data: An Options-Based Approach", *International Journal of Forecasting*, 26(4), pp. 858–884

[22] Niemira M.P. and T.L. Saaty (2004) "An Analytic Network Process Model for Financial Crises Forecasting", *International Journal of Forecasting*, 20(4), pp. 573-587

[23] Sandoval Junior L. and I. De Paula Franca (2012) "Correlation of Financial Markets in Times of Crisis", *Physica A*, 391(1), pp. 187–208

[24] Singleton J.C. and J. Wingender (1986) "Skewness Persistence in Common Stock Returns", *Journal of Financial and Quantitative Analysis*, 21(3), pp. 335-341

[25] Singh A. and D. Xu (2013) "Random Matrix Application to Correlations Among Volatility of Assets" (2013), *arxiv.org/abs/1310.1601*

[26] Snarska M. (2007) "Financial Applications of Random Matrix Theory, Dynamics of the Covariance Matrix", *Cracow University of Economics - SSRN-ID = 2150559*

[27] Sornette D. (2009) "Dragon-Kings, Black Swans and the Prediction of Crises", *Swiss Finance Institute Research Paper No. 09-36 - SSRN-ID = 1470006*

[28] Sornette D. and A. Johansen (2010) "Shocks, Crashes and Bubbles in Financial Markets", *Brussels Economic Review*, 53(2), pp. 201-253

[29] Stanley H.E. , P. Gopikrishnan , V. Plerou and L.A.N. Amaral (2000) "Quantifying Fluctuations in Economic Systems by Adapting Methods of Statistical Physics", *Physica A*, 287(3-4), pp. 339-361

[30] Stekler H. and H. Symington (2016) "Evaluating Qualitative Forecasts: The FOMC minutes, 2006-2010", *International Journal of Forecasting*, 32(2), pp. 559-570

[31] Van den Berg J., B. Candelon and J-P. Urbain (2008) "A Cautious Note on the Use of Panel Models to Predict Financial Crises", *Economics Letters*, 101(1), pp. 80-83

Appendix

Reference Distributions for all Datasets

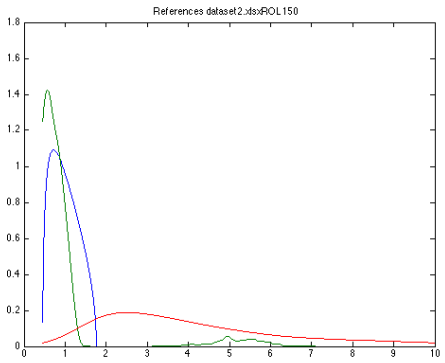

(a) Dataset 2

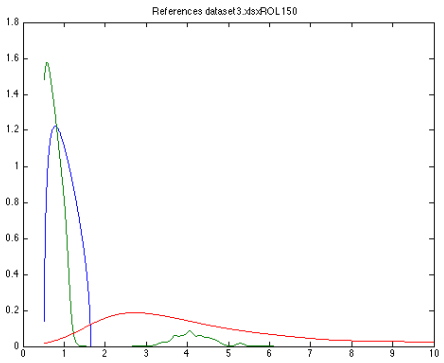

(b) Dataset 3

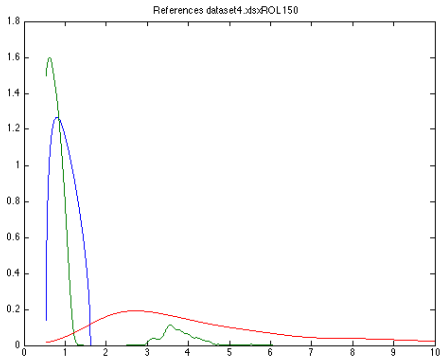

(c) Dataset 4

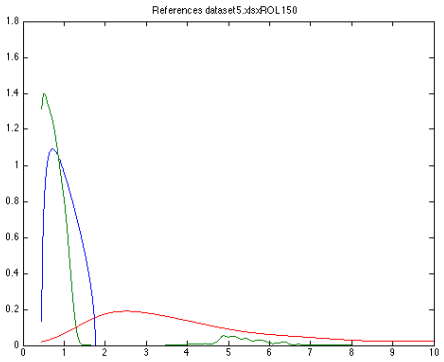

(d) Dataset 5

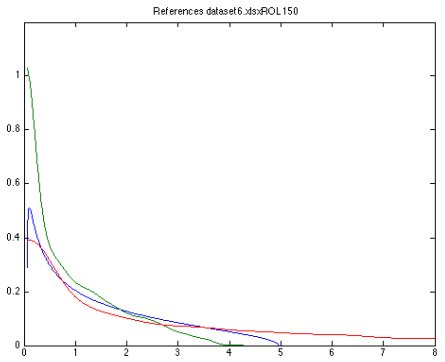

(e) Dataset 6

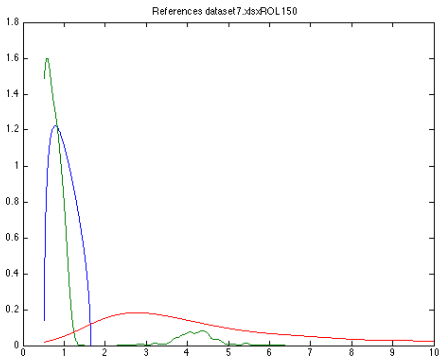

(f) Dataset 7

Reference distributions computed for Dataset 2 to Dataset 7, with a rolling window of 150 days (Blue: Marchenko Pastur (Θ1), Green: Θ2, Red: Θ3).

Composition of Dataset 6 (226 assets)

AA, AAPL, ABT, ADM, ADSK, AEP, AFL, AIG, ALTR, AMAT, AMGN, AON, APA, APC, APD, ARG, AVY, AXP, BA, BAC, BAX, BBY, BCR, BDX, BEN, BHI, BK, BLL, BMY, C, CAG, CAT, CB, CCE, CELG, CI, CINF, CL, CLX, CMA, CMCSA, CMI, CMS, CNP, COP, CPB, CSC, CSX, CTAS, CTL, CVS, CVX, D, DD, DE, DHR, DIS, DOV, DOW, DTE, DUK, EA, ECL, ED, EFX, EIX, EMC, EMR, EOG, EQT, ES, ETN, ETR, EXC, EXPD, F, FAST, FDO, FDX, FISV, FITB, FMC, GAS, GCI, GD, GE, GIS, GLW, GPC, GPS, GWW, HAL, HAR, HBAN, HCP, HD, HES, HOG, HON, HOT, HP, HPQ, HRB, HRL, HRS, HSY, HUM, IBM, IFF, INTC, IP, IPG, IR, ITW, JCI, JEC, JNJ, JPM, K, KLAC, KMB, KO, KR, KSU, L, LB, LEG, LEN, LLTC, LLY, LM, LNC, LOW, LRCX, LUK, LUV, MAS, MCD, MDT, MHFI, MMC, MMM, MO, MRK, MSFT, MSI, MUR, NBL, NEE, NEM, NI, NOC, NSC, NTRS, NUE, NWL, OKE, OXY, PAYX, PBCT, PBI, PCAR, PCG, PCL, PCP, PEG, PEP, PFE, PG, PGR, PH, PHM, PKI, PNC, PNW, PPG, PPL, PVH, R, ROST, RTN, SCG, SHW, SIAL, SLB, SNA, SO, SPLS, STI, SWK, SWN, SYMC, SYY, T, TE, TEG, TGT, THC, TIF, TJX, TMK, TMO, TROW, TRV, TSO, TSS, TXT, TYC, UNM, UNP, USB, UTX, VAR, VFC, VMC, VZ, WEC, WFC, WHR, WMB, WMT, WY, XEL, XOM, XRAY, XRX

Funding

This work was achieved through the Laboratory of Excellence on Financial Regulation (Labex RéFi) supported by PRES heSam under the reference ANR10LABX-0095. It benefited from a French government support managed by the National Research Agency (ANR) within the project Investissements d'Avenir Paris Nouveaux Mondes (Investments for the Future Paris New Worlds) under the reference ANR11IDEX000602.

Chapter 2

Winning Investment Strategies Based on Financial Crisis Indicators

Winning Investment Strategies Based on Financial Crisis Indicators

Antoine Kornprobst *

Université Paris 1 Panthéon-Sorbonne, Labex ReFi

September 7th 2017

Abstract

The aim of this work is to create systematic trading strategies built upon several financial crisis indicators based on the spectral properties of market dynamics. Within the limitations of our framework and data, we will demonstrate that our systematic trading strategies are able to make money, not as a result of pure luck but, in a reproducible way and while avoiding the pitfall of over fitting, as a result of the skill of the operators and their understanding and knowledge of the financial market. Using singular value decomposition (SVD) techniques in order to compute all spectra in an efficient way, we have built two kinds of financial crisis indicators with a demonstrable power of prediction. Firstly, there are those that compare at every date the distribution of the eigenvalues of a covariance or correlation matrix to a distribution of reference representing either a calm or agitated market reference. Secondly, we have those that merely compute at every date a chosen spectral property (trace, spectral radius or Frobenius norm) of a covariance or correlation matrix. Aggregating the signals provided by all the indicators in order to minimize false positive errors, we then build systematic trading strategies based on a discrete set of rules governing the investment decisions of the investor. Finally, we compare our active strategies to a passive reference as well as to random strategies in order to prove the usefulness of our approach and the added value provided by the out-of-sample predictive power of the financial crisis indicators upon which our systematic trading strategies are built.

Keywords :
Prediction Methods, Financial Crisis, Financial Forecasting, Random Matrix Theory.

1 Introduction

Our goal in this paper is to build active trading strategies that are able to make money in a reproducible fashion, not as a result of luck but as a result of skill. While using only commercially available data [1], we attempt to anticipate market movements and act on them beforehand by using the financial crisis indicators based on random matrix theory that were developed in the work of Douady and Kornprobst (2015). Simply speaking, our objective is to liquidate our positions before the prices start to drop and to acquire them back before the prices go back up again. The portfolios that we consider are constituted of a mix of ETF shares replicating an

*Electronic address: antoinekor9042@gmail.com

[1] All the data in this study ha been obtained from Bloomberg

equity index and cash. The financial crisis indicators will work on the stock components of the equity index and make a determination about whether it is prudent to convert the shares into cash because the probability of a crisis happening in the near future is getting higher, or on the contrary whether it is advisable to convert the cash into shares because the market is in a calm phase and the probability of a sudden price drop within a given forecast horizon is low. The cash, if present in a portfolio, earns the risk-free Libor rate.

We consider that our actions have no direct influence on the market and that we are always price takers. In other words, we consider that our trading operations are small enough to generate neither slippage nor feedback in the order book. This is of course a simplification, as even the smallest trades have some kind of impact on the order book. Our assumption however, is that this impact is negligible for our operations and that ignoring it does not change anything to our approach and the validity of the situations that we are attempting to describe. In order to focus entirely on demonstrating the power of predictions of our strategies and their potential for making money, we decided against modeling market frictions like transaction fees associated with our trading operations. While these market frictions do exist and represent a very real cost for market agents, our ambition at this stage is not to build a realistic simulation of market operation, which by the way would include many other variables than those we have considering here, but rather to provide a credible technical framework and methods that are ready to be applied by professionals.

There is a large literature, both applied and theoretical, on the topic of building successful systematic trading strategies, especially for the hedge fund industry as explained in Fung and Hsieh (1997). A first approach relies on what is commonly known in the financial world as *technical analysis*. This mostly empirical approach aims at predicting market movements and stock returns by identifying certain well known patterns in stock prices and other market vital signs. Technical analysis shares a lot of similarities with our approach since our aim is also to empirically detect reproducible crisis announcing patterns inside the market data and use that knowledge as a financial crisis indicator. The efficiency of optimized systematic trading strategies based on technical analysis has been demonstrated in the work of Gençay (1998). Indeed, clever technical analysis is usually able to do better than passive buy-and-hold strategies. This predictability of stock returns as a way to establish successful investment strategies is also described in details in the work of Pesaran and Timmermann (1995), who discuss from a historical point of view how the predictability of U.S stock returns have been routinely exploited by investors since the 1960' and especially since the 1970's. Indeed, it is at times of higher market volatility that technical analysis strategies can reach their full potential. Technical analysis strategies of various kinds (momentum, mean reverting, moving average, etc...) have also been successfully tested by Ratner and Leal (1999) where they discuss systematic trading strategies based on technical analysis and applied to the Latin American and Asian equity markets. The relevance of systematic trading strategies based on technical analysis, versus passive buy-and-hold strategies, has been also statistically demonstrated in the work of Kwon and Kish (2002) about the predictability of NYSE stocks.

Another approach successfully used in the financial industry in order to build systematic trading strategies is the dynamic time-series process and signal processing approach. This approach also shares a lot of similarities with our systematic trading strategies based on financial crisis indicators. Indeed we use a rolling window on market data time-series, which are constituted of the log-returns of the stock components of an equity index. The financial crisis indicators that we compute then produce a signal that is used in the decision-making process governing the active

trading strategy. This time-series based approach to trading is discussed in the work of Farmer and Shareen (2002) about the price dynamics of trading strategies seen through the lenses of signal processing theory. While some strategies based on technical analysis techniques might increase undesirable noise inside a market and create volatility as well as instability, especially when a large proportions of investors is using them at the same time, their efficiency and their power to make money is usually proven beyond a reasonable doubt as demonstrated in the work of Brock, Lakonishok and LeBaron (1992).

Our own approach to systematic trading strategies based on financial crisis indicators combines elements from all of the approaches that we described previously: technical analysis, time-series, signal processing, statistical considerations. We thus create a new framework that is grounded in a solid theoretical background, while still remaining flexible enough in order to be able to be applied in the real world and in order to be useful to traders and investors.

2 The Data

We work exclusively with daily data, because data with a daily frequency is more readily available, but there is nothing in our framework that would prevent the use of intraday data. Besides, working with daily data was easier because intraday datasets can become extremely large and require a lot of computing power to be properly exploited in a timely fashion. Our data is constituted of five global equity indices. We use the Standard & Poor's 500 (SP500), the Bloomberg European 500 (BE500), the Shanghai-Shenzhen CSI 300 (SHSZ300), the NASDAQ and the CAC40. For all those equity indices, we also have at our disposal all of their respective components as well as a matching time-series of the U.S Government Bond of maturity 1 month (US0001M) that is going to be used as the riskless asset to compute what the cash earns, whenever it is present in one of our portfolios, at a given date. The data for the equity indices themselves is comprised of the closing price $P_0(t)$ at each date of the time period on which our study is conducted. The data for the N the components is comprised, for all $i \in [\![1, N]\!]$ of the closing price $P_i(t)$, the daily volume traded $V_i(t)$, the closing market capitalization $C_i(t)$ and the closing financial leverage $L_i(t)$, which is the quotient of the total debt by the market capitalization. All prices have been adjusted for dividends and splits. At every time t, we compute the daily log-returns for both the index itself and its components. It is defined as the log-return between a given trading day and the previous trading day. For all $i \in [\![0, N]\!]$: $r_i(t) = log(\frac{P_t}{P_{t-1}})$.

The composition of the equity indices is dynamic over time, but our datasets need to have a stable composition. Indeed, if we consider a given index, companies regularly drop out and are replaced by new ones that better fit the membership criteria, which are defined by a committee and most often based on the listed companies' market capitalization. In order to conduct our study, we need to have for each of the five indices a stable set of index stock components over a sufficiently long period of time. Therefore it was not possible to keep all the current components of the indices. A compromise had to be found between keeping enough of the components of each index in order to have a sample of companies that is representative of the state of the financial market and the necessity to have a sufficient depth for our time-series in order to conduct a statistical study over a long enough period of time. All our datasets span between June 13th 2006 and March 15th 2016. The details about the five datasets that we are going to use in our study are the following. The exact composition of each dataset, given as a list of Bloomberg tickers, is given in appendix for each of the datasets.

- **Dataset-SP500** is comprised of 420 components of the Standard and Poor's 500 index, plus the index itself, which contains 500 of the largest companies ranked by market capitalization, having stock listed on the NYSE or NASDAQ stock exchanges.
- **Dataset-BE500** is made of 419 components of the Bloomberg European 500 index plus the index itself, which is the European counterpart to the SP500 and contains 500 of the largest companies listed on European stock exchanges.
- **Dataset-SHSZ300** is comprised of 147 components of the Shanghai-Shenzhen CSI 300 index, plus the index itself. The composition of this index, which has only been in existence since April 2005, is very much in a state of flux and its evolution reflects the profound transformations of the Chinese economy over the past decade. For that reason, less than half of the companies in the index today were already there at the time of its creation. We still decided to go forward and keep using this basket of 147 Chinese companies which are representative of the Chinese financial market since 2006 and which reflect its current state.
- **Dataset-NASDAQ** is comprised of 69 components of the NASDAQ Composite Index, plus the index itself which contains 100 of the largest companies, excluding financial companies, with respect to market capitalization, listed on the NASDAQ stock exchange.
- **Dataset-CAC40** is constituted of 37 components of the CAC40 index, plus the index itself, which contains 40 of the most important (selection by a committee) companies among the 100 companies with the highest market capitalization listed on the Euronext Paris stock exchange.

For all the datasets, we considered only the trading days, excluding week-ends and holidays. Moreover, when a specific stock wasn't traded on a given day or whenever an entry was missing in the data, we carried over the last valid available value to fill the gap in order to avoid neutralizing a large number of trading days in our study.

3 The Financial Crisis Indicators

The financial crisis indicators used as decision making tools in our systematic investment strategies are based on the work of Douady and Kornprobst (2017). For a given dataset constituted of the N stock components of an equity index, we start by choosing the length T of a rolling window. This choice has to be made carefully and is important for the quality of the financial crisis forecasts and therefore important for the success of the systematic trading strategies based upon those forecasts. T represents the number of observations of the log-returns of the components of the equity index and it needs to be large enough for a given dataset to enable us to obtain a whole meaningful spectrum of the covariance or correlation matrix of the stock components, but it should also not be too large in order to preserve the responsiveness of the indicators and avoid giving them a too long memory.

To obtain a whole spectrum of the matrices, we must have $T > N$ otherwise the asset vectors are not long enough (there are not enough observations inside the rolling window) and thus can never be linearly independent and the covariance and correlation matrices will be degenerate. Although that would have been a sufficient size for T, we discard the possibility of choosing $T = N$. This is a technical requirement. Indeed, since we plan on using the singular value decomposition

(SVD) of the rolling window to obtain the eigenvalues of the covariance and correlation matrices, the rolling window cannot be a square matrix, as explained in Horn and Johnson (2013) as well as in Golub and Van Loan (2013).

The requirement of having $T > N$ may however be in theory somewhat relaxed because the only part of the spectrum that really interests us is the larger eigenvalues. Larger eigenvalues are indicative of dynamical instability and our financial crisis indicators are based on that property. If $T < N$, we will not be able to obtain the whole meaningful spectrum of the matrices, but as long as T is not too small, the eigenvalues that we will miss are going to be the smaller ones, which are the ones that are less interesting to us. That is why the indicators in Douady and Kornprobst (2017) do still work when applied on a dataset containing 226 components of the SP500, while using a rolling window of only 150 days. In practice however in this study, where we are going to aggregate the signals produced by many different indicators, truncating the spectrum of the covariance or correlation matrix in any way did create technical problems and tended to degrade the quality of the forecasts, especially for the indicators that are called the A-series in Douady and Kornprobst (2017) and which compare the distribution of the whole spectrum to chosen references that represents either a calm or an agitated market.

We therefore decided to choose from now on in this paper $T = 1.1 \times N$ (1) for all the datasets. Even though it means that the rolling window becomes quite large for the datasets that contain the most assets, like Dataset-SP500 or Dataset-BE500, the benefit of working with a spectrum that has not been truncated outweighs the drawbacks in terms of loss of responsiveness of our indicators due to their longer memory for some of our datasets. We therefore choose for the whole study the following sizes for the rolling window of each of the datasets ; 462 days for Dataset-SP500, 461 days for Dataset-BE500, 162 days for Dataset-SHSZ300, 76 days for Dataset-NASDAQ and 41 days for Dataset-CAC40.

For a given dataset and at a given date t_0, we consider the matrix of the log-returns :

$$A(t_0) = (a_{i,j}(t_0))_{i \in [\![1,N]\!]; j \in [\![t_0 - T, t_0 - 1]\!]}$$

The rows of $A(t_0)$ represent time-series of individual stock component and the columns of $A(t_0)$ represent the observation dates. The coefficients of this matrix are the scaled and centered daily log-returns of the stock components of one of the equity indices considered in this study :

$$a_{i,j}(t_0) = \frac{1}{\sqrt{T}} \{ r_i(j) - \frac{\sum_{k=1}^{T} r_i(t_0 - k)}{T} \} \quad (2)$$

From the matrix A, we derive five matrices of interest :

- The unmodified matrix $A(t_0)$ itself enables us, through its singular value decomposition, which we will write in details below, to compute the spectrum of the covariance matrix of the N stock components over the time period T. The covariance matrix contains both the correlation and volatility effects of the stock components of a given equity index and both of those signals are going to be useful.
- The matrix $B_0(t_0) = (b^0_{i,j}(t_0))_{i \in [\![1,N]\!]; j \in [\![t_0 - T, t_0 - 1]\!]}$ is obtained by normalizing each coefficient of A with the standard deviation of the row to which it belongs. This normalization removes the volatility information that was contained in $A(t_0)$ and $B_0(t_0)$ contains only the pure correlation effect between the stock components.

$$b^0_{i,j}(t_0) = \frac{a_{i,j}(t_0)}{std([\![a_{i,t_0-T} \dots a_{i,t_0-1}]\!])} \quad (3)$$

From the singular value decomposition of $B_0(t_0)$ we obtain the spectrum of the correlation matrix of the N stock components over the time period T.

- The matrix $B_1(t_0) = (b^1_{i,j}(t_0))_{i\in[\![1,N]\!];j\in[\![t_0-T,t_0-1]\!]}$ is obtained by weighting each of the coefficients of $B(t_0)$ by the relative importance of the corresponding stock's daily traded volume at $t_0 - 1$, with respect to all the other components of the index. The idea behind B_1 is to build a different flavor of the correlation matrix, one which gives more importance to the stocks which are the most liquid and the most traded inside the index. Indeed, those liquid stocks are more susceptible to drive the movements of the market, especially the down movements during and preceding a crisis event.

$$b^1_{i,j}(t_0) = b^0_{i,j}(t_0)\frac{V_i(t_0)}{\sum_{k=1}^N V_k(t_0)} \quad (4)$$

From the singular value decomposition of $B_1(t_0)$ we will obtain the spectrum of the correlation matrix of the N stock components over the time period T weighted by volume traded.

- The matrix $B_2(t_0) = (b^2_{i,j}(t_0))_{i\in[\![1,N]\!];j\in[\![t_0-T,t_0-1]\!]}$ is constructed by applying to each of the coefficients of $B(t_0)$ a weight proportional to the market capitalization of the corresponding company. The idea is to give more importance in the computation of the spectrum of the correlation matrix to the companies which have the largest market capitalization and which may therefore drive the movements, though their sheer size, of their entire industry sector or of the financial market as a whole. By computing the singular value decomposition of $B_2(t_0)$ we will obtain the spectrum of another flavor of the correlation matrix, one which is weighted by market capitalization.

$$b^2_{i,j}(t_0) = b^0_{i,j}(t_0)\frac{C_i(t_0)}{\sum_{k=1}^N C_k(t_0)} \quad (5)$$

- Finally, the matrix $B_3(t_0) = (b^3_{i,j}(t_0))_{i\in[\![1,N]\!];j\in[\![t_0-T,t_0-1]\!]}$ is another flavor of the weighted correlation matrix. This time, we apply to the each of the coefficients a weight proportional to the financial leverage of the corresponding firm. Since the financial leverage can be interpreted as a measure of the financial health of a company, it provides us with a valuable way of giving more importance in our computations to the firms which are, because of their higher financial leverage, more exposed to the risk of suffering major adverse effects during a crisis or to start a domino effect. Indeed, their higher proportion of debt with respect to their own assets, puts them in a more precarious financial situation, or at least in a situation where a sudden random downturn of the market would render them unable to service that debt and therefore prone to failure. Many global financial institutions fell prey to this vicious circle during the 2007-2008 financial crisis for example.

$$b^3_{i,j}(t_0) = b^0_{i,j}(t_0)\frac{L_i(t_0)}{\sum_{k=1}^N L_k(t_0)} \quad (6)$$

We then apply the singular value decomposition (SVD) technique, as detailed in Horn and Johnson (2013) as well as in Golub and Van Loan (2013), to our five rolling matrices (A, B_0, B_1, B_2 and B_3) in order to obtain at each date t_0 the spectrum of the corresponding covariance, correlation or weighted correlation matrix. The main advantage that we obtain from using SVD is that the algorithm computing the singular values does not require any matrix multiplication like in Douady and Kornprobst (2017), where obtaining the covariance and correlation matrices required the product of a matrix by its transpose. Therefore, there will not be any added numerical errors during execution of the code on a computer. Indeed, a classical spectrum determination approach would start by computing the product of the rolling matrix by its transpose before applying standard techniques, like numerically finding all the roots of the characteristic polynomial using Newton-Raphson's method or similar techniques as detailed in the work of Abbasbandy (2003). The SVD approach bypasses the need to use those multiplications of matrices.

Taking into consideration an $N \times T$, with $(N < T)$, matrix M with $M = A$ or $M = B_k$ for $k \in [\![0, 3]\!]$), the singular value decomposition is written :

$$M = U\ \Sigma V^T; \Sigma = \left[\begin{array}{cccc|ccc} \sigma_1 & 0 & \dots & 0 & 0 & \dots & 0 \\ 0 & \sigma_2 & \dots & 0 & 0 & \dots & 0 \\ \vdots & \vdots & \ddots & \vdots & \vdots & \ddots & \vdots \\ 0 & 0 & \dots & \sigma_N & 0 & \dots & 0 \end{array}\right] \quad (7)$$

The eigenvalues λ_i of MM^T are obtained from the singular values σ_i found in Σ :

$$\forall i \in [\![1, N]\!], \lambda_i = \sigma_i^2 \quad (8)$$

After computing the whole spectrum of the rolling matrices at each date t_0, we can then use the two kinds of financial crisis indicators described in the work of Kornprobst and Douady (2017).

- Firstly, there are the indicators that compare the whole spectrum of the covariance, correlation or weighted correlation matrices associated with our five rolling matrices, to a reference spectrum distribution. We call these financial crisis indicators the α-series. The reference distribution may represent either an agitated or a calm market reference. Following the work of Douady and Kornprobst (2017), we consider three different references distributions. Two represent a calm market and one represents an agitated market. In the sense of the Hellinger distance, which is the metric adopted, the observed empirical distribution is expected to move away from a calm reference distribution and move closer to an agitated reference distribution when the risk of a financial crisis is increasing in the market. The main idea is to measure when the whole spectrum of the eigenvalues of the covariance matrix, correlation matrix or weighted correlation matrix shifts towards the higher eigenvalues, which is a situation indicative of instability in the market and therefore may indicate the possibility of an upcoming crisis. The first reference distribution modeling an ideal calm market, called $\mathscr{R}_1$, is the Marchenko-Pastur distribution, introduced in Marchenko and Pastur (1967). It is the distribution of the spectrum of a correlation matrix corresponding to a rolling matrix constituted of independent identically distributed normal Gaussian coefficients. The second reference distribution, called $\mathscr{R}_2$ represents a more realistic calm market. This numerically computed reference is the distribution of the eigenvalues of the covariance matrix corresponding to a rolling matrix constituted of Gaussian coefficients correlated to one another at the level of the mean of the long term correlation coefficients between all the assets of the whole sample contained in the chosen

dataset (around 50%), as explained in Douady and Kornprobst (2017). The distribution $\mathscr{R}_3$ representing an agitated market reference is the numerically computed distribution of the eigenvalues of a covariance matrix corresponding to a rolling matrix constituted of Student ($t = 3$) coefficients which are correlated to one another by the same method as the one used in $\mathscr{R}_2$. The resulting coefficients follow a fat tailed distribution and are correlated and therefore constitute an adequate representation of an agitated market, where the log-returns of the stock component of an equity index are highly volatile and prone to extreme losses. These market conditions simulate the kind of situation we expect to exist in days the days leading to a financial crisis. To summarize, we are considering five matrices (A, B_0, B_1, B_2 and B_3) and three references ($\mathscr{R}_1$, $\mathscr{R}_2$ and $\mathscr{R}_3$), which therefore gives us 15 financial crisis indicators of the α-series.

- Secondly, there are the financial crisis indicators that compute a specific spectral property of the covariance matrix, correlation matrix or weighted correlation matrices. We call these financial crisis indicators the β-series. We take into consideration three spectral properties: the spectral radius (the largest of the eigenvalues), the trace (the sum of the eigenvalues) and the Frobenius norm (the sum of the squared eigenvalues). The basic idea behind those indicators is similar than in the case of the indicators of the α-series, which compare the whole distribution of the spectrum to a reference distribution. Indeed, a shift of the spectrum to the right, toward the larger eigenvalues is indicative of market instability. It means increased correlation and volatility in the market and therefore an increased risk of a crisis taking place. These effects are studied under different points of views corresponding to the five rolling matrices considered. We therefore take into consideration five matrices (A, B_0, B_1, B_2 and B_3) and three spectral properties (spectral radius, trace and Frobenius norm), which gives us 14 financial crisis indicators of the β-series. Indeed the trace of the covariance matrix is useless as an indicator because it is constant and equal to the number N of stock components in the equity index considered. The traces of the weighted correlation matrices obtained from B_1 (volume traded), B_2 (market capitalization) and B_3 (financial leverage) are on the other hand perfectly valid indicators which bring their unique point of view to the study and are therefore very valuable. Indeed, as written in equations (4), (5) and (6), the weighting is applied to the coefficients of the rolling matrix B_0 and not to the coefficients of A. Therefore the normalization is applied before the weighting and the sum of the eigenvalues of the weighted correlation matrices, which are obtained par SVD decomposition of B_1, B_2 and B_3, has no reason to be constant.

When aggregating the indicators of the α-series and of the β-series, we therefore obtain 29 financial crisis indicators overall. At a given date t_0, when an investment decision needs to be made, each of those financial crisis indicators is considered as a expert opinion. When a strategy has to be defined, the core of our approach is going to be to attempt to find a consensus among those 29 opinions.

4 Calibration

The daily results provided by our 29 financial crisis indicators are just numbers at the moment. We need to translate those numbers in terms of financial crisis forecasts. We must define an in-sample calibration period and recognize patterns in the values taken by the 29 indicators during that calibration period that are reproducible and that we are going to use later in the out-of-sample study to make previsions.

In order to quantitatively define a financial crisis, we introduce at each given date t_0 the notion of maximum draw down ($MDD(t_0)$) at a given time horizon H in the future. We will choose H at 100 days for the remainder of our study since it's a commonly used value, both in the literature and in the industry. We define a *financial crisis* or *market event* as the crossing of a chosen threshold of maximum draw down, which can be for example down to 5% if we want to consider mild market events, or up to 40%, if our intention is to consider mostly very large crises. The order of magnitude of the maximum draw down never climbs much higher than 40% for most indices, not even at the height of the 2008 crisis during the failure of Lehman Brothers. The choice of a maximum draw down threshold is an important part of the construction of a successful systematic trading strategy in the framework that we are building. For a given dataset, the reference asset for which the maximum draw down is computed is the index itself (or an ETF replicating the index) and the price considered is the last price of the day $P_0(t_0)$.

$$MDD(t_0) = \max_{t_0 \leq t \leq \tau \leq t_0 + H} \{1 - \frac{P_0(\tau)}{P_0(t)}\} \quad (9)$$

Obviously, in the out-of-sample study, the value at a date t_0 of $MDD(t_0)$ is not known at t_0, we would need knowledge from the future for that. Indeed, we want interpret the value of our indicators as a probability of crossing a chosen maximum draw down threshold over the course of the forecast horizon H in the future. In the in-sample, training period of our indicators, we will however match the value of our indicators at a given date t_0 with the value of $MDD(t_0)$, computed in advance by using data from the future from the point of view of an observer who exists at the date t_0. We will do this in order to precisely learn which are the values taken by our indicators which correspond to the crossing of a given MDD threshold in the future within the forecast horizon H. That process is at the heart of the calibration of our 29 indicators.

We must choose two things in the calibration process. Firstly, we decide the size K of the in-sample calibration period during which our indicators learn how to recognize which are the values they take that match the largest MDD values. Obviously, the larger the calibration period, the better in theory, but since our data spans only around 10 years, we must preserve a large enough out-of-sample period to make previsions and validate the viability of our systematic trading strategies. It is also necessary that the 2007-2008 financial crisis be included in that calibration period because the indicators must be confronted at least once to a major crisis in order to learn its signature and hopefully be able to recognize similar events in advance in the out-of sample period. Besides all those considerations, the calibration period K must at the very least fit the rolling window T for a given dataset, which as we explained before in Equation (1) is equal to $1.1 \times N$, with N the number of stock components present in the dataset. Using those notations, there are going to $K - T$ usable dates for the training of the indicators and the previsions will be able to start at the date $K + H$. Figure 1 summarizes the situation of the calibration period with the rolling window represented as an orange rectangle.

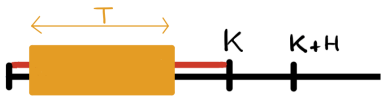

Figure 1 : Calibration period (red) and rolling window (orange)

In order to give the indicators the chance to have enough usable calibration dates for every one of our five datasets and keeping in mind that we must try to treat them as equally as possible, even though they are of very different sizes in terms of the number of stock components that

they contain, we establish the following rule :

$$K = max(500, T + 50) \quad (10)$$

This seems like a reasonable choice. Indeed, Formula (10) guarantees that the indicators will encounter the 2007-2008 financial crisis for all the datasets, even the smaller ones like the CAC40. It assures that the training period will not significantly be larger than 2 years (assuming around 250 trading days per year), even for the larger datasets like the SP500 and BE500. Finally, the indicators are guaranteed at least 50 training dates for all the datasets, even the larger ones, which is the minimum to guarantee their proper calibration. Using Formula (10), we obtain an in-sample calibration period of 512 days for Dataset-SP500, 511 days for Dataset-BE500 and 500 days for Dataset-SHSZ300, Dataset-NASDAQ and Dataset-CAC40.

For a given dataset and for each of our 29 financial crisis indicators, we draw the scatter plot of the maximum draw down at a given date versus the numerical value of the indicator at the same date. The plots for all the five datasets and the 29 financial crisis indicators of both the α-series and the β-series are provided in appendix. The points corresponding to the dates of the in-sample calibration period are in red and the points corresponding to the dates of the out-of sample prediction period are in blue. The most notable feature that immediately emerges from observing all those plots is that they are all roughly bell-shaped and, most importantly, that bell-shaped structure is present both in the calibration period and the prediction period. The values of the indicator corresponding to the higher values of MDD are the same during the in-sample training period and the out-of-sample prediction period. That means that it makes sense to teach the indicators during their calibration period which ones are the values they take that actually correspond to the highest values of MDD (i.e the financial crises). Those structures are obviously easier to see when the number of usable dates inside the calibration period is larger (i.e for the smaller datasets in terms of the number of stock components inside the equity index), but it is almost always visible nonetheless.

We can interpret that bell-shaped structure from a financial point of view in the following manner. When the value of an indicator is very small (resp. very high for the indicators based on $\mathscr{R}_3$), it means that the probability of a crisis happening withing the chosen 100 days time horizon H is very small. On the other hand, when the value of an indicator is very high (resp. very small for the indicators based on $\mathscr{R}_3$), then it means that the market is very likely already in the midst of a crisis and what the indicators are seeing at the $H = 100$ days horizon is the post-crisis recovery. That leaves in the middle a *danger zone* which corresponds to the values taken by an indicator which corresponds to the highest values of MDD at the 100 days horizon. In light of the previous discussion, "calibrating the indicators" therefore means "finding the danger zone for each indicator " and in order to do this in a quantitative and reproducible manner, we need to choose the first of the two parameters that define a systematic trading strategy in our framework: the MDD threshold $\mathscr{T}$. This choice is very important and will have profound implications for the eventual success of a systematic trading strategy.

By choosing an MDD threshold $\mathscr{T}$, we tell each of the 29 indicators to forget any point below $\mathscr{T}$ in the scatter plot (value vs. MDD) graph drawn during the calibration period and then to place its danger zone (which is of a fixed width equal to 15% of the total width of the graph, after having discarded possible outliers) such that the number of points inside it, is maximum. The choice of $\mathscr{T}$ determines whether we decide to design our strategies to attempt to detect in advance a large number of small crises (we choose in that case a low $\mathscr{T}$ around 5% or 10%) or whether we prefer to bet on the successful forecasts of a small number of large crises (we choose

in that case a $\mathscr{T}$ of 15% or more). We must find the good balance because both cases, large or small $\mathscr{T}$, present advantages and drawbacks.

If we choose $\mathscr{T}$ to be small, then according to the work of Douady and Kornprobst (2017), there is going to be some false positives (i.e. an indicator forecasts a crisis within its 100 days horizon of previsions, but nothing actually happens) and some false negatives as well (i.e. an indicator fails to predict a market event). The relatively low number of false positives for an individual indicator is clearly an advantage and will give more focus to our systematic trading strategies. The presence of some false negatives is potentially more dangerous but this may not be a disaster however, because the market events that we are betting on forecasting in order to build our strategy are typically small in that case, so even if a few of them are missed, we could still obtain acceptable results in terms of performance. If on the other hand we choose $\mathscr{T}$ quite high, then there is going to be much more false positives, further increasing the noise in the signal of an individual indicator, but there is going to be only a small risk that the indicators will miss a large market event. If we bet on accurately forecasting large financial crises, there is a lower risk of missing one, however if the indicators still do fail to correctly forecast a large market event, then in that case we would be instantly ruined.

As an illustration of the process of calibration of the indicators, we consider Dataset-CAC40 and the financial crisis indicator defined by the Hellinger distance between the empirical distribution of the spectrum of the correlation matrix weighted by financial leverage and the reference distribution $\mathscr{R}_2$ (calm market reference). In Figure 2a, we draw the scatter plot (indicator value vs. MDD), with the MDD represented on the y-axis. The bell-shaped structure is clearly visible, both for the red dots, which represent the calibration period and the blue dots, which represent the out-of-sample forecast period. In Figure 2b, we have chosen $\mathscr{T} = 10\%$ and all the red points below $\mathscr{T}$ are forgotten. The danger zone is represented as the area between the two vertical red lines and it is chosen automatically by the computer code, which maximizes the number of remaining red points inside a vertical stripe of width 15% of the total width of the scatter plot. In that example, the danger zone is defined by values of the indicator roughly between 224 and 238 for the Hellinger distance.

Figure 2a: MDD vs. Hellinger distance between $\mathscr{R}_2$ and the distribution of the eigenvalues of the correlation matrix weighted by financial leverage for Dataset-CAC40

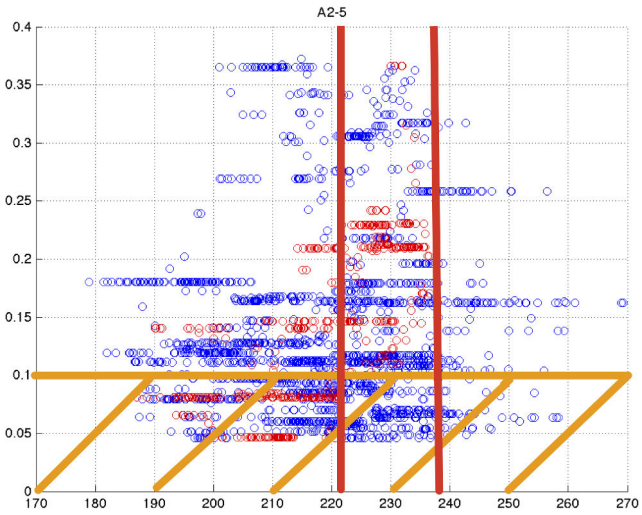

Figure 2b: $\mathscr{T}$ is represented an horizontal orange line (10% in this example), any point below $\mathscr{T}$ is not taken into consideration. The danger zone is represented as the area between the vertical red lines.

5 Systematic Trading Strategies

The 29 financial crisis indicators, both of the α-series and of the β-series are now properly calibrated, which means that they each have discovered where their danger zone is located during their in-sample training period, according to the choice that was made for the value of the MDD threshold $\mathscr{T}$. Like we have already stated, we view those 29 indicators as expert opinions and we try to reach consensus among them at a given date t_0 in order to make a trading decision. Following the work of Clemen (1989), our intention is to combine multiple individual forecasts, provided by our 29 indicators, in order to improve the quality and focus of our previsions and therefore to increase to chances of success of the systematic trading strategies, which are based on those previsions. Since it was stated in the work of Douady and Kornprobst (2017) that one of the main limitations to the predictive power of each individual financial crisis indicator of either the α-series or the β-series, was the presence of false positives inside the results, our expectation is that combining the signals of many different indicators will reduce the influence of those false positives. The strategies that are going to be considered in this study are applied to a portfolio containing both cash, which earns the riskless Libor rate, and ETF stocks, which replicates an equity index. At each date t_0, according to the aggregated signal produced by our financial crisis indicators, we can choose to do nothing if the situation is unclear, convert some cash to shares if the market forecast is good or convert some shares to cash if the risk of a crisis happening is increasing. There are no market frictions or transaction fees in our modeling and there are no considerations of liquidity either, since major equity indices ETF (SP500, BE500, SHSZ300, NASDAQ or CAC40) are extremely liquid securities in all market conditions.

We illustrate our approach with the drawing in Figure 3. At each date t_0 of the active trading period that starts at $K + H$, we look 100 days in the past and count for each of the 29 financial crisis indicators the number of times it takes a value which is inside its danger zone. We have talked about the MDD threshold $\mathscr{T}$ in the previous section and we now introduce the second of the two parameters that define a systematic trading strategy in our framework: the indicator

sensitivity $\mathscr{S}$. This indicator sensitivity $\mathscr{S}$ is a number between 0 and 100 that defines a threshold above which an indicator gives a *red flag*. For any one of our 29 indicators, if the indicator takes values inside its danger zone more than $\mathscr{S}$ times inside the interval $[\![t_0 - 100, t_0 - 1]\!]$, then it produces a red flag at t_0, which indicates a higher risk of a financial crisis happening (defined as the crossing of the threshold $\mathscr{T}$) during the time period $[\![t_0 + 1, t_0 + H]\!]$ in the future. Like the choice of $\mathscr{T}$ before, the choice of $\mathscr{S}$ is a very important part of the eventual success of a systematic trading strategy based on our financial crisis indicators. Indeed the parameter $\mathscr{S}$ controls the "aggressiveness" of a strategy, which is its tendency to react very quickly to the first signs of deteriorating market conditions and convert shares to cash immediately or, on the contrary, its tendency for showing patience and restraint and only act and sell shares when the signs of an impending crisis in the market are more clear.

If $\mathscr{S}$ is chosen to be small (around 50% or 60%), then red flags are easier to achieve and the strategy is going to be very aggressive and convert the shares to cash at the first sign of danger. This behavior may be considered prudent in some circumstances, but it will also severely damage the performance prospects of the strategy because there will often be only cash (which earns very little) inside the portfolio and we will fail to take advantage of periods of market growth. On the other hand if $\mathscr{S}$ is chosen very high (for example 85% or 90%), then the red flags are going to be very hard to obtain and the strategy is going to be very patient and keep the shares inside the portfolio until the signs indicative of an impending crisis become impossible to ignore. Such a behavior might maximize profit in some cases because the shares are kept for as long as possible, in particular during the periods of market growth, but the risk is to keep the shares for too long while their value starts to decline and to have a strategy so apathetic that it follows the ETF down during a crash and does not convert the shares into cash when it is needed. Like with the choice of $\mathscr{T}$ before, the choice of the indicator sensitivity $\mathscr{S}$ is about finding the right balance between responsiveness (low $\mathscr{S}$) and apathy (high $\mathscr{S}$).

Figure 3: Representation of the calibration period (red) and of the computation period at the date t_0 (purple).

We then count the total number of red flags produced by the indicators at the date t_0. It is an integer between 0 and 29 that we call $\Gamma(t_0)$. This number contains the aggregated crisis forecasting signal of all the indicators of the α-series and of the β-series. Finally we define a set of discrete rules that define what the strategy is going to do regarding the cash and ETF shares mix inside the portfolio.

We had initially also pursued an approach where, instead choosing an indicator sensitivity $\mathscr{S}$, then a function Γ and finally a set of rules on Γ, we chose a response function $f : [0, 2900] \longrightarrow [0, 1]$ that gave the percentage of cash inside the portfolio as a function of the total number of times the 29 indicators were inside their respective danger zone in the time period $[\![t_0 - 100, t_0 - 1]\!]$. This approach did not however prove itself viable as the performances of the resulting active strategies were very sensitive to the exact form of the graph of the function f chosen empirically by the operator. This lack of robustness of the approach relying on a response function seemed unacceptable and moreover it would have invited concerns about over-fitting in our framework.

The set of discrete rules on Γ are very robust and are chosen once and for all for five datasets and for the duration of the study. The rules that we choose for this study may still probably be refined and made more realistic in a real world situation, but they have experimentally proven their worth for the all datasets and the time periods that we have studied. Dealing with a portfolio constituted of a mix of cash and ETF shares, the discrete rules on Γ are the following at the date t_0 of the out-of-sample active trading period:

- $\Gamma(t_0) = 0$ or $\Gamma(t_0) = 1$: we buy 10% more of the ETF shares on top of those already present inside the portfolio, unless there is already no more cash inside the portfolio because it has already been entirely previously converted to ETF shares.

- $\Gamma(t_0) \in [\![2, 4]\!]$: we do nothing.

- $\Gamma(t_0) > 4$: we sell 10% of the ETF shares present inside the portfolio, unless there is already no more shares inside the portfolio because they have already been entirely previously converted to cash.

Those rules on Γ are designed to filter out the false positives in the forecasts provided by our financial crisis indicators, which are the main limitation of our framework, as explained in Douady and Kornprobst (2017). We achieve this goal by combining the opinion of several of them and try to reach a consensus before selling shares and act on the prevision that a market downturn is becoming more likely within the given time horizon $H = 100$ days. The occurrence of false negative errors on the other hand is rarer in our framework, but we did also design the rules such that the indicators have to agree among themselves that the risk of a market downturn is low before triggering the purchase of more shares.

We may now summarize our framework for the construction of systematic trading strategies based on our financial crisis indicators. Once the rules for Γ have been fixed beforehand for the whole study, the operator decides which parameters are the best given the dataset being studied and the market conditions. The skills and experience of the person making the decisions for the parameters $\mathscr{T}$ and $\mathscr{S}$ are a very important part of the potential for success of a strategy. We recall that:

- The operator first chooses a MDD threshold $\mathscr{T}$ to calibrate the indicators (i.e. find their danger zone) over the in-sample calibration period). A high $\mathscr{T}$ means that we bet on accurately forecasting a small number of large market downturns and a low $\mathscr{T}$ means that we bet on forecasting a large number of small market downturns.
- The operator then chooses an indicator sensitivity $\mathscr{S}$. It determines the level of aggressiveness of the strategy. A high $\mathscr{S}$ means that the red flags are difficult to obtain and therefore that the strategy is very apathetic. A low $\mathscr{S}$ means that the red flags are easier to obtain and therefore that the strategy is very aggressive ans sells the shares at the first sign of danger.

Once these choices have been made for a given equity index dataset, the systematic trading strategy that we have designed is able to decide at every date of the out-of sample period

what to do regarding the composition of the portfolio constituted of a mix of cash and ETF shares replicating the index. We are now going to compare the performances of our active trading strategies to a passive buy-and-hold strategy as well as to random strategies in order to demonstrate their worth, which is built upon the predictive power of our 29 financial crisis indicators of both the α-series and the β-series.

6 Numerical Results

We now switch our attention to the application of our systematic trading strategies inside the framework defined in the previous sections to our five datasets: SP500, BE500, SHSZ300, NASDAQ and CAC40. As usual, we compute the financial crisis indicators on the components of the index present inside each dataset and the financial instrument that we trade is an ETF share replicating the equity index.

For each dataset, we will consider three investors:

- A passive investor who hold the portfolio PP. That investor starts with 10.000 shares of the ETF replicating the index and 10 millions in cash, which earns the riskless monthly Libor rate. That investor keeps those assets for the duration of the study.
- An active investor who holds the portfolio PA. That investor starts with 10.000 shares of the index and 10 millions in cash and then chooses a set of parameters ($\mathscr{T}$, $\mathscr{S}$) in order to create a systematic trading strategy governing the composition of PA and deciding automatically what to do according the set of discrete rules that was detailed in the previous section. We do not consider fractional ETF shares and round the number of shares to the closest lower integer.
- An active investor who holds a portfolio PR and who starts with 10.000 shares of the index and 10 millions in cash and adopts a random strategy. At each date, the random strategy governing a path of PR chooses to buy more shares (unless there is already no more cash), do nothing or sell some shares (unless there are already no more shares) in a random fashion, but in such a manner that the proportion of "buy", "do nothing" and "sell" orders is the same as in PA. Those random strategies are similar in nature to the *random same proportion* (RSP) strategies described in Douady and Kornprobst (2017). The role of the PR paths is to demonstrate that our active strategy PA does bring added value and (hopefully, as we will discuss below) beats an average of random strategies.

For every decision date in the out-of-sample period, the riskless asset TB is chosen as the one month U.S Treasury Bond (US0001M) and the cash, if present inside a portfolio, earns this rate as well. Considering an asset A, which can represent either PP, PA or one path of PR, we define the following benchmarks, Sharpe ratio and Calmar ratio. We also define the investment ratio IR and we recall the Maximum Draw Down (MDD), that we have already defined in Equation (9). Here, we compute the MDD(A) over the entire period of study and not at a 100 days horizon like when we were calibrating the indicators.

- The investment ratio IR, that is computed for PA only, is simply a measure of the proportion of riskless cash inside the active portfolio. It measures whether the strategy is choosing to convert the cash into ETF shares or the ETF shares into cash. $IR = 1$ means we are fully invested and $IR = 0$ means the strategy has decided to convert all the ETF shares

into cash because, according to its parameters, it sees a high risk of a crisis happening within the 100 days forecast horizon of the financial crisis indicators.

$$IR = \frac{PA - cash}{PA} = \frac{shares}{PA} \quad (11)$$

- To compute the yearly Sharpe ratio, we proceed in the following manner. The Sharpe ratio measures the quotient of the excess performance with respect to a riskless asset over the volatility. To achieve the desired highest Sharpe possible, a strategy has to maximize return while at the same time minimize volatility, which represents risk.

  - At every date t of the out-of-sample period, $ExcessReturn_A(t) = \frac{A(t)}{A(t-1)} - \frac{TB(t-1)}{12} - 1$
  - With the notations of Figure 3, we compute the annualized performance, assuming 30 days per month $Perf(A) = (\frac{A(S)}{A(K+H)})^{\frac{360}{S-(K+H)}} - 1$
  - $Vol(A) = stdev(ExcessReturn_A).\sqrt{12}$ (Annualized volatility)

$$Sharpe(A) = \frac{Perf(A) - mean(TB)}{Vol} \quad (12)$$

- We define the yearly Calmar ratio as the quotient of the performance by the maximum draw down (MDD).

$$Calmar(A) = \frac{Perf(A)}{MDD(A)} \quad (13)$$

Regarding the set of parameters ($\mathscr{T}$, $\mathscr{S}$) that we choose, we divide the five equity indices studied into three groups, detailed below, with similar characteristics. Our intention is to standardize the choice of $\mathscr{T}$ and $\mathscr{T}$ and therefore demonstrate that our framework does not suffer from over-fitting and the selection of ad-hoc parameters that would work only for a specific index in a particular situation. Indeed the results that will be provided by our successful systematic trading strategies are robust and able to be generalized to other datasets and many market regimes.

- The first group contains the BE500, the CAC40 and the SP500. Those are are equity indices containing stocks belonging to companies from all the sectors of activity in large mature economies. We choose $\mathscr{T} = 20$ and $\mathscr{S} = 75$. According to the discussion in the previous sections, it means that we intend to bet on the detection of a small number of large crises and that we want the strategy to be relatively calm and patient. Indeed, market events representing a MDD of 20% or more are already very significant and asking the indicators to return a red flag when they are at least 75% of the time inside their danger zone in the 100 days preceding a decision makes the red flags relatively hard to achieve and therefore it makes the strategy less likely to sell the shares too early at the first sign of danger.

- The second group contains the NASDAQ index only. This equity index contains many high tech companies, which are often younger and sometimes more prone to volatility in the prices of their respective shares. We choose $\mathscr{T} = 15$ and $\mathscr{S} = 80$. We therefore decide to bet on relatively large market event that will however still be more numerous and smaller than those we had decided to bet on for the large generalist equity indices like the SP500.

The choice of $\mathscr{S}$ reflects our desire to have very patient strategies, that will not panic at the first sign of danger and wait until the signs of an impending crisis are undeniable to start converting the ETF shares into cash.

- Finally, the third group is constituted of the SHSZ300 index alone. Like we are going to see when we will comment the results obtained, building a winning systematic trading strategy for the Chinese index has been a challenging task. Indeed, the Chinese market has undergone a lot of profound structural transformations, from being a large emerging market to being the world's second largest, during the period of study covered by Dataset-SHSZ300 (June 2006 to March 2016). This inherent instability is reflected in the very composition of Dataset-SHSZ300, since it contains only 147 of the current 300 components, meaning that more than half of the companies that are currently part of the index were not present ten years ago. Because of all those uncertainties creating instability and volatility inside the SHSZ300 index, we chose $\mathscr{T} = 10$ and $\mathscr{S} = 70$. Our choice is to bet on the detection of a large number of small crises (MDD threshold = 10%) and to have relatively aggressive strategies, with an indicator sensitivity of only 70% that will react quickly to signs indicative of a higher risk of a crisis happening withing the forecast horizon and not wait to too long to take action in a structurally chaotic financial market.

The results that we obtain for Dataset-BE500 with our systematic trading strategy, defined by all the parameters chosen as discussed above ($\mathscr{T} = 20$, $\mathscr{S} = 75$), are presented in Figure 4a, Figure 4b and Figure 4c. We recall that the rolling window is of 461 days in length and that the calibration period is 511 days. Over the course of the out-of-sample prediction period, the active strategy governing PA issued 983 buy orders, 357 stay orders and 556 sell orders. By examining all the calibration graphs provided in appendix for the 29 indicators of both the α-series and of the β-series, we notice that most of them have the expected bell-shaped structure, both the in-sample calibration period (red dots) and the out-of-sample test period (blue dots). This guarantees a proper calibration of the indicators and therefore the quality of the active strategy based on their aggregated signals. In Figure 4a, the active portfolio PA does much better than the passive portfolio PP in terms of Sharpe ratio (increase to 0.43 from 0.27), performance (increase to 8.5% from 5.2%). PA does slightly better than PP in terms of Calmar ratio as well, but it is less significant (increase to 0.28 from 0.26). This is due to the fact that PA has an higher MDD over the course of the out-of-sample period than PP. This drawback of the active strategy results from the fact than whenever $IR = 1$ (PA is fully invested), if there is drop in the ETF share prices, PA suffers more locally than PP, which still contains its cash. Excluding the considerations on the MDD, PA still beats PP on all the other market benchmarks. The graph of Γ is represented in Figure 4c and has to be studied in concert with the graph of IR in Figure 4a. We notice that the active strategy, with its rules on Γ that we have detailed earlier, correctly anticipates the the big crises, IR falls to zero at mostly the rights times, but it is a bit too bad that the strategy decides to sell all the shares too early in 2014, which results in a performance that does not reach its full potential. We talked a lot about the limitations in our framework induced by the false positive signals sent by the indicators and combining the signals of 29 of them to compute the function Γ did help a lot, but there is still room for improvement. In figure 4b, we have represented PA against 50,000 paths of PR. The average Sharpe of the random strategies is only 0.29, while PA has a Sharpe of 0.43. PA beats 100% of the random paths on that important benchmark. While the average MDD of the paths of PR is slightly smaller than the MDD of PA for the reasons we have given just before (the presence of cash in PA does boost the MDD at some point, unfortunately), the active portfolio PA still beats nearly 69% of the random paths in terms of Calmar because PA features a better overall performance than most random paths PR. The examination of the plane area (in green on Figure 4b) created by the

random paths underlines the fact that the active strategy governing PA takes the right decisions at the right time, especially in late 2011, but decides to sell the ETF shares too soon in early 2014, which somewhat reduced the overall performance of PA.

The results that we obtain for Dataset-CAC40 ($\mathscr{T} = 20$, $\mathscr{S} = 75$) are presented in Figure 5a, Figure 5b and Figure 5c. We recall that the rolling window was 41 days in length and that the calibration period was 500 days. Over the course of the out-of-sample forecast period, the strategy governing PA has issued 1152 buy orders, 711 stay orders and only 36 sell orders, but as we are going to discover, those few sell orders were given just at the right time, before a major drop in price and have made all the difference, making PA on Dataset-CAC40 very successful. The success of PA is rooted in the excellent calibration of the indicators, as highlighted by the 29 scatter plots provided in appendix. The danger zones were very accurately defined and the structure of the (MDD vs. Indicator Value) scatter plots is for most indicators very regular, both in the in-sample and out-of-sample periods. Moreover the small number of assets inside Dataset-CAC40, resulting in a small rolling window, allowed the indicators the have many usable calibration points inside the calibration period (the red dots in the scatter plots), which boosted the accuracy of the determination of the danger zones even more for all the 29 financial crisis indicators. In Figure 5a, we see that the Sharpe of PA is 0.40, while the Sharpe of PP is only 0.19. While PA has an annualized volatility similar to the one of PP, the overall performance of PA jumps to 11%, while it was only 6% for PP. Even though PA and PA have a similar MDD (the MDD of PA is slightly better: 0.31 against 0.32), the Calmar ratio of PA (0.37) is much better than the Calmar ratio of PP (0.20). We also notice by examining IR that the active strategy governing PA takes the right decisions at the right time. It does not sell the ETF shares often, but when it does it is in anticipation of crises and drop in ETF prices that did happen, especially in 2011 and late 2015. It is also fully invested ($TR = 1$) at the right times of market growth, which boosted the performance of PA. This is confirmed by Figure 5c, which shows the spikes in the value of Γ happening at the right times. When we switch our attention to Figure 5b which shows PA and 50,000 paths of PR, the success of our active systematic trading strategy is very impressive. Because the active strategy sold the shares in PA just at the right moment in anticipation of a significant drop in the CAC40 index in late 2011, probably a consequence of the the European Debt Crisis, the value of the active portfolio soars above the random paths. PA beats 100% of the PR paths in terms of Sharpe ratio, and the average of the Sharpe for the random paths is only 0.19. PA is also less volatile than all the random paths, even though the volatility of PA at 0.26 is close to the average volatility of PR, which is 0.28. PA performs better than all the random paths in terms of overall performance and in terms of Calmar ratio. Even when we examine the MDD, which is usually the weak point of PA because it may contain no cash at all, while PR does often keep some (we recall that PP always keep its cash), the success of PA is striking. Indeed, PA has an MDD of 0.31 while the average of the random paths' MDD is 0.33 and it beats the PR paths in terms of MDD 99.9% of the time.

The results obtained for Dataset-SP500 ($\mathscr{T} = 20$, $\mathscr{S} = 75$) are presented in Figure 6a, Figure 6b and Figure 6c. For this dataset, the rolling window was made of 462 days and the calibration period was therefore 512 days, according to Formula (10). The active trading strategy governing PA issued 934 buy orders, 748 stay orders and 162 sell orders. The calibration of the financial crisis indicators was generally good, as we can see with the graphs in appendix for the SP500 index and the indicators of both the α-series and the β-series. Therefore, the forecasts of the indicators were often accurate, which resulted in the right decisions taken at the right times by the active strategy. Since there were few large drops in the value of the SP500 during our out-of-sample prediction period, there were few sell orders given by the strategy and the IR

graph on Figure 6a shows that we are most of time fully invested (i.e no cash left in PA). In the rare instances when the strategy did decide the sell the ETF shares, those decisions were taken at the right time, as seen in the graph of Γ in Figure 6c as well, in anticipation of significant drops in the index, which is good and underlines the predictive power of the aggregated signal produced by our 29 financial crisis indicators and the added value of the systematic trading strategy based on them. The performance of PA is 19.3% and beats the performance of PP which is only 16.6%. PA is slightly less volatile than PP, which again is a good result and the Sharpe ratio of PA reaches 0.90 while PP had only 0.72 for a Sharpe ratio. As we have seen with the previous indices, in the case of the SP500 too PA has a slightly higher MDD than PP. This is due to the fact that PA is most of the time fully invested, while PP still holds its cash. As a result, the Calmar of PA is similar and only marginally higher than the Calmar of PP. Switching our attention to Figure 6b, we can compare PA to 50,000 paths of PR. PA beats the random paths in terms of Sharpe ratio 100% of the time, is less volatile than all the random paths as well and achieves a better performance 99.97% of the time. Those are very reassuring results. In terms of MDD, as we expected, PA tends to be a little disappointing and beats the random paths of PR only 22% of the time. However, since PA performs overall so much better than the paths of PR, it still manages to beat the random paths 97.18% of the time in terms of Calmar, which is a remarkable result.

We present the results for Dataset-NASDAQ ($\mathscr{T} = 15$, $\mathscr{S} = 80$) in Figure 7a, Figure 7b and Figure 7c. For this dataset, the rolling window was made of 76 days and the calibration period was therefore 500 days, according to Formula (10). The active trading strategy governing PA issued 1533 buy orders, 287 stay orders and 36 sell orders. The calibration of the 29 financial crisis indicators was mostly good, as we can see in appendix for the NASDAQ, with most scatter plots (MDD vs. Indicator Value) featuring the usual bell-shape. Besides, the structure of the red dots (in-sample) and blue-dots (out-of-sample) is similar, which validates the possibility of forecasting the future by studying the past in the case of the Dataset-NASDAQ. The NASDAQ index was mostly in a pattern of growth from 2009 to 2016, without any large scale market downturn, therefore our active investment strategy has issued mostly buy and stay orders and very few sell orders, mostly in the first half of 2009, as we can see on Figure 7a and Figure 7c. The consequence of this is that PA and PP perform in a similar fashion, with PA still keeping a clear advantage, because the few sell orders were issued at an appropriate time. Those few sell orders issued at the right time did not however have a massive positive impact on the quality of the results provided by PA, like it was the case when considering the CAC40 index. It is a little disappointing that the active strategy governing PA did not issue sell orders in late 2015 and early 2016, when a possible larger drop in the value of the NASDAQ becomes a possibility, but it did not change much the fact that PA and PP perform mostly in a similar fashion because the out-of-sample forecasting period that we chose did not feature major market events that we could have accurately predicted and acted upon. The overall performance of PA and PP is very close, with a slight advantage for PA, essentially explained by the fact that PA was fully invested ($IR = 1$) for most of the out-of-sample period, while PP was static and kept its cash, which earned only the Libor. PA and PP have almost identical volatility as well, which explains that they also have similar Sharpe ratios: 0.88 for PA and 0.84 for PP. PP has a slightly lower MDD than PA because of the cash it contains which acts as a stabilizer, and that explains the slight advantage in terms of MDD that PP holds over PA, while PA holds a slight performance advantage as we have explained. The study of the random paths of PR and their comparison to PA confirms our analysis that PA did not get a chance, for this index over this time period, to predict many crises because there were indeed few to predict. The active strategy still manages to do better than the random paths in a significant and reproducible manner, proving the validity

of our approach. Indeed, PA beats the random paths 99.9% of the time in terms of Sharpe ratio, has an overall performance better than the PR paths in 82% of the cases and achieves a better Calmar ratio than the PR paths more than 66% of the time.

Finally, the results obtained for Dataset-SHSZ300 ($\mathscr{T} = 10$, $\mathscr{S} = 70$) are presented in Figure 8a, Figure 8b and Figure 8c. For this dataset, the rolling window was made of 162 days and the calibration period was therefore 500 days. The active trading strategy governing PA issued 1063 buy orders, 484 stay orders and 228 sell orders. Even though PA manages to produce fairly good results over the whole period of the out-of-sample forecasting period, the study of the graphs in Figure 8a and the graph of Γ in Figure 8c reveals that the quality of the financial crisis forecasts provided by our 29 financial crisis indicators can probably be made better in the case of the SHSZ300 index. Indeed, the large drop in the value of the index in 2015 is not anticipated and the times when $IR = 0$ are not always perfectly well in sync with the times when the SHSZ300 index experiences a drop in value. This relatively poor performance of our financial crisis indicators when applied to the Chinese index, in comparison to their excellent behavior when applied to the other four equity indices of this study, takes its roots in the poor quality of the calibration of the indicators, as we can see in the appendix where the scatter plots (MDD vs. Indicator value) are presented for all our 29 financial crisis indicators of both the α-series and the β-series when applied to the SHSZ300 index. Indeed, many of those scatter plots do not feature the usual bell shape, as we have discussed before, and the structure of the in-sample graph (red dots) is not stable and preserved into the out-of-sample period (blue dots), thus rendering the calibration useless and the determination of the danger zone of many of the indicators meaningless for forecasting purposes. Fortunately, some of our financial crisis indicators are properly calibrated, but many are not and extreme cases of deformities in the scatter plots for our financial crisis indicators applied to the SHSZ300 index can be found, for example, in the α-series, graph (n) (reference : $\mathscr{R}_3$; matrix: correlation weighted by market capitalization) or in the α-series, graph (h) (trace of the correlation matrix weighted by market capitalization). In those instances the scatter plot is almost bi-modal, with the high values of MDD in the in-sample calibration period corresponding to completely different values of the indicator than in the out-of-sample forecasting period. Of course, when there is little stability for a given index in the behavior of our indicators over time, then accurately forecasting the future by looking at the past becomes an impossibility. Regardless of the difficulties encountered in the calibration of several of our financial crisis indicators, PA in the case of the SHSZ300 index still manages to produce fairly good results. That is the advantage of using the aggregated signal coming from our 29 financial crisis indicators. Even though a large amount of them might in some cases fail to be calibrated properly, enough remain useful to provide the investor holding PA with enough accurate previsions to beat PP and most the random paths PR. Indeed the Sharpe of PA still reaches 0.49 while PP only had a Sharpe of 0.29, PA is slightly less volatile than PP and the performance of PA (15%) beats the performance of PP (10%). While the MDD of PA is marginally higher than the MDD of PP, the Calmar ratio of PA (0.32) still shows a significant improvement with respect to the Calmar ratio of PP (0.23). When considering random paths of PR, as shown in Figure 8b, the results that we obtain are very reassuring and attest to the resilience of our framework that is still able to produce useful active trading strategies, even when many of the financial crisis indicators upon which they rely are giving flawed signals. Indeed, PA beats the PR paths 99.9% of the time in terms of Sharpe ratio and volatility and 99.5% of the time in terms of performance. The MDD of the random paths are usually better than the MDD of PA, but the advantage that PA hold over the 50,000 random paths in terms of performance still permit our active strategy to beat the PR paths 97.2% of the time in terms of Calmar ratio.

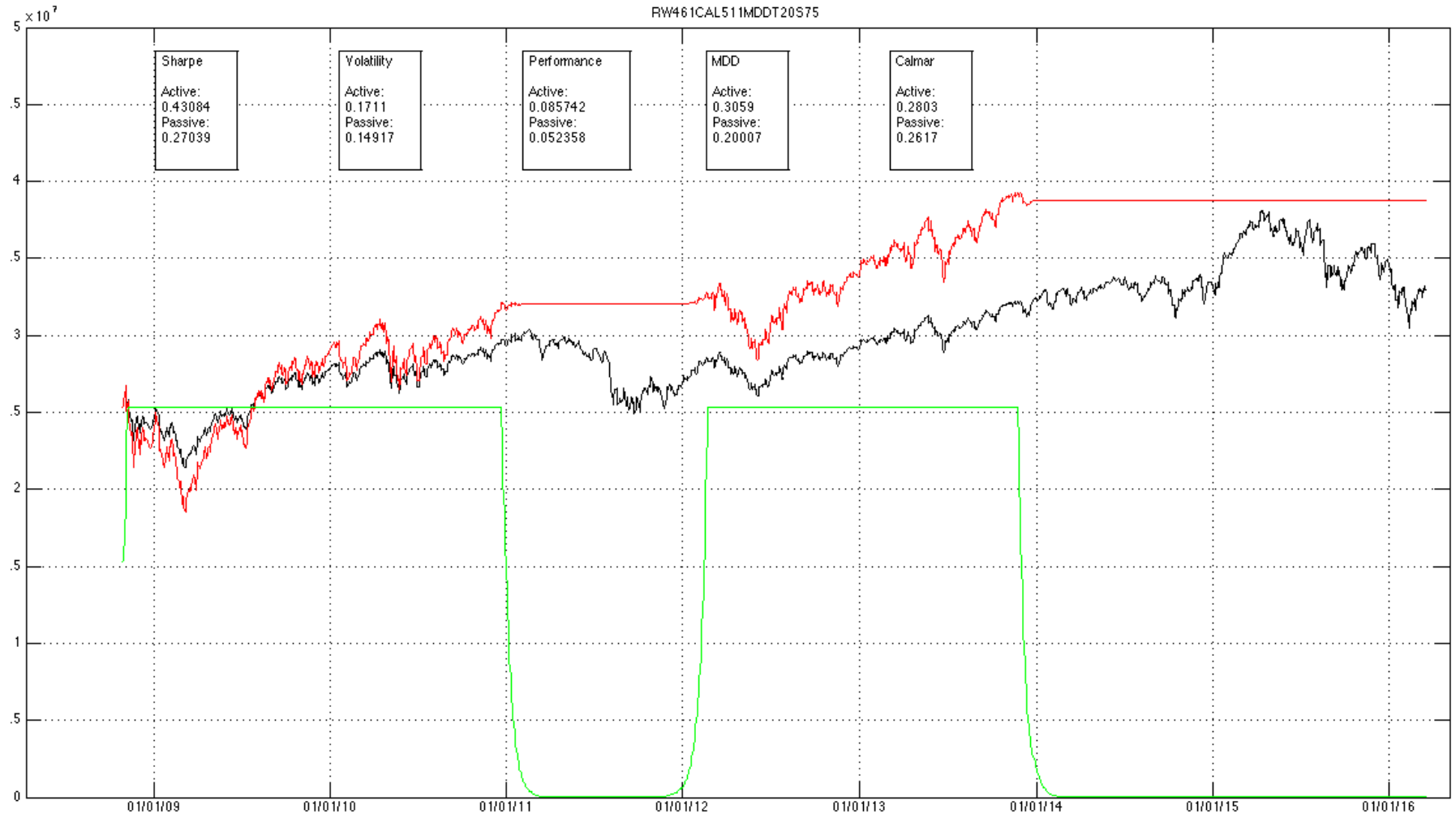

Figure 4a: Dataset-BE500. Red: PA; Black: PP; Green: IR

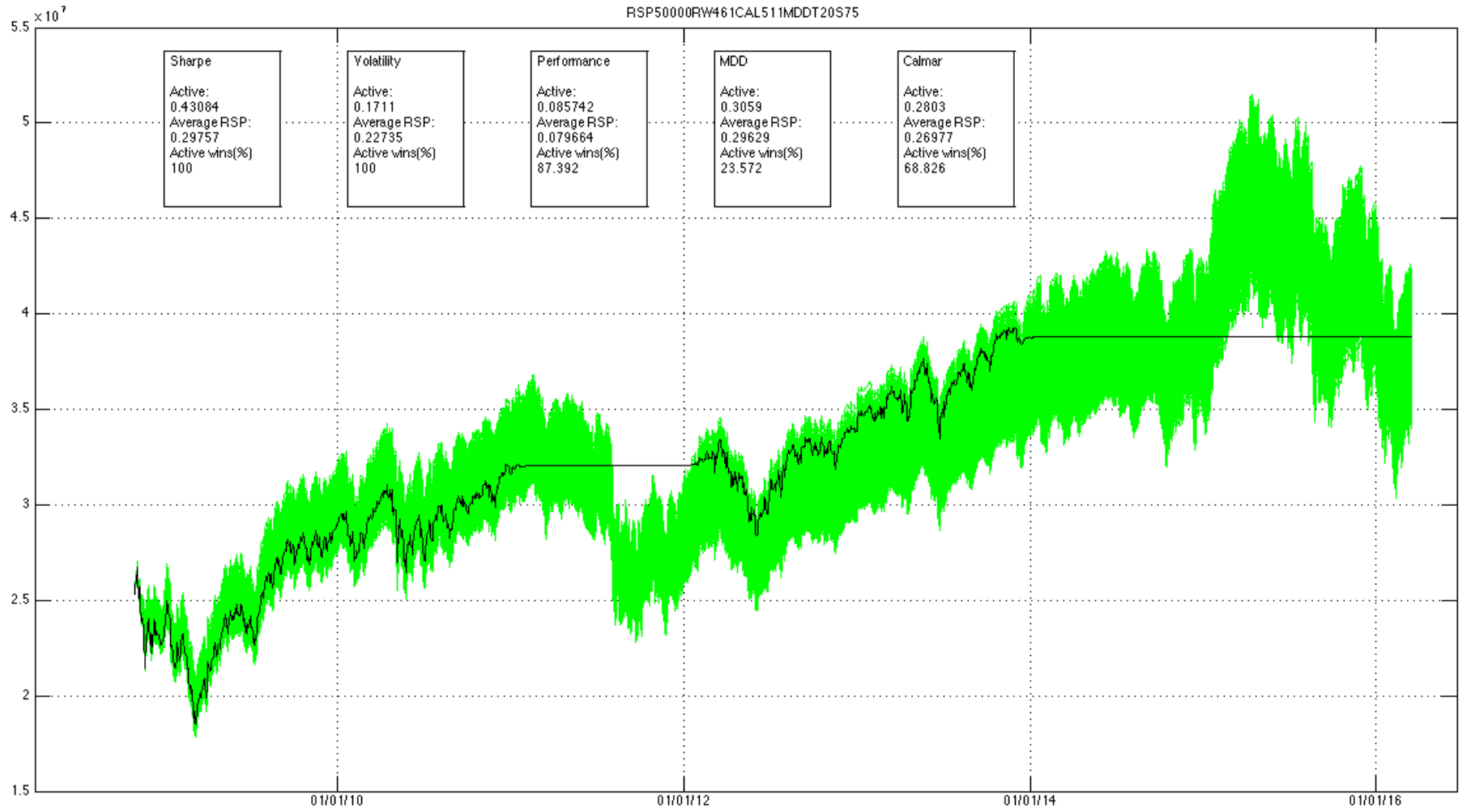

Figure 4b: Dataset-BE500. Black: PA; Green: 50,000 paths of PR

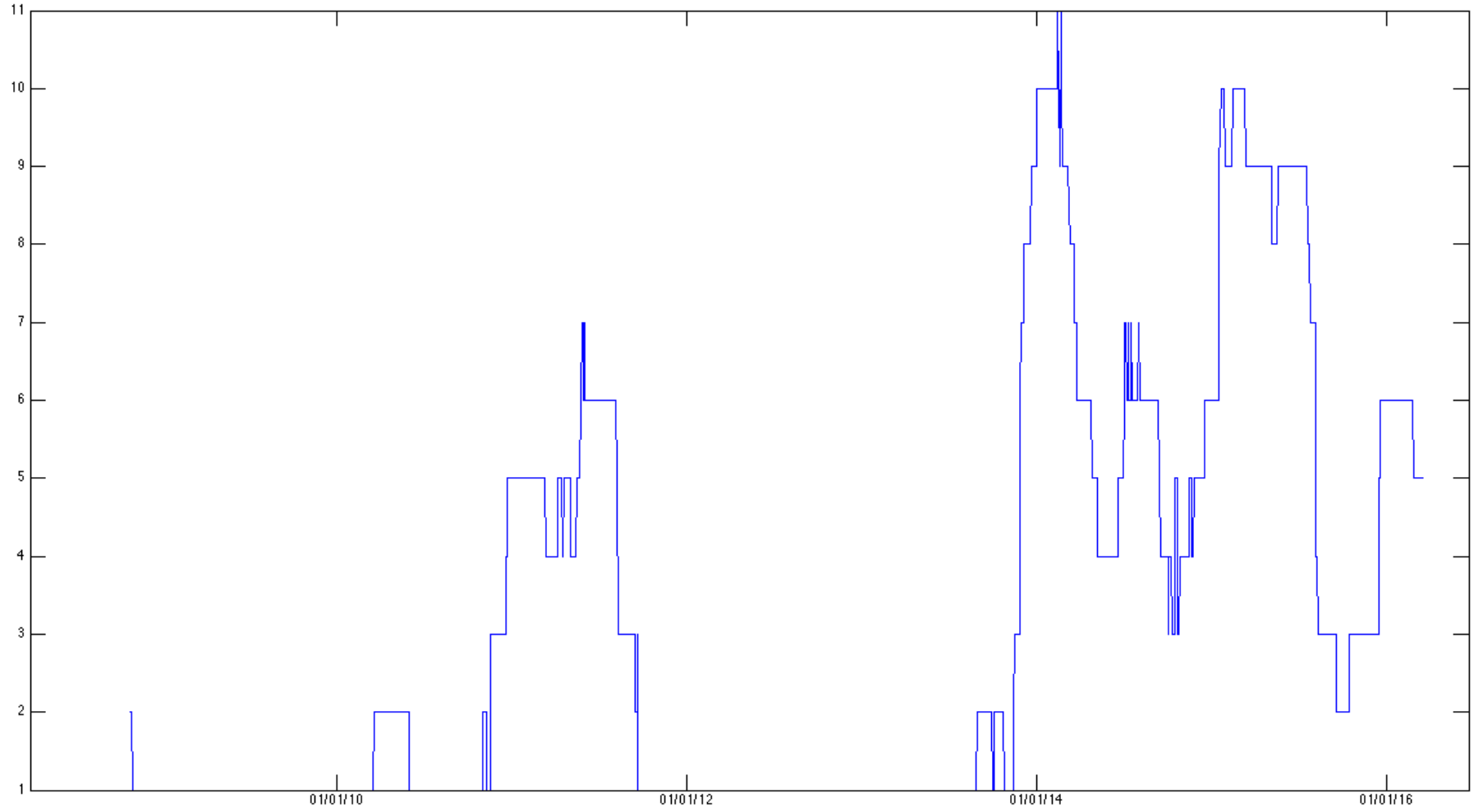

Figure 4c: Graph of Γ for PA on Dataset-BE500

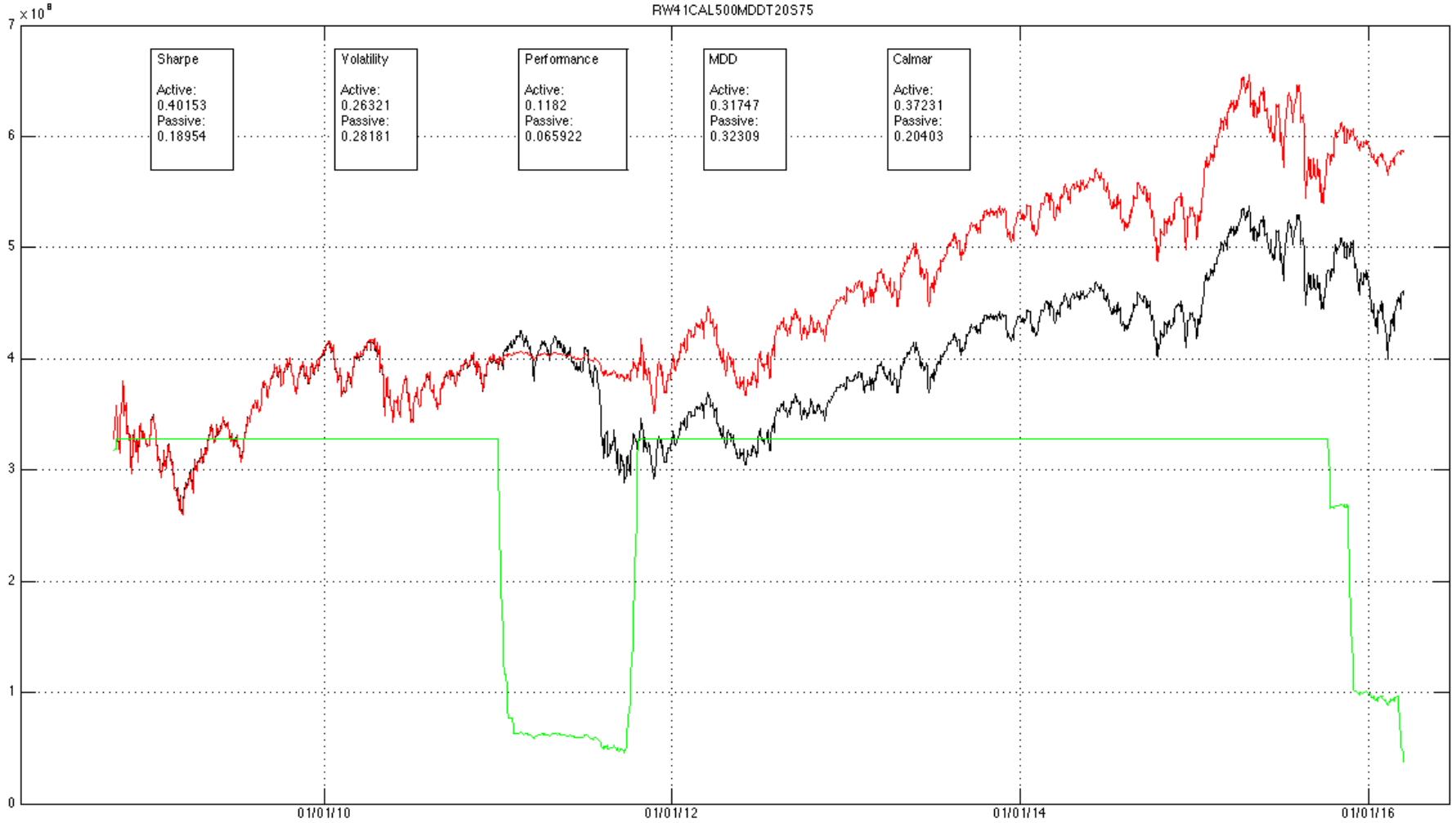

Figure 5a: Dataset-CAC40. Red: PA; Black: PP; Green: IR

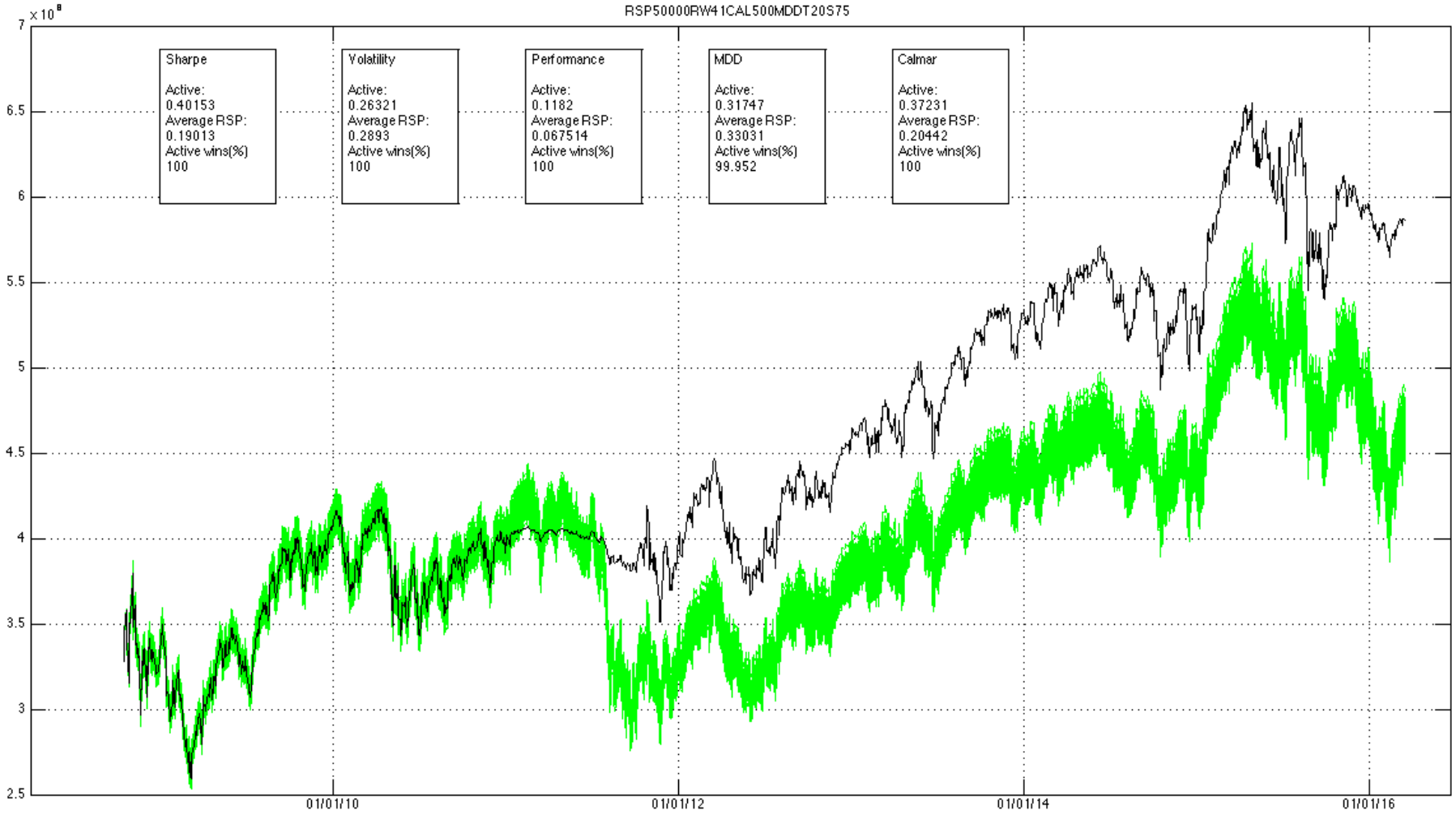

Figure 5b: Dataset-CAC40. Black: PA; Green: 50,000 paths of PR

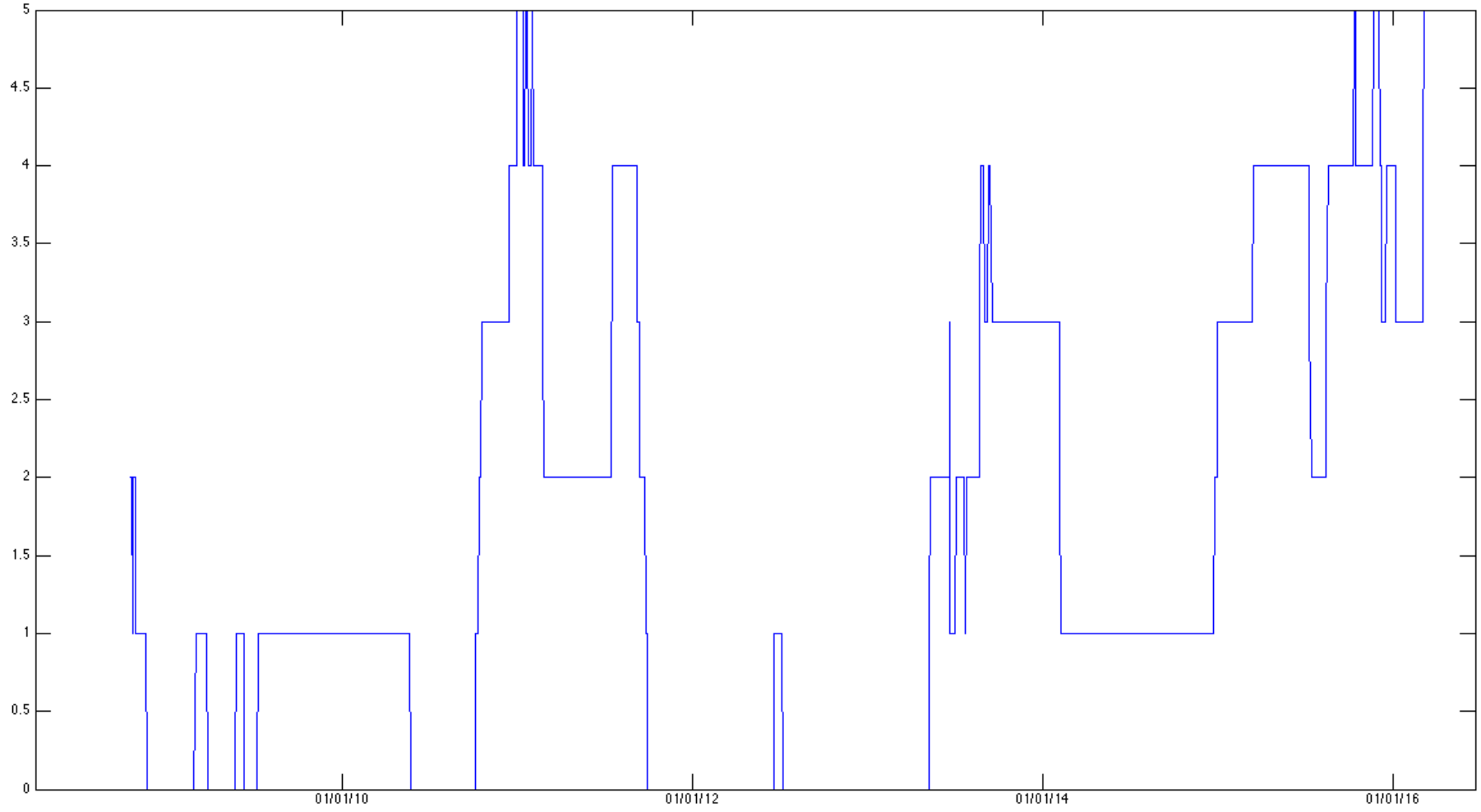

Figure 5c: Graph of Γ for PA on Dataset-CAC40

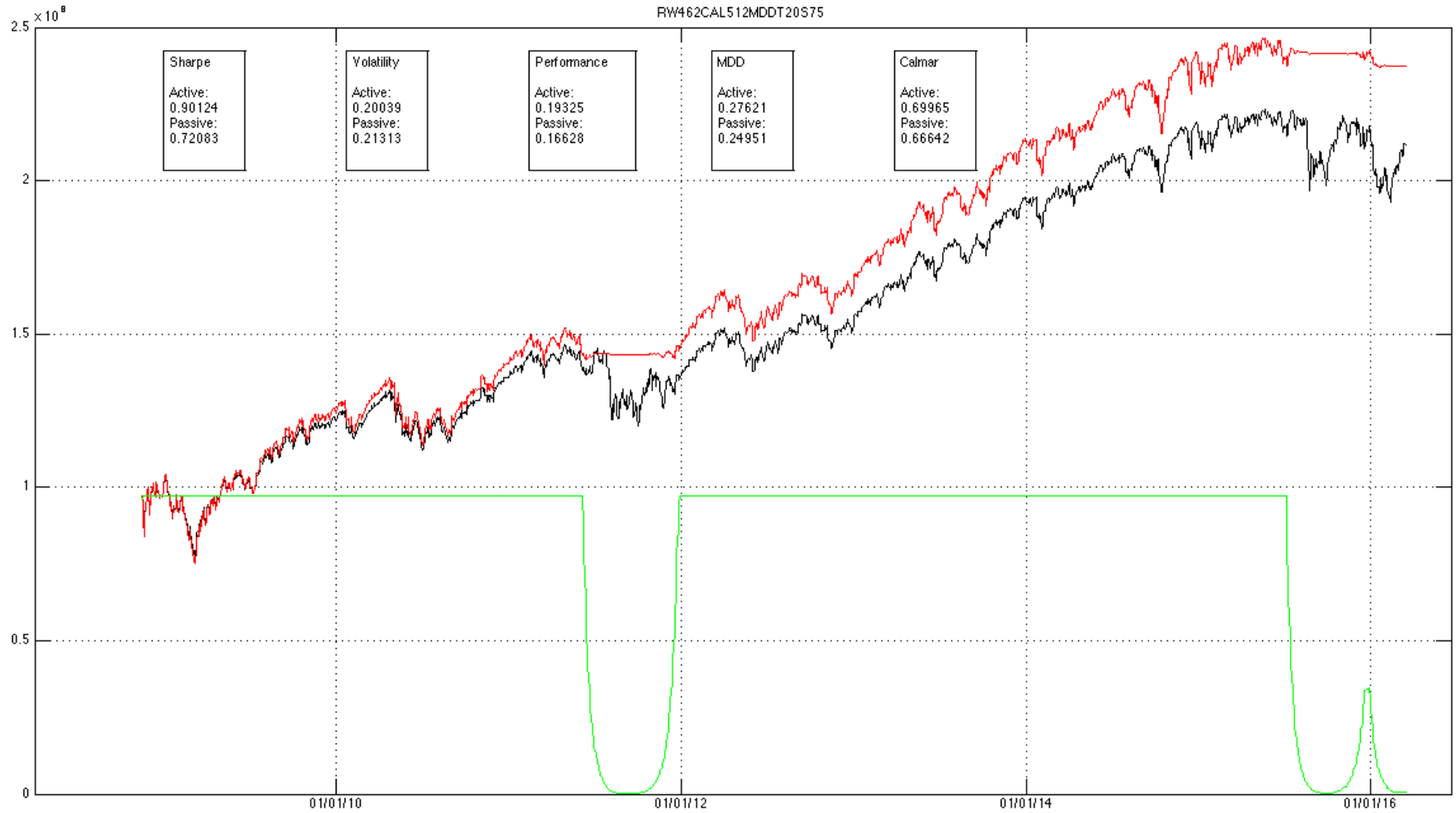

Figure 6a: Dataset-SP500. Red: PA; Black: PP; Green: IR

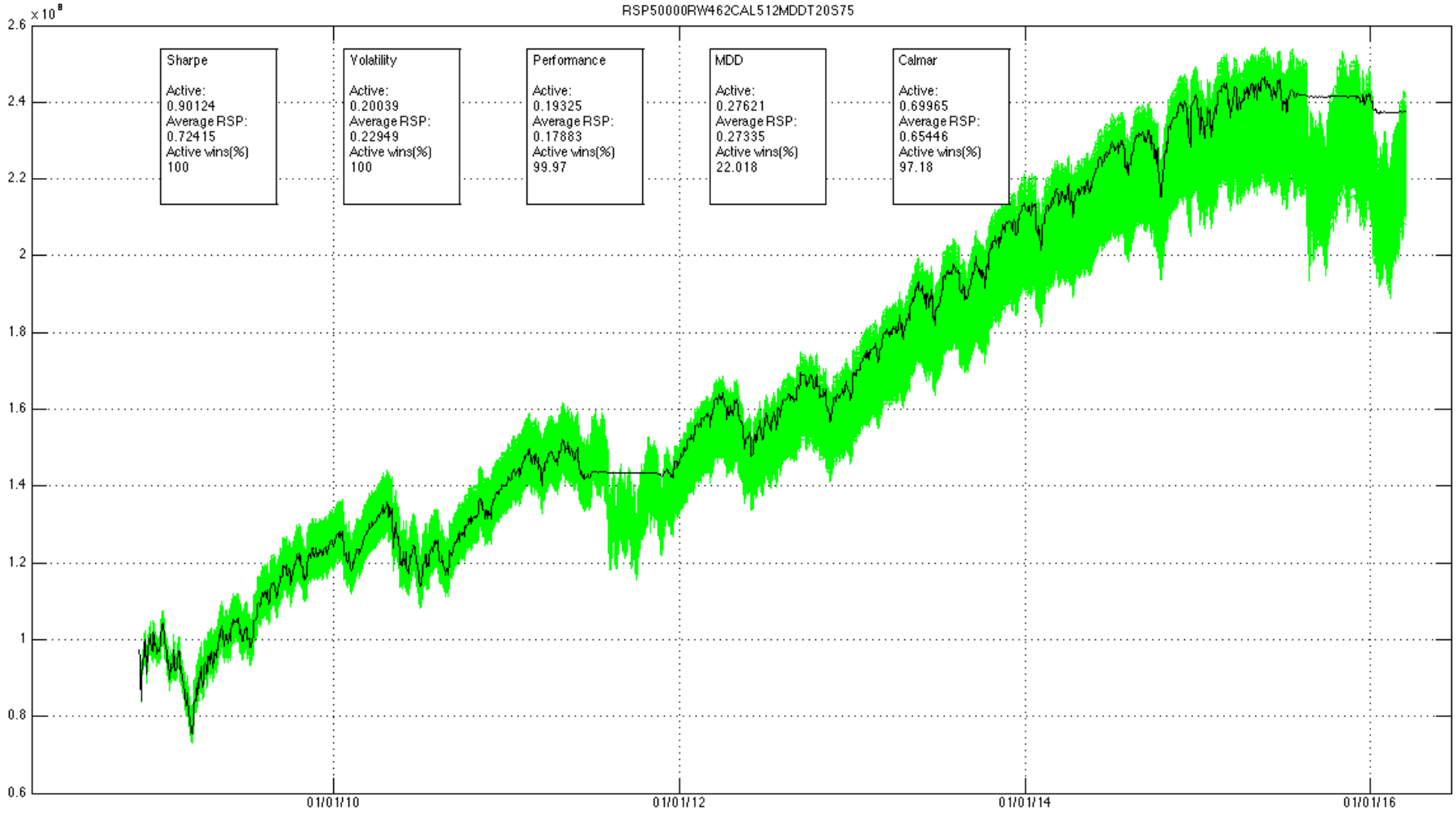

Figure 6b: Dataset-SP500. Black: PA; Green: 50,000 paths of PR

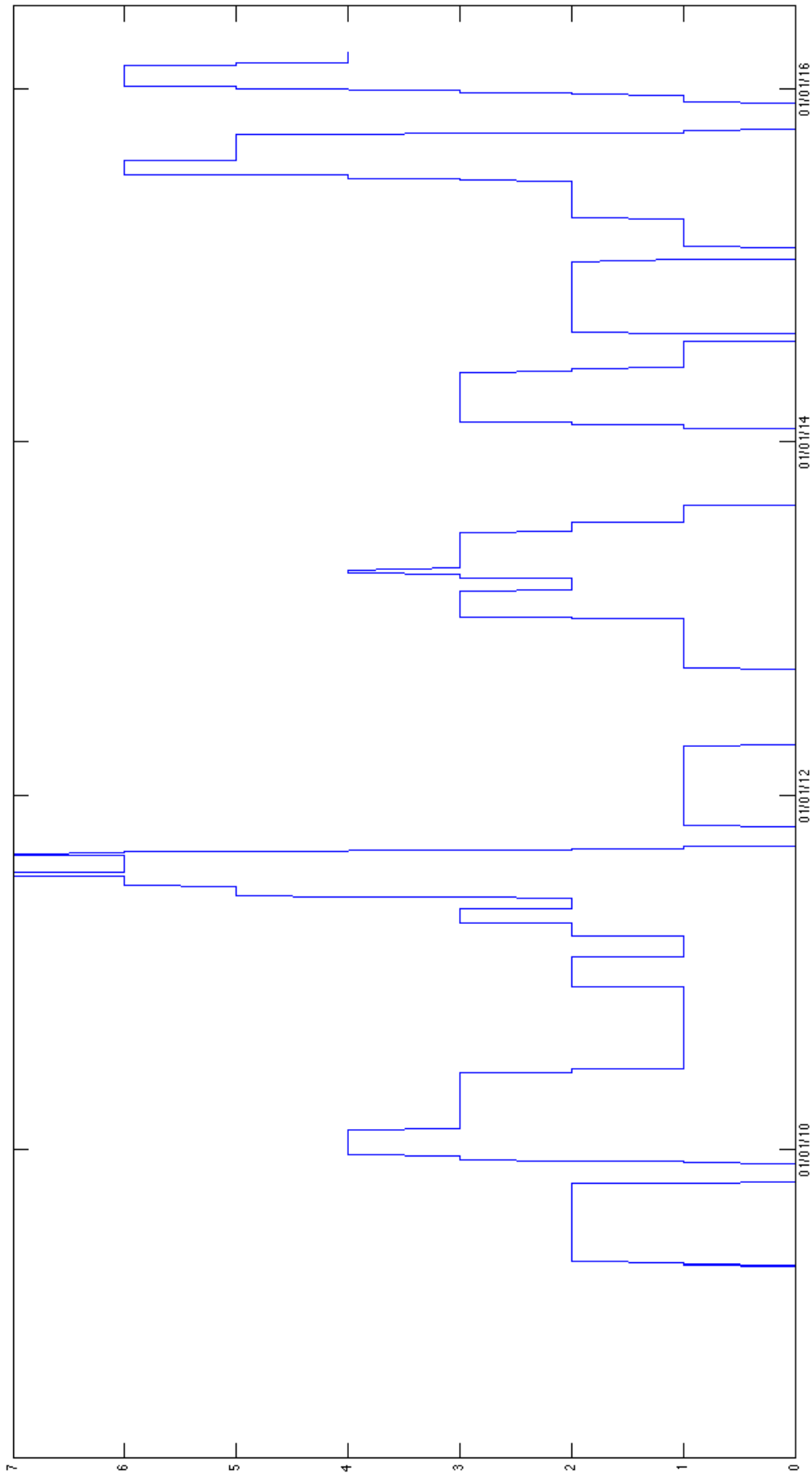

Figure 6c: Graph of Γ for PA on Dataset-SP500

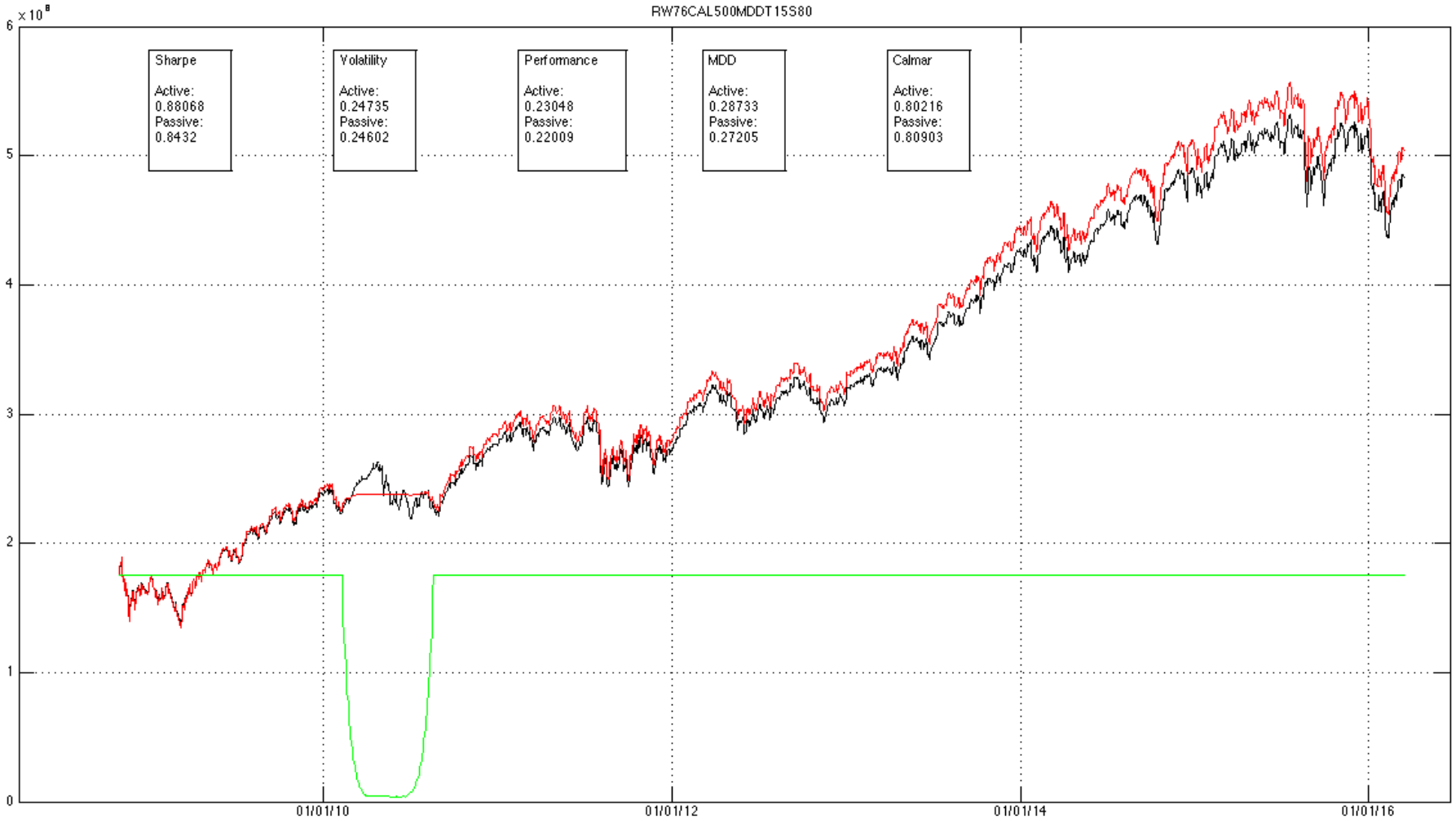

Figure 7a: Dataset-NASDAQ. Red: PA; Black: PP; Green: IR

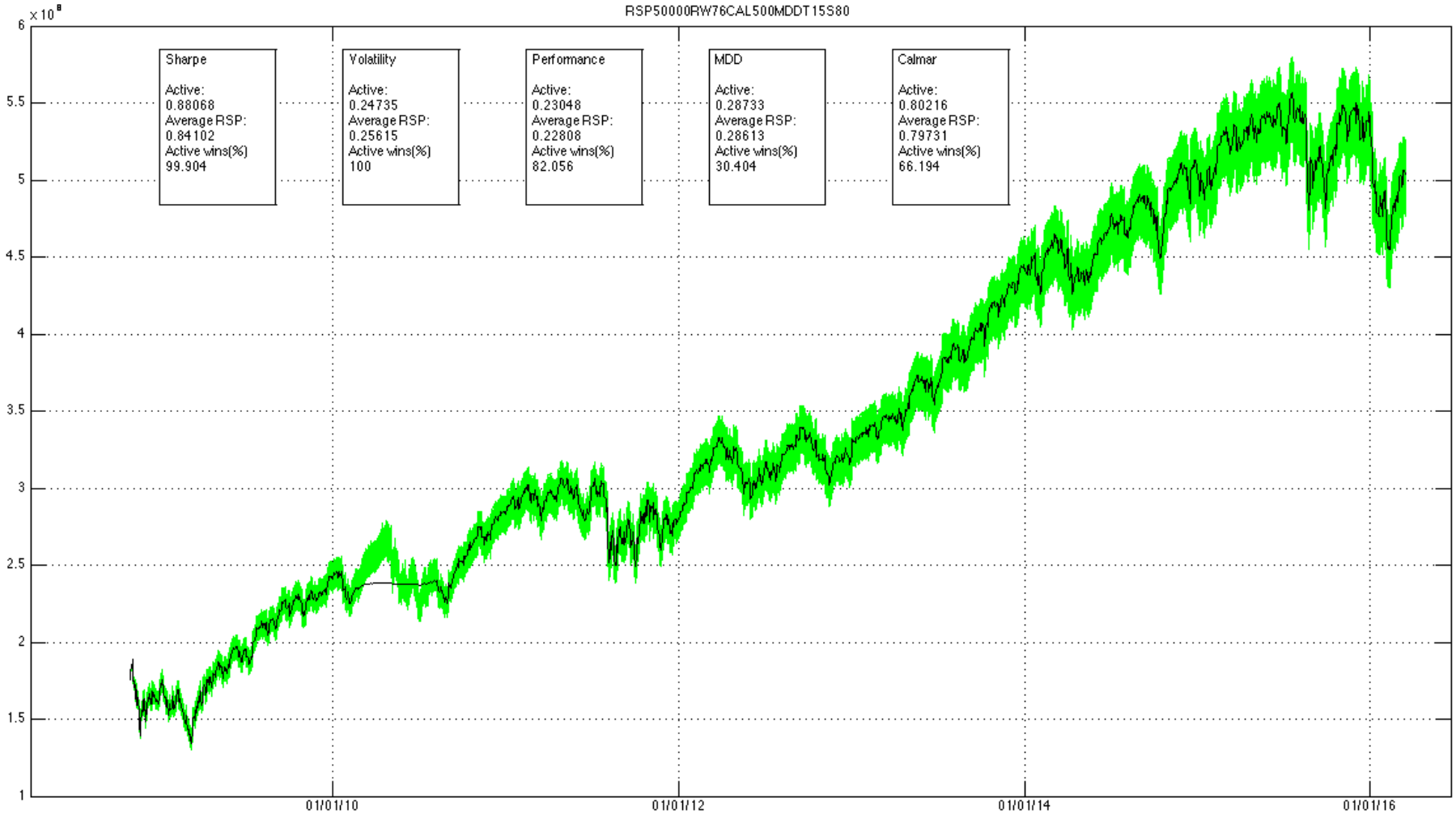

Figure 7b: Dataset-NASDAQ. Black: PA; Green: 50,000 paths of PR

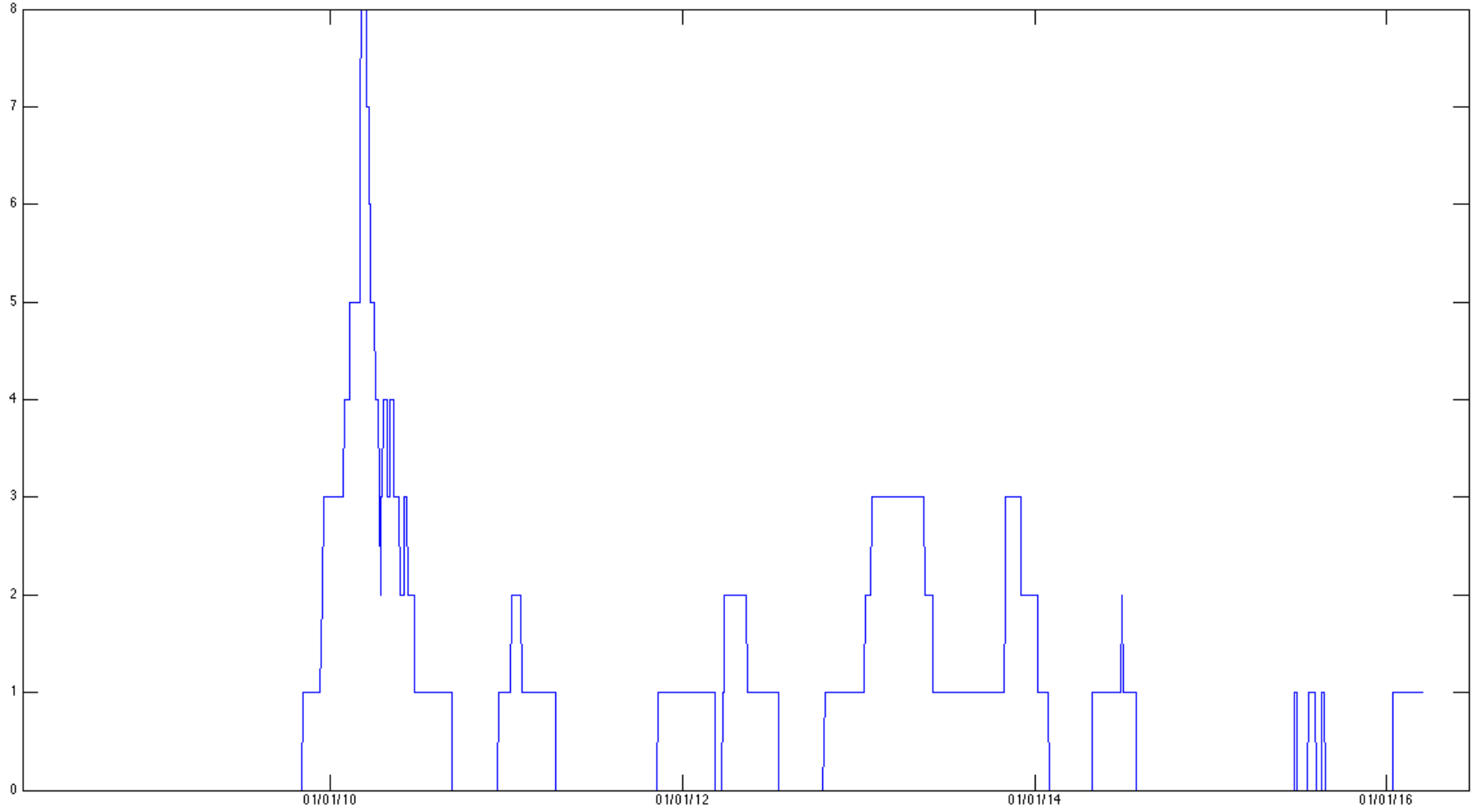

Figure 7c: Graph of Γ for PA on Dataset-NASDAQ

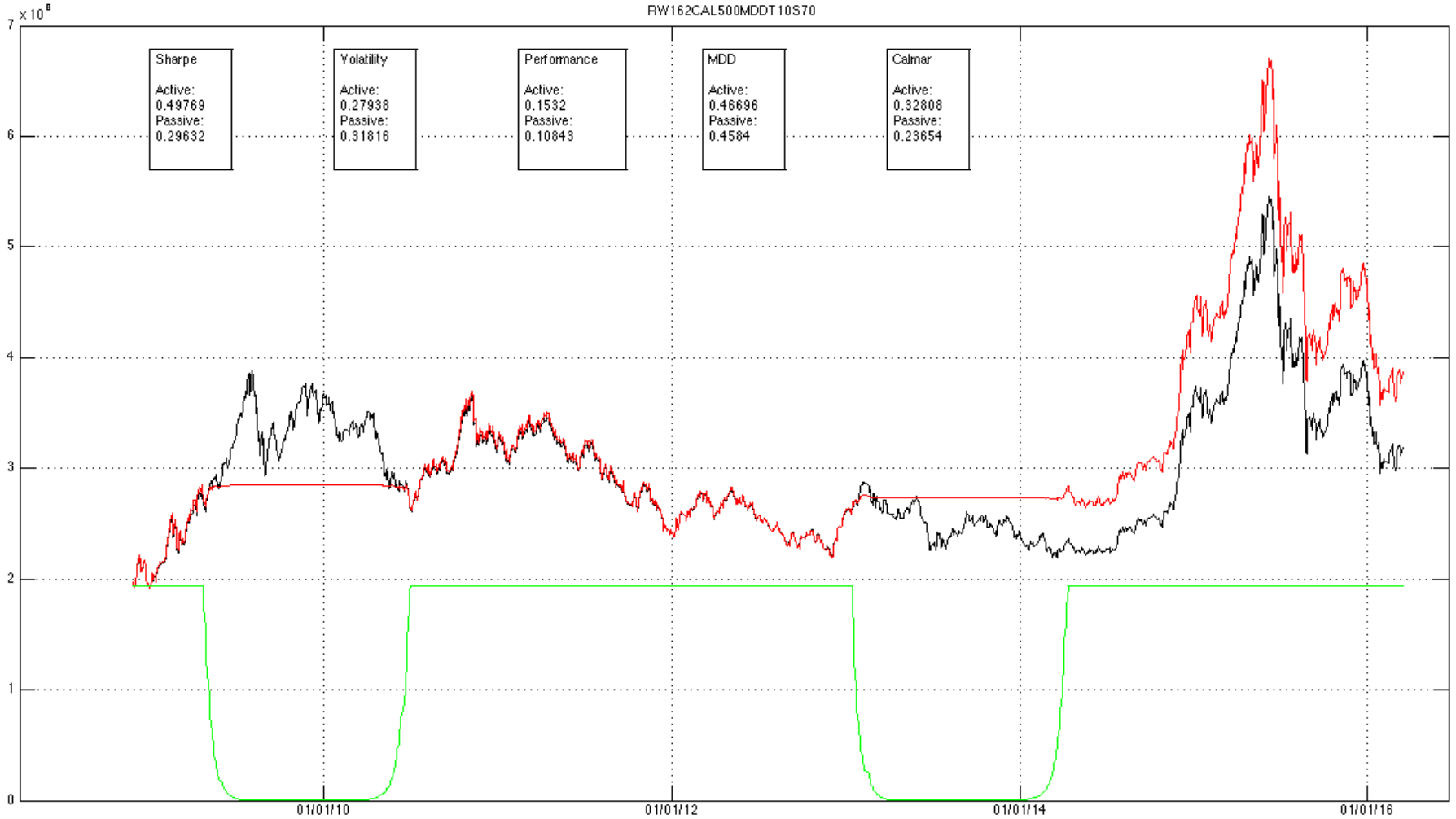

Figure 8a: Dataset-SHSZ300. Red: PA; Black: PP; Green: IR

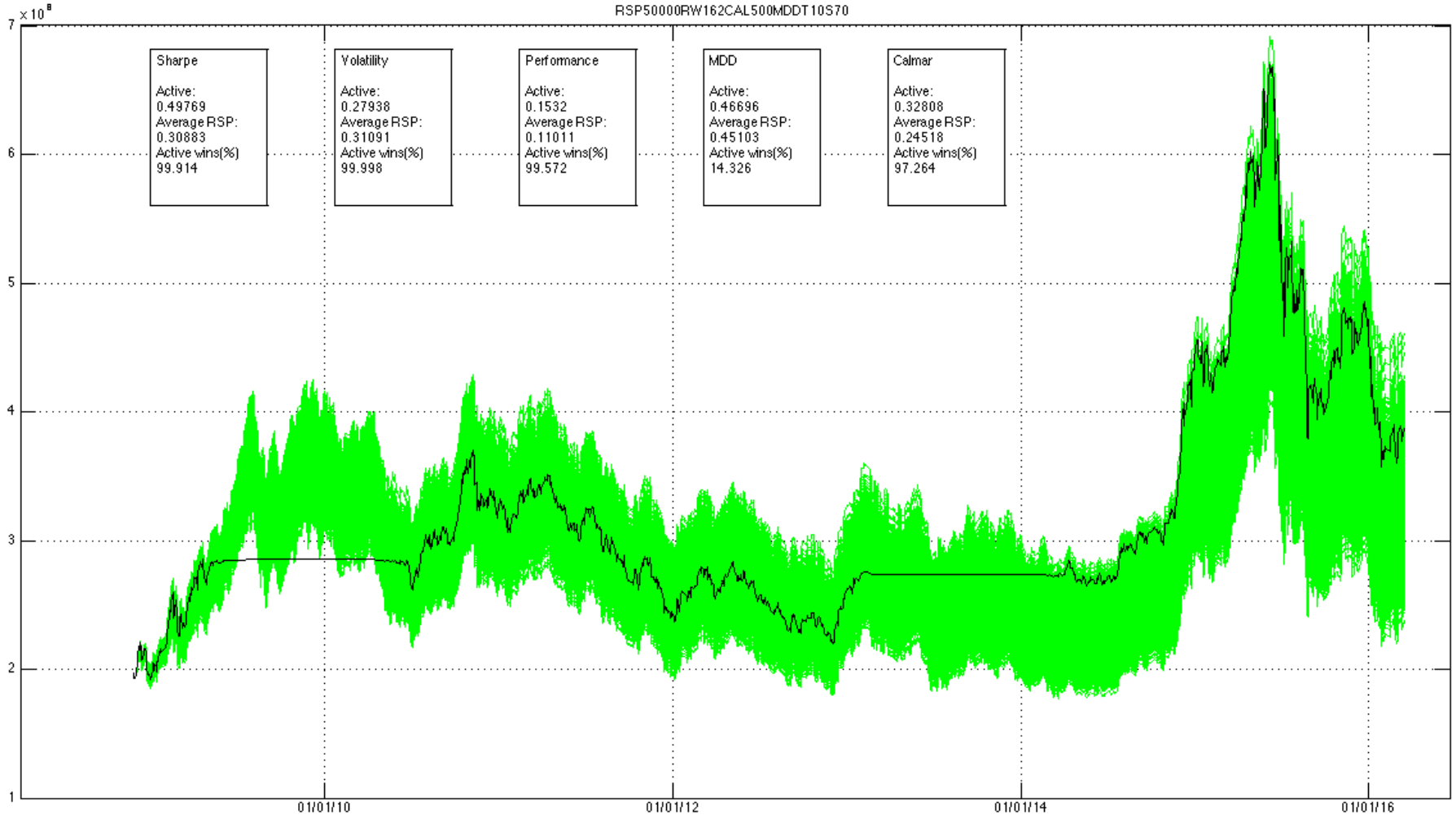

Figure 8b: Dataset-SHSZ300. Black: PA; Green: 50,000 paths of PR

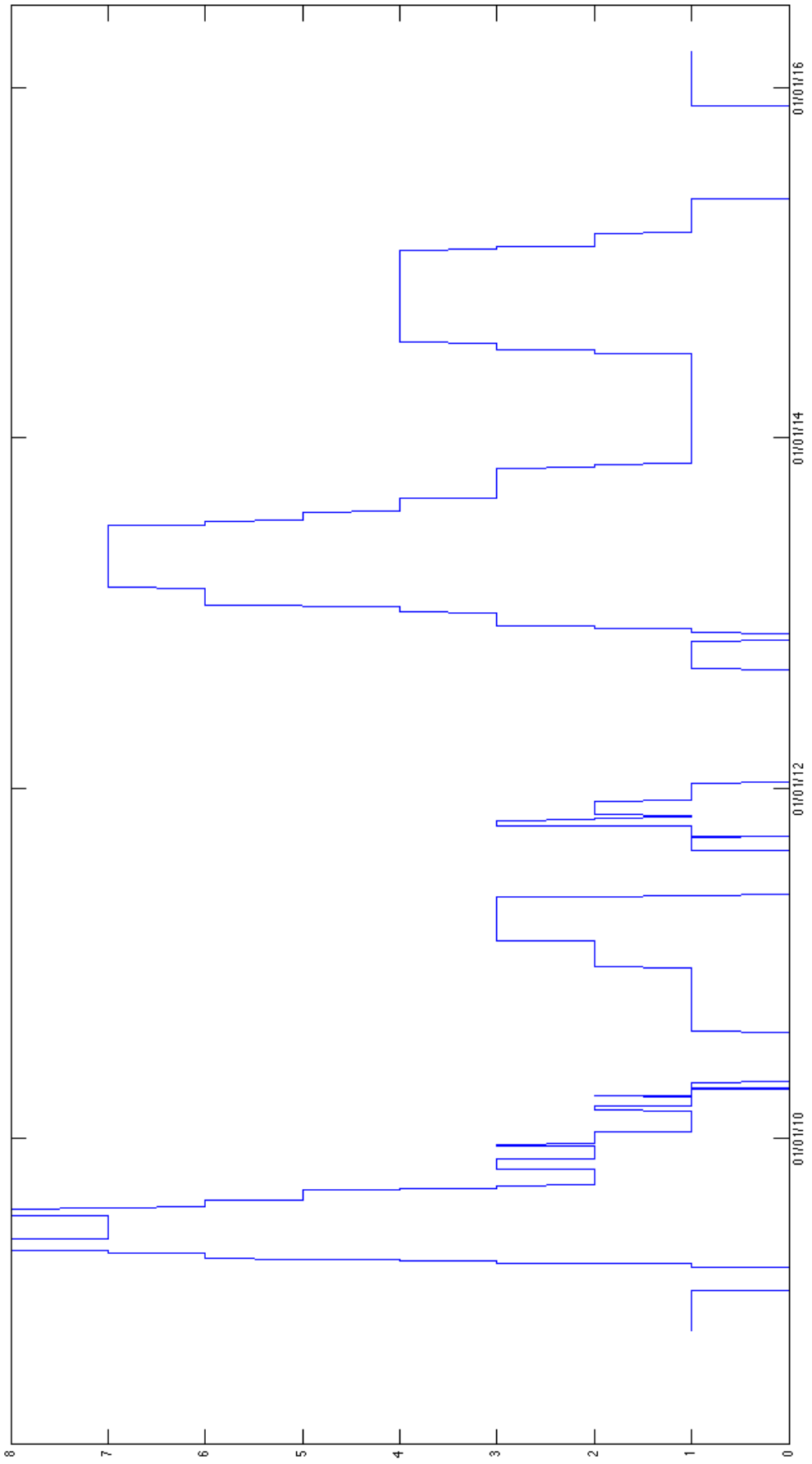

Figure 8c: Graph of Γ for PA on Dataset-SHSZ300

7 Conclusion

As a conclusion, we would like first to underline the excellent results provided by our systematic trading strategies based on the forecasting power of our 29 financial crisis indicators, both of the α-series and of the β-series. For every one of the five datasets that we have built by considering a major equity index and its respective stock components (BE500, CAC40, SP500, NASDAQ, SHSZ300), our systematic trading strategies are always able to beat in a clear and reproducible fashion a passive buy-and-hold strategy. Our active systematic investment strategy is also able to beat random strategies, which feature the same proportion of 'buy', 'sell' and 'stay' orders, in an overwhelming majority of the cases.

Indeed, for the equity indices that we have considered in this study, the active portfolio PA beats the passive portfolio PP and the random paths PR in terms of Sharpe ratio, performance, volatility and Calmar ratio. Only in terms of maximum-draw-dawn do the passive and random strategies sometimes give better results than the active one but this is only because, by design in this study, PP always contains some cash and a PR path usually contains cash as well, while PA may be fully invested most of the time. Only in the case of the Chinese SHSZ300 index, did some of our financial crisis indicators provide flawed predictions, regardless of the skills deployed by the operator in choosing the right parameters $\mathscr{T}$ and $\mathscr{S}$. That may have been due to the poor quality of the historical data on the Chinese market or the fact, which definitely introduced survivorship bias in our study, that we had to consider less than half of the current 300 components because of the profound transformations of the Chinese market over the last 10 years.

To summarize our method, we start by establishing a simple rule for the length of the rolling window (Formula (1)) for all of our five datasets and we proceed to establishing another simple rule for the length of the calibration period (Formula (10)). We then choose two parameters that govern the behavior of a systematic trading strategy. The first parameter is the MDD Threshold $\mathscr{T}$, the value of which determines whether we wish to bet on accurately forecasting a large number of small crises or a small number of large crises. The second parameter, the Indicator Sensitivity $\mathscr{S}$ is then chosen and its value determines the level of aggressiveness of a systematic trading strategy. Low value of $\mathscr{S}$ will produce very aggressive strategies that will start converting the ETF shares into cash inside the active portfolio at the first sign of danger, because the red flags provided by the indicators will be easier to obtain. Higher values of $\mathscr{S}$ will make a systematic trading strategy more calm and patient because the red flags provided by the financial crisis indicators will be harder to achieve and the strategy will therefore wait to take action and start converting the shares into cash until the risk of a crisis happening within the 100 days forecasting horizon of our financial crisis indicators becomes impossible to ignore.

The choice of the two parameters $\mathscr{T}$ and $\mathscr{S}$ is robust and once an operator has chosen a value for $\mathscr{T}$ and $\mathscr{S}$, using his or her experience and knowledge of the equity index being considered, then those parameters may be used for similar equity indices over large periods of time, excluding any possibility of over-fitting our model. In other words, it is the skill of the operator setting-up those strategies, not luck, which is the determining factor that makes the difference between a winning and a failing active trading strategy.

Future developments of this work could include designing a real-time system of ratings in order to give more weight in the decision and the computation of Γ at a given time to the indicators, among the 29 we have built, that have had the most accurate forecasts in a given past period. Indeed, in our work in its present form, all those expert's opinions carry the same

weight, regardless of the past accuracy of their prediction and their respective proportions of false positive (more rarely false negative) errors regarding financial crisis prediction. In a future work, one could envision giving all those indicators a rating on a given scale and then modulate in a strategy's decision process the importance of each indicator with respect to its rating. We also plan to incorporate transaction costs and market frictions in our study. Indeed, those transaction costs are especially important for smaller transactions and providing a proper modeling of their influence is important to give our trading strategies a better chance of being useful regardless of the size of the portfolio that they are being applied to. Concerning the question of scalability again, we also plan to take into account the impact that the investors have on the market when they execute sell or buy orders. Even though they are price takers and not market makers, their actions do have a small influence on the order book and may in particular create slippage, no matter how small the orders are in comparison to the size of the market. That effect will in the future be integrated to our approach in order to make it fully scalable.

References

[1] Abbasbandy S. (2003) "Improving Newton-Raphson Method for Nonlinear Equations by Modified Adomian Decomposition Method", *Applied Mathematics and Computation*, 145(2-3), pp. 887-893

[2] Brock W., J. Lakonishok and B. LeBaron (1992) "Simple Technical Trading Rules and the Stochastic Properties of Stock Returns", *The Journal of the American Finance Association*, 47(5), pp. 1731-1764

[3] Clemen R.T. (1989) "Combining Forecasts: A Review and Annotated Bibliography", *International Journal of Forecasting*, 5(4), pp. 559-583

[4] Douady R. and A. Kornprobst (2017) "An Empirical Approach to Financial Crisis Indicators Based on Random Matrices", *https://arxiv.org/abs/1506.00806*

[5] Farmer J.D and J. Shareen (2002) "The Price Dynamics of Common Trading Strategies", *Journal of Economic Behavior & Organization*, Vol. 49(2), pp. 149-171

[6] Fung W. and D.A Hsieh (1997) "Empirical Characteristics of Dynamic Trading Strategies: The Case of Hedge Funds", *Review of Financial Studies*, 10(2), pp. 275-302

[7] Gençay R. (1998) "Optimization of Technical Trading Strategies and the Profitability in Security Markets", *Economics Letters*, 59(2), pp. 249-254

[8] Golub G.H. and C.F. Van Loan C.F. (2013) "Matrix Computations (4th Edition)", *The Johns Hopkins University Press*, pp. 76-81

[9] Horn R.A and C.R Johnson (2013) "Matrix Analysis (2nd Edition)", *Cambridge University Press*, pp. 242-259

[10] Kwon K.Y. and R. Kish (2002) "Technical Trading Strategies and Return Predictability: NYSE", *Journal of Applied Financial Economics*, 12(9), pp. 639-653

[11] Marchenko V. A. and L.A. Pastur (1967) "Distribution of Eigenvalues for Some Sets of Random Matrices", Mathematics of the USSR-Sbornik, 1(4), pp. 457–483

[12] Pesaran M.H. and A. Timmermann (1995) "Predictability of Stock Returns: Robustness and Economic Significance", *The Journal of Finance*, 50(4), pp. 1201-1228

[13] Ratner M. and R. Leal (1999) "Tests of Technical Trading Strategies in the Emerging Equity Markets of Latin America and Asia", *Journal of Banking and Finance*, 23(12), pp. 1887-1905

Appendices

Dataset-SP500

A UN ; AA UN ; AAP UN ; AAPL UW ; ABC UN ; ABT UN ; ACN UN ; ADBE UW ; ADM UN ; ADS UN ; ADSK UW ; AEE UN ; AEP UN ; AES UN ; AET UN ; AFL UN ; AGN UN ; AIG UN ; AIV UN ; AIZ UN ; AKAM UW ; ALL UN ; ALXN UW ; AMAT UW ; AME UN ; AMG UN ; AMGN UW ; AMP UN ; AMT UN ; AMZN UW ; AN UN ; ANTM UN ; AON UN ; APA UN ; APC UN ; APD UN ; APH UN ; ARG UN ; ATVI UW ; AVB UN ; AVY UN ; AXP UN ; AZO UN ; BA UN ; BAC UN ; BAX UN ; BBBY UW ; BBT UN ; BBY UN ; BCR UN ; BDX UN ; BEN UN ; BF/B UN ; BHI UN ; BIIB UW ; BK UN ; BLK UN ; BLL UN ; BMY UN ; BRK/B UN ; BSX UN ; BWA UN ; BXP UN ; C UN ; CAG UN ; CAH UN ; CAM UN ; CAT UN ; CB UN ; CBG UN ; CBS UN ; CCE UN ; CCI UN ; CCL UN ; CELG UW ; CERN UW ; CF UN ; CHD UN ; CHK UN ; CHRW UW ; CI UN ; CINF UW ; CL UN ; CLX UN ; CMA UN ; CMCSA UW ; CMG UN ; CMI UN ; CMS UN ; CNP UN ; COF UN ; COG UN ; COH UN ; COL UN ; COP UN ; COST UW ; CPB UN ; CRM UN ; CSCO UW ; CTAS UW ; CTL UN ; CTSH UW ; CTXS UW ; CVC UN ; CVS UN ; CVX UN ; D UN ; DD UN ; DE UN ; DGX UN ; DHI UN ; DHR UN ; DIS UN ; DISCA UW ; DLTR UW ; DNB UN ; DO UN ; DOV UN ; DOW UN ; DRI UN ; DTE UN ; DUK UN ; DVA UN ; DVN UN ; EA UW ; EBAY UW ; ECL UN ; ED UN ; EFX UN ; EIX UN ; EL UN ; EMC UN ; EMN UN ; EMR UN ; ENDP UW ; EOG UN ; EQIX UW ; EQR UN ; EQT UN ; ES UN ; ESRX UW ; ESS UN ; ESV UN ; ETN UN ; ETR UN ; EW UN ; EXC UN ; EXPD UW ; EXPE UW ; EXR UN ; F UN ; FAST UW ; FCX UN ; FDX UN ; FE UN ; FFIV UW ; FIS UN ; FISV UW ; FITB UW ; FLIR UW ; FLR UN ; FLS UN ; FMC UN ; FRT UN ; FTI UN ; GAS UN ; GD UN ; GE UN ; GILD UW ; GIS UN ; GLW UN ; GME UN ; GOOGL UW ; GPC UN ; GPS UN ; GRMN UW ; GS UN ; GWW UN ; HAL UN ; HAR UN ; HBAN UW ; HCN UN ; HCP UN ; HD UN ; HES UN ; HIG UN ; HOG UN ; HON UN ; HOT UN ; HP UN ; HPQ UN ; HRB UN ; HRL UN ; HRS UN ; HSIC UW ; HST UN ; HSY UN ; HUM UN ; IBM UN ; ICE UN ; IFF UN ; ILMN UW ; INTC UW ; INTU UW ; IP UN ; IPG UN ; IR UN ; IRM UN ; ISRG UW ; ITW UN ; IVZ UN ; JBHT UW ; JCI UN ; JEC UN ; JNJ UN ; JPM UN ; JWN UN ; K UN ; KEY UN ; KIM UN ; KLAC UW ; KMB UN ; KMX UN ; KO UN ; KR UN ; KSS UN ; KSU UN ; L UN ; LB UN ; LEG UN ; LEN UN ; LH UN ; LLL UN ; LLTC UW ; LLY UN ; LM UN ; LMT UN ; LNC UN ; LOW UN ; LRCX UW ; LUK UN ; LUV UN ; M UN ; MA UN ; MAC UN ; MAS UN ; MCD UN ; MCHP UW ; MCK UN ; MCO UN ; MDT UN ; MET UN ; MHFI UN ; MHK UN ; MKC UN ; MLM UN ; MMC UN ; MMM UN ; MNST UW ; MO UN ; MON UN ; MOS UN ; MRK UN ; MRO UN ; MS UN ; MSFT UW ; MSI UN ; MTB UN ; MUR UN ; NBL UN ; NDAQ UW ; NEE UN ; NEM UN ; NFLX UW ; NFX UN ; NI UN ; NKE UN ; NOC UN ; NOV UN ; NRG UN ; NSC UN ; NTAP UW ; NTRS UW ; NUE UN ; NVDA UW ; NWL UN ; O UN ; OI UN ; OKE UN ; OMC UN ; ORLY UW ; OXY UN ; PAYX UW ; PBCT UW ; PBI UN ; PCAR UW ; PCG UN ; PCLN UW ; PDCO UW ; PEG UN ; PEP UN ; PFE UN ; PFG UN ; PG UN ; PGR UN ; PH UN ; PHM UN ; PKI UN ; PLD UN ; PNC UN ; PNR UN ; PNW UN ; POM UN ; PPG UN ; PPL UN ; PRU UN ; PSA UN ; PVH UN ; PWR UN ; PX UN ; PXD UN ; QCOM UW ; R UN ; RAI UN ; RCL UN ; REGN UW ; RF UN ; RHI UN ; RIG UN ; RL UN ; ROK UN ; ROP UN ; ROST UW ; RRC UN ; RSG UN ; RTN UN ; SBUX UW ; SCG UN ; SEE UN ; SHW UN ; SIG UN ; SJM UN ; SLB UN ; SLG UN ; SNA UN ; SNDK UW ; SO UN ; SPG UN ; SPLS UW ; SRCL UW ; SRE UN ; STI UN ; STJ UN ; STT UN ; STZ UN ; SWK UN ; SWKS UW ; SWN UN ; SYK UN ; SYMC UW ; SYY UN ; T UN ; TAP UN ; TE UN ; TGNA UN ; TGT UN ; THC UN ; TIF UN ; TJX UN ; TMK UN ; TMO UN ; TROW UW ; TRV UN ; TSCO UW ; TSN UN ; TSO UN ; TSS UN ; TWX UN ; TXT UN ; TYC UN ; UDR UN ; UHS UN ;

UNH UN ; UNM UN ; UNP UN ; UPS UN ; URBN UW ; URI UN ; USB UN ; UTX UN ; VAR UN ; VFC UN ; VLO UN ; VMC UN ; VNO UN ; VRSN UW ; VRTX UW ; VTR UN ; VZ UN ; WAT UN ; WEC UN ; WFC UN ; WFM UW ; WHR UN ; WM UN ; WMB UN ; WMT UN ; WY UN ; WYNN UW ; XEC UN ; XEL UN ; XL UN ; XLNX UW ; XOM UN ; XRAY UW ; XRX UN ; YHOO UW ; YUM UN ; ZBH UN ; ZION UW

Dataset-BE500

A2A IM ; AAL LN ; AALB NA ; ABBN VX ; ABE SM ; ABF LN ; ABI BB ; AC FP ; ACA FP ; ACS SM ; ADEN VX ; ADM LN ; ADN LN ; ADS GR ; AGK LN ; AGN NA ; AGS BB ; AH NA ; AHT LN ; AI FP ; AIR FP ; AKE FP ; AKZA NA ; ALFA SS ; ALO FP ; ALU FP ; ALV GR ; AMEAS FH ; ANA SM ; ANDR AV ; ARM LN ; ASC LN ; ASML NA ; ASSAB SS ; ATCOA SS ; ATL IM ; ATLN VX ; ATO FP ; AV/ LN ; AXFO SS ; AZN LN ; BA/ LN ; BAB LN ; BALDB SS ; BALN VX ; BARC LN ; BAS GR ; BATS LN ; BAYN GR ; BBVA SM ; BDEV LN ; BEI GR ; BG LN ; BILL SS ; BKG LN ; BKIR ID ; BKT SM ; BLND LN ; BMED IM ; BMW GR ; BN FP ; BNP FP ; BNZL LN ; BOK LN ; BOKA NA ; BOL FP ; BOL SS ; BOSS GR ; BP LN ; BRBY LN ; BT/A LN ; BTG LN ; BWY LN ; CA FP ; CAP FP ; CARLB DC ; CBK GR ; CFR VX ; CLN VX ; CLS1 GR ; CNA LN ; CNP FP ; CO FP ; COB LN ; COLOB DC ; COLR BB ; CON GR ; CPG LN ; CPI LN ; CPR IM ; CRDA LN ; CRH ID ; CS FP ; CSGN VX ; CWC LN ; DAI GR ; DANSKE DC ; DB1 GR ; DBK GR ; DCC LN ; DEC FP ; DELB BB ; DG FP ; DGE LN ; DLG IM ; DLN LN ; DMGT LN ; DNB NO ; DPW GR ; DSM NA ; DSV DC ; DSY FP ; DTE GR ; DUFN SW ; DWNI GR ; EBS AV ; EDF FP ; EDP PL ; EI FP ; ELE SM ; ELI1V FH ; ELUXB SS ; EMG LN ; EN FP ; ENEL IM ; ENG SM ; ENGI FP ; ENI IM ; EO FP ; EOAN GR ; ERICB SS ; ETL FP ; EZJ LN ; FER SM ; FGR FP ; FME GR ; FNC IM ; FP FP ; FR FP ; FRA GR ; FRE GR ; FUM1V FH ; G IM ; G1A GR ; GAM SM ; GAS SM ; GBLB BB ; GEBN VX ; GEN DC ; GETIB SS ; GFS LN ; GKN LN ; GLB ID ; GLE FP ; GNK LN ; GPOR LN ; GSK LN ; GTO NA ; HAV FP ; HEI GR ; HEIA NA ; HEIO NA ; HER IM ; HEXAB SS ; HGG LN ; HLMA LN ; HMB SS ; HMSO LN ; HNR1 GR ; HO FP ; HOT GR ; HSBA LN ; HTO GA ; HUH1V FH ; HUSQB SS ; HWDN LN ; IAG LN ; IAP LN ; IBE SM ; ICA SS ; IFX GR ; IGG LN ; IHG LN ; III LN ; IMB LN ; IMI LN ; INCH LN ; INDUA SS ; INF LN ; ING FP ; INTU LN ; INVEB SS ; ISAT LN ; ISP IM ; IT IM ; ITRK LN ; ITV LN ; ITX SM ; JD/ LN ; JMAT LN ; JMT PL ; JYSK DC ; KBC BB ; KER FP ; KESBV FH ; KGF LN ; KINVB SS ; KN FP ; KNEBV FH ; KNIN VX ; KPN NA ; KSP ID ; KU2 GR ; KYG ID ; LAND LN ; LGEN LN ; LHA GR ; LHN VX ; LI FP ; LIN GR ; LLOY LN ; LONN VX ; LR FP ; LSE LN ; LUN DC ; LUPE SS ; LUX IM ; LXS GR ; MAP SM ; MB IM ; MC FP ; MCRO LN ; MEDAA SS ; MEO GR ; MEO1V FH ; MGGT LN ; MHG NO ; MKS LN ; ML FP ; MMB FP ; MRK GR ; MRW LN ; MS IM ; MT NA ; MTX GR ; MUV2 GR ; NCCB SS ; NDA SS ; NESN VX ; NESTE FH ; NG LN ; NHY NO ; NIBEB SS ; NOKIA FH ; NOS PL ; NOVN VX ; NOVOB DC ; NRE1V FH ; NXT LN ; NZYMB DC ; OERL SW ; OML LN ; OMV AV ; OR FP ; ORA FP ; ORK NO ; ORP FP ; PFC LN ; PFG LN ; PHIA NA ; PLT IM ; PMI IM ; PNN LN ; POM FP ; POP SM ; PPB ID ; PROX BB ; PRU LN ; PSM GR ; PSN LN ; PSON LN ; PUB FP ; RAND NA ; RB/ LN ; RBI AV ; RBS LN ; RCO FP ; RDSA LN ; REC IM ; REE SM ; REL LN ; REN NA ; REP SM ; REX LN ; RGU LN ; RI FP ; RIO LN ; RMV LN ; RNO FP ; ROG VX ; RPC LN ; RR/ LN ; RRS LN ; RSA LN ; RTO LN ; RWE GR ; RYA ID ; SAABB SS ; SAB LN ; SAB SM ; SAF FP ; SAMAS FH ; SAN FP ; SAN SM ; SAND SS ; SAP GR ; SBMO NA ; SBRY LN ; SCAB SS ; SCHA NO ; SCHP VX ; SCMN VX ; SCR FP ; SDF GR ; SDR LN ; SEBA SS ; SECUB SS ; SGE LN ; SGO FP ; SGRO LN ; SHB LN ; SHBA SS ; SHP LN ; SIE GR ; SKAB SS ; SKFB SS ; SKY LN ; SLHN VX ; SMDS LN ; SMIN LN ; SN LN ; SNH GR ; SOLB BB ; SOON VX ; SPM IM ; SPR GR ; SPSN SW ; SREN VX ; SRG IM ; SSE LN ; STAN LN ; STERV FH ; STJ LN ; STL NO ; STM IM ; SU FP ; SVT LN ; SW FP ; SWEDA SS ; SWMA SS ; SYNN VX ; SZU GR ; TATE LN ; TDC DC ; TEC FP ; TEF SM ; TEL NO ; TEL2B SS ; TEMN SW ; TEN IM ; TIT IM ; TKA AV ; TKA GR ; TL5 SM ; TLSN SS ; TNET BB ; TPK LN ; TRELB SS ; TRN IM ; TRYG DC ; TSCO LN ; TW/ LN ; UBI IM ; UBM LN ; UBSG VX ; UCB BB ; UCG IM ; UG FP ;

UHR VX ; ULVR LN ; UMI BB ; UPM1V FH ; US IM ; UTDI GR ; UU/ LN ; VER AV ; VIE FP ; VIG AV ; VIV FP ; VOD LN ; VOE AV ; VOLVB SS ; VOW GR ; VPK NA ; VWS DC ; WCH GR ; WDH DC ; WDI GR ; WG/ LN ; WKL NA ; WMH LN ; WOS LN ; WPP LN ; WRT1V FH ; WTB LN ; YAR NO ; ZC FP ; ZOT SM ; ZURN VX

Dataset-SHSZ-CSI300

000001 CH ; 000002 CH ; 000009 CH ; 000027 CH ; 000039 CH ; 000046 CH ; 000060 CH ; 000061 CH ; 000063 CH ; 000069 CH ; 000100 CH ; 000157 CH ; 000400 CH ; 000402 CH ; 000413 CH ; 000415 CH ; 000423 CH ; 000425 CH ; 000503 CH ; 000538 CH ; 000539 CH ; 000540 CH ; 000559 CH ; 000568 CH ; 000581 CH ; 000598 CH ; 000625 CH ; 000629 CH ; 000651 CH ; 000686 CH ; 000709 CH ; 000712 CH ; 000725 CH ; 000728 CH ; 000729 CH ; 000738 CH ; 000768 CH ; 000778 CH ; 000792 CH ; 000793 CH ; 000800 CH ; 000825 CH ; 000826 CH ; 000858 CH ; 000876 CH ; 000883 CH ; 000898 CH ; 000917 CH ; 000937 CH ; 000983 CH ; 000999 CH ; 002007 CH ; 002008 CH ; 002024 CH ; 002038 CH ; 600000 CH ; 600005 CH ; 600008 CH ; 600009 CH ; 600010 CH ; 600011 CH ; 600015 CH ; 600016 CH ; 600019 CH ; 600021 CH ; 600028 CH ; 600029 CH ; 600030 CH ; 600031 CH ; 600036 CH ; 600038 CH ; 600050 CH ; 600060 CH ; 600066 CH ; 600068 CH ; 600085 CH ; 600089 CH ; 600100 CH ; 600104 CH ; 600109 CH ; 600111 CH ; 600115 CH ; 600118 CH ; 600150 CH ; 600157 CH ; 600166 CH ; 600170 CH ; 600177 CH ; 600188 CH ; 600196 CH ; 600208 CH ; 600221 CH ; 600252 CH ; 600256 CH ; 600271 CH ; 600276 CH ; 600309 CH ; 600317 CH ; 600332 CH ; 600340 CH ; 600350 CH ; 600352 CH ; 600362 CH ; 600373 CH ; 600398 CH ; 600406 CH ; 600415 CH ; 600485 CH ; 600489 CH ; 600518 CH ; 600519 CH ; 600535 CH ; 600547 CH ; 600549 CH ; 600570 CH ; 600578 CH ; 600583 CH ; 600585 CH ; 600588 CH ; 600600 CH ; 600642 CH ; 600648 CH ; 600660 CH ; 600663 CH ; 600674 CH ; 600688 CH ; 600690 CH ; 600717 CH ; 600718 CH ; 600739 CH ; 600741 CH ; 600783 CH ; 600795 CH ; 600804 CH ; 600820 CH ; 600827 CH ; 600837 CH ; 600839 CH ; 600863 CH ; 600867 CH ; 600873 CH ; 600875 CH ; 600886 CH ; 600887 CH ; 600895 CH ; 601607 CH ; 601988 CH

Dataset-NASDAQ

AAPL UW ; ADBE UW ; ADSK UW ; AKAM UW ; ALXN UW ; AMAT UW ; AMGN UW ; AMZN UW ; ATVI UW ; BBBY UW ; BIDU UW ; BIIB UW ; BMRN UW ; CELG UW ; CERN UW ; CHKP UW ; CMCSA UW ; COST UW ; CSCO UW ; CTRP UW ; CTSH UW ; CTXS UW ; DISCA UW ; DISH UW ; DLTR UW ; EA UW ; EBAY UW ; ENDP UW ; ESRX UW ; EXPE UW ; FAST UW ; FISV UW ; GILD UW ; GOOGL UW ; HSIC UW ; ILMN UW ; INCY UW ; INTC UW ; INTU UW ; ISRG UW ; LBTYA UW ; LBTYK UW ; LLTC UW ; LRCX UW ; MNST UW ; MSFT UW ; NFLX UW ; NTAP UW ; NTES UW ; NVDA UW ; ORLY UW ; PAYX UW ; PCAR UW ; PCLN UW ; QCOM UW ; QVCA UW ; REGN UW ; ROST UW ; SBAC UW ; SBUX UW ; SIRI UW ; SRCL UW ; SWKS UW ; SYMC UW ; TSCO UW ; VRTX UW ; WFM UW ; XLNX UW ; YHOO UW

Dataset-CAC40

AC FP ; ACA FP ; AI FP ; AIR FP ; ALO FP ; BN FP ; BNP FP ; CA FP ; CAP FP ; CS FP ; DG FP ; EI FP ; EN FP ; ENGI FP ; FP FP ; FR FP ; GLE FP ; KER FP ; LI FP ; LR FP ; MC FP ; ML FP ; MT NA ; OR FP ; ORA FP ; PUB FP ; RI FP ; RNO FP ; SAF FP ; SAN FP ; SGO FP ; SOLB BB ; SU FP ; TEC FP ; UG FP ; VIE FP ; VIV FP

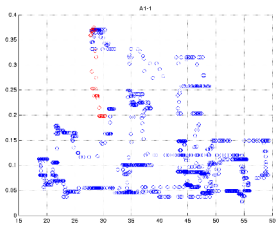

(a) $\mathscr{R}_1$covar

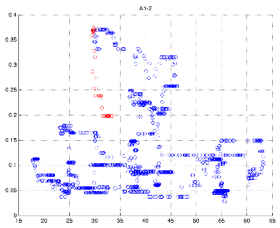

(b) $\mathscr{R}_1$correl

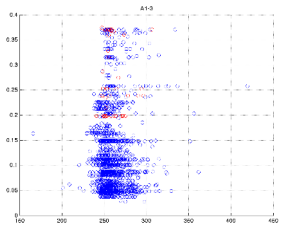

(c) $\mathscr{R}_1$correl-volume

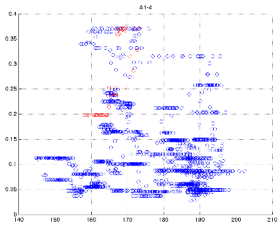

(d) $\mathscr{R}_1$correl-mcap

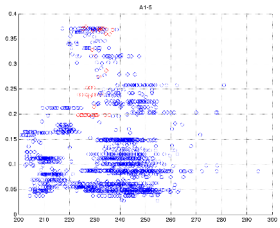

(e) $\mathscr{R}_1$correl-leverage

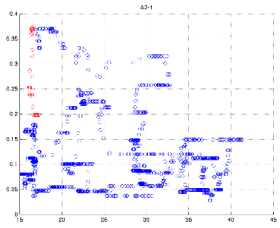

(f) $\mathscr{R}_2$covar

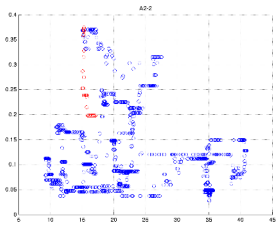

(g) $\mathscr{R}_2$correl

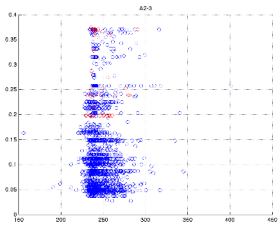

(h) $\mathscr{R}_2$correl-volume

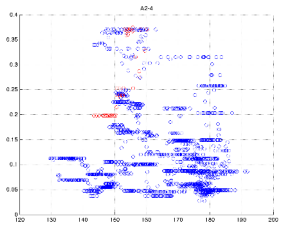

(i) $\mathscr{R}_2$correl-mcap

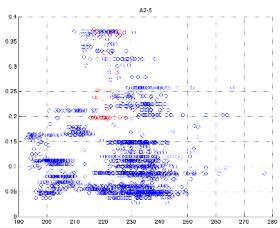

(j) $\mathscr{R}_2$correl-leverage

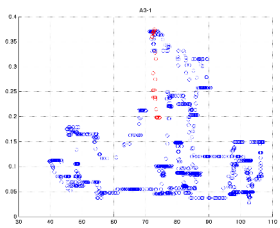

(k) $\mathscr{R}_3$covar

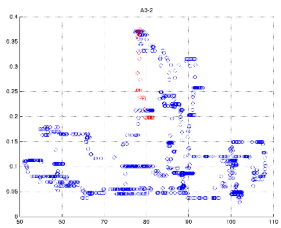

(l) $\mathscr{R}_3$correl

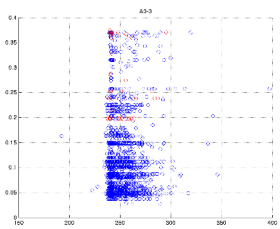

(m) $\mathscr{R}_3$correl-volume

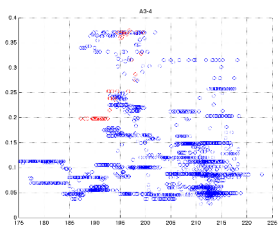

(n) $\mathscr{R}_3$correl-mcap

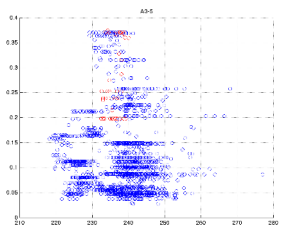

(o) $\mathscr{R}_3$correl-leverage

BE500: Indicators of the α-series. Red: in-sample ; Blue: out-of-sample

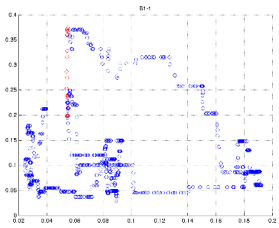

(a) rspec-covar

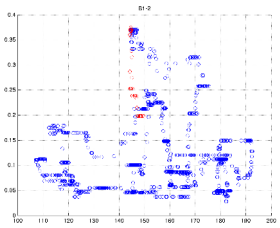

(b) rspec-correl

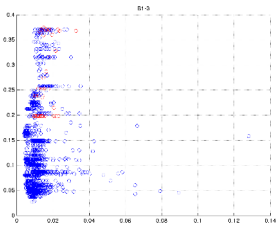

(c) rspec-correl-volume

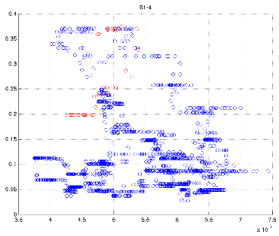

(d) rspec-correl-mcap

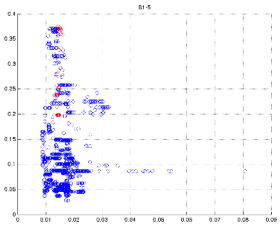

(e) rspec-correl-leverage

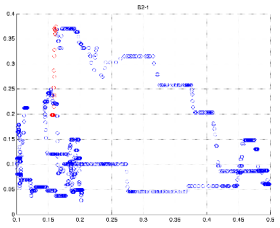

(f) trace-covar

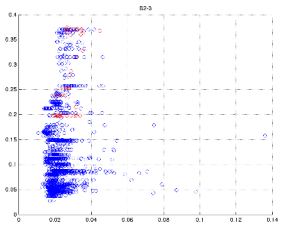

(g) trace-correl-volume

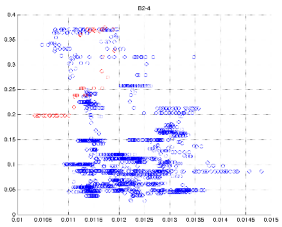

(h) trace-correl-mcap

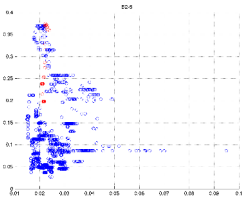

(i) trace-correl-leverage

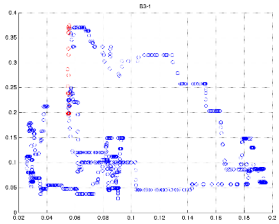

(j) froben-covar

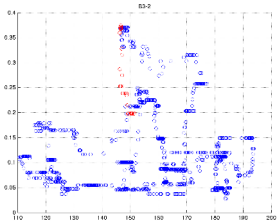

(k) froben-correl

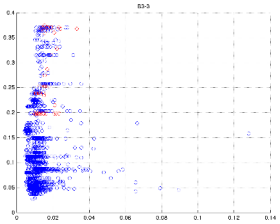

(l) froben-correl-volume

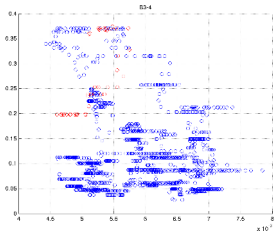

(m) froben-correl-mcap

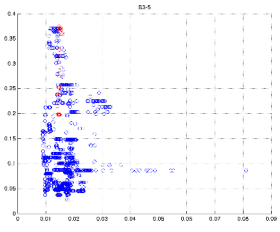

(n) froben-correl-leverage

BE500: Indicators of the β-series. Red: in-sample ; Blue: out-of-sample

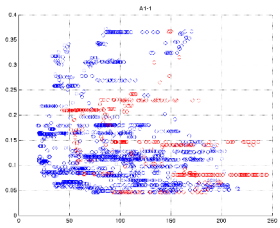

(a) $\mathscr{R}_1$covar

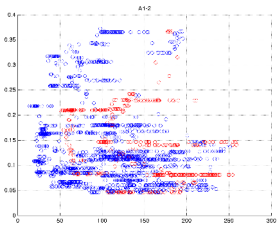

(b) $\mathscr{R}_1$correl

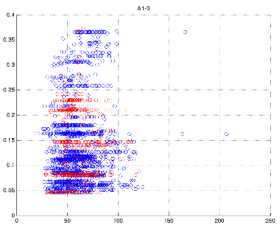

(c) $\mathscr{R}_1$correl-volume

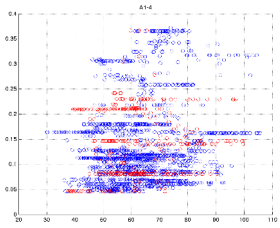

(d) $\mathscr{R}_1$correl-mcap

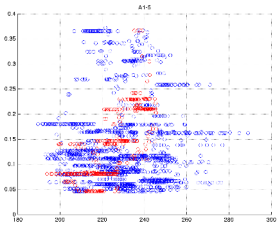

(e) $\mathscr{R}_1$correl-leverage

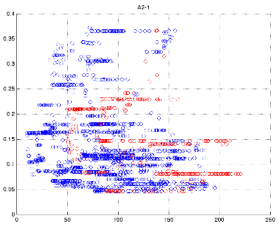

(f) $\mathscr{R}_2$covar

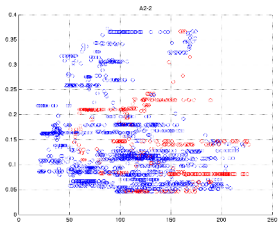

(g) $\mathscr{R}_2$correl

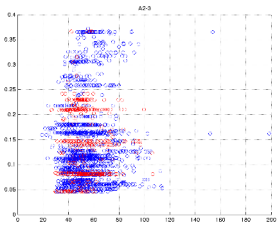

(h) $\mathscr{R}_2$correl-volume

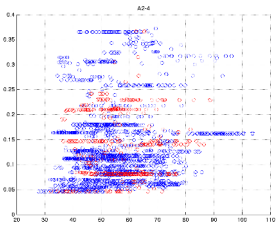

(i) $\mathscr{R}_2$correl-mcap

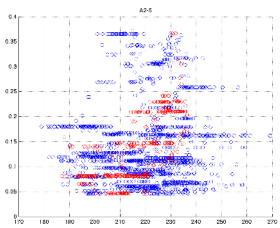

(j) $\mathscr{R}_2$correl-leverage

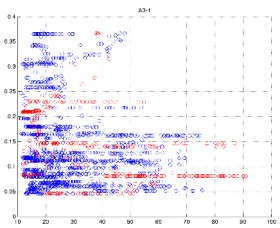

(k) $\mathscr{R}_3$covar

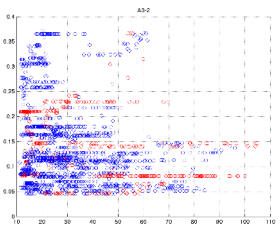

(l) $\mathscr{R}_3$correl

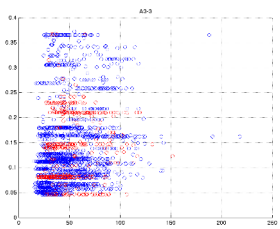

(m) $\mathscr{R}_3$correl-volume

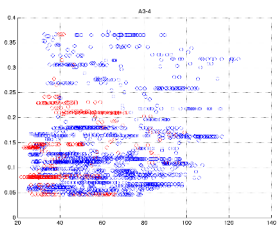

(n) $\mathscr{R}_3$correl-mcap

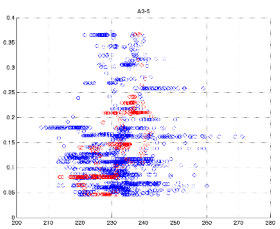

(o) $\mathscr{R}_3$correl-leverage

CAC40: Indicators of the α-series. Red: in-sample ; Blue: out-of-sample

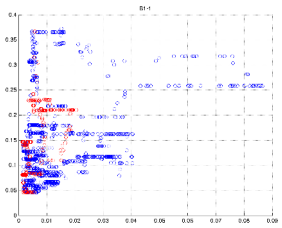

(a) rspec-covar

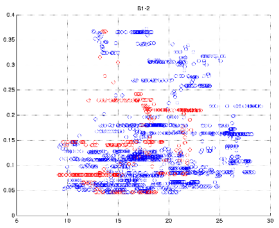

(b) rspec-correl

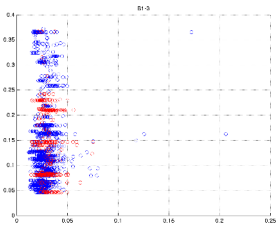

(c) rspec-correl-volume

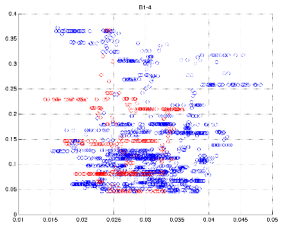

(d) rspec-correl-mcap

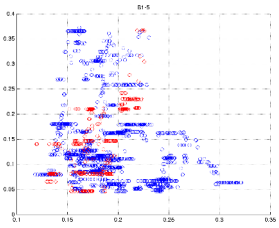

(e) rspec-correl-leverage

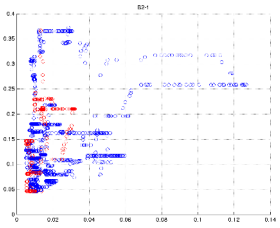

(f) trace-covar

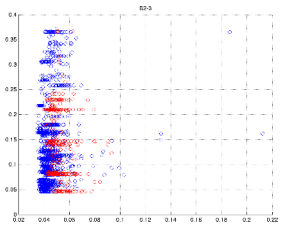

(g) trace-correl-volume

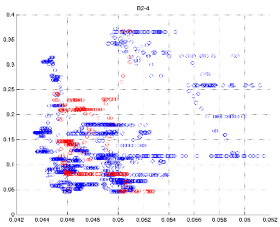

(h) trace-correl-mcap

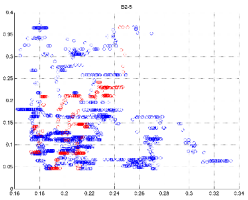

(i) trace-correl-leverage

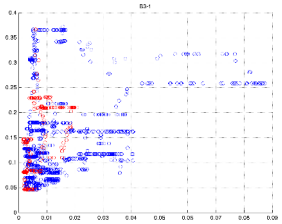

(j) froben-covar

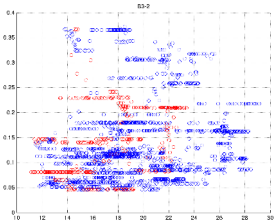

(k) froben-correl

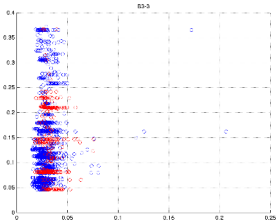

(l) froben-correl-volume

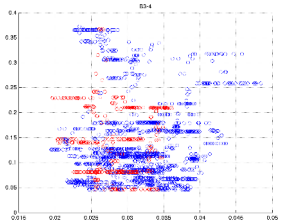

(m) froben-correl-mcap

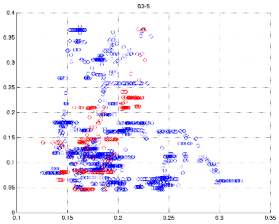

(n) froben-correl-leverage

CAC40: Indicators of the β-series. Red: in-sample ; Blue: out-of-sample

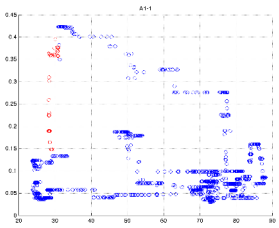

(a) $\mathscr{R}_1$covar

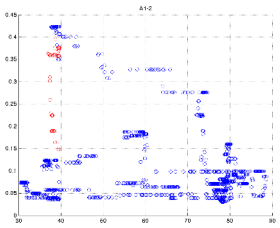

(b) $\mathscr{R}_1$correl

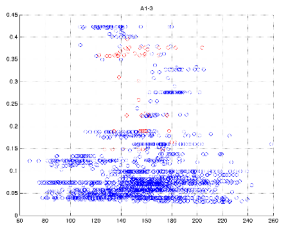

(c) $\mathscr{R}_1$correl-volume

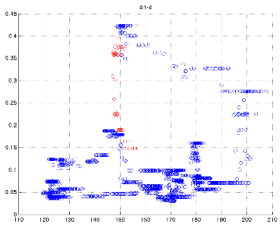

(d) $\mathscr{R}_1$correl-mcap

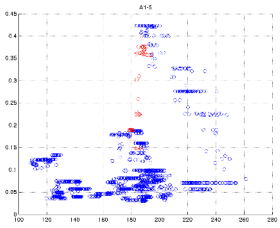

(e) $\mathscr{R}_1$correl-leverage

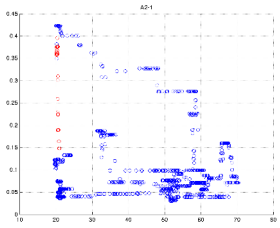

(f) $\mathscr{R}_2$covar

(g) $\mathscr{R}_2$correl

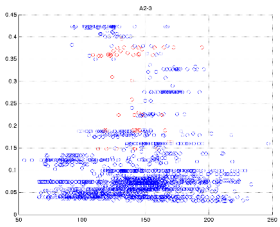

(h) $\mathscr{R}_2$correl-volume

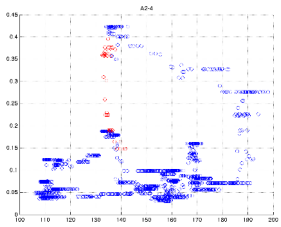

(i) $\mathscr{R}_2$correl-mcap

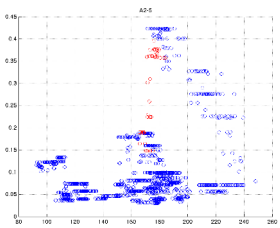

(j) $\mathscr{R}_2$correl-leverage

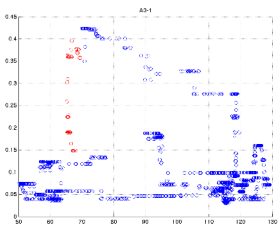

(k) $\mathscr{R}_3$covar

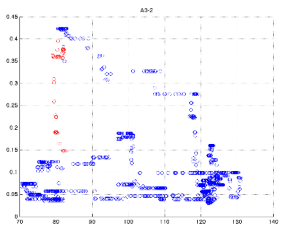

(l) $\mathscr{R}_3$correl

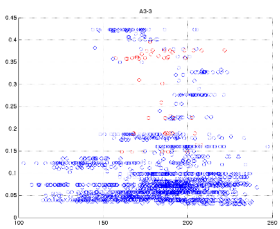

(m) $\mathscr{R}_3$correl-volume

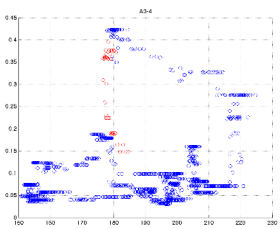

(n) $\mathscr{R}_3$correl-mcap

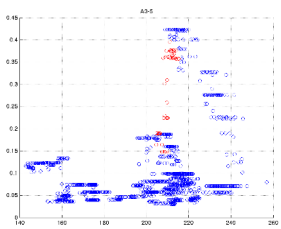

(o) $\mathscr{R}_3$correl-leverage

SP500: Indicators of the α-series. Red: in-sample ; Blue: out-of-sample

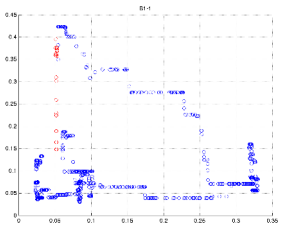

(a) rspec-covar

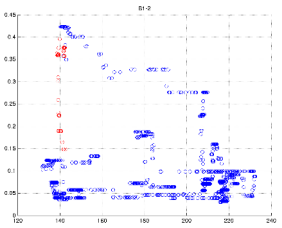

(b) rspec-correl

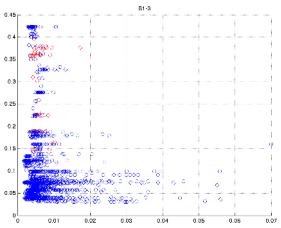

(c) rspec-correl-volume

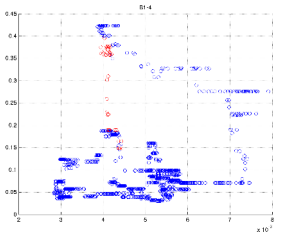

(d) rspec-correl-mcap

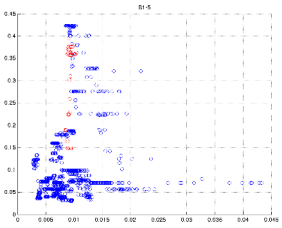

(e) rspec-correl-leverage

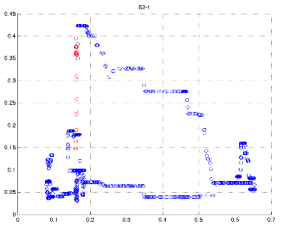

(f) trace-covar

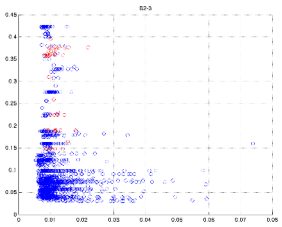

(g) trace-correl-volume

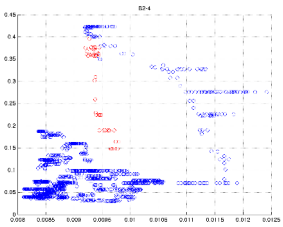

(h) trace-correl-mcap

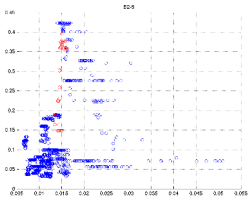

(i) trace-correl-leverage

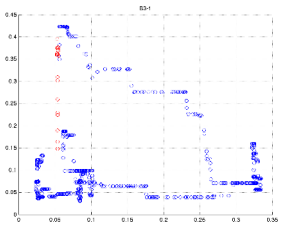

(j) froben-covar

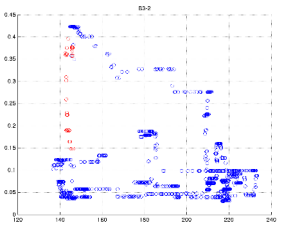

(k) froben-correl

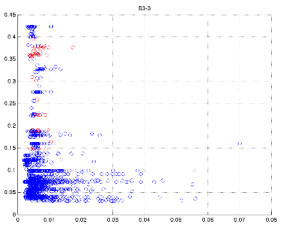

(l) froben-correl-volume

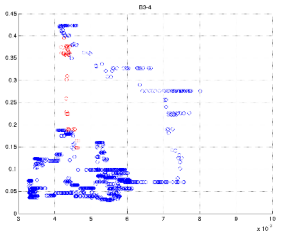

(m) froben-correl-mcap

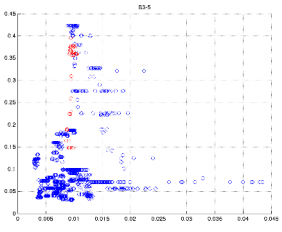

(n) froben-correl-leverage

SP500: Indicators of the β-series. Red: in-sample ; Blue: out-of-sample

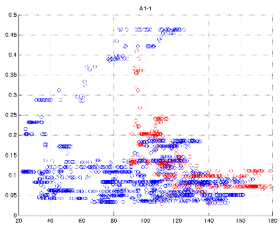

(a) $\mathscr{R}_1$covar

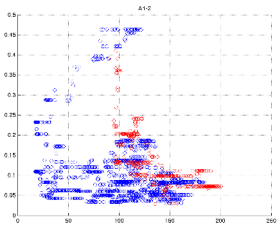

(b) $\mathscr{R}_1$correl

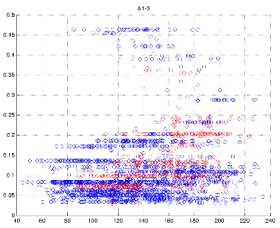

(c) $\mathscr{R}_1$correl-volume

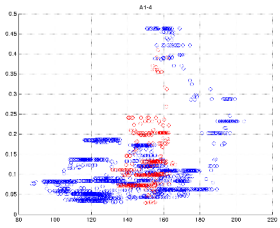

(d) $\mathscr{R}_1$correl-mcap

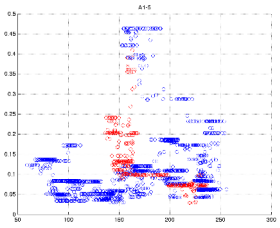

(e) $\mathscr{R}_1$correl-leverage

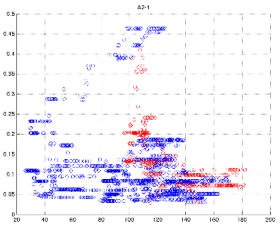

(f) $\mathscr{R}_2$covar

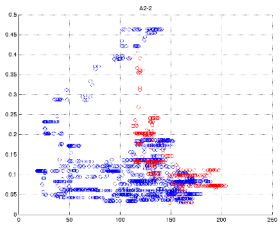

(g) $\mathscr{R}_2$correl

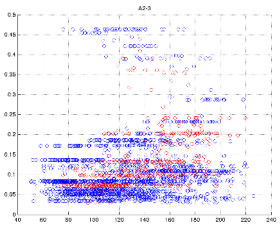

(h) $\mathscr{R}_2$correl-volume

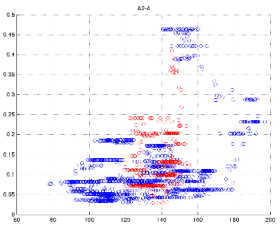

(i) $\mathscr{R}_2$correl-mcap

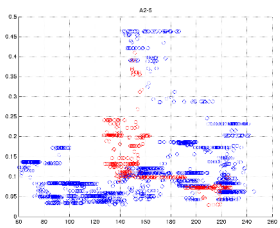

(j) $\mathscr{R}_2$correl-leverage

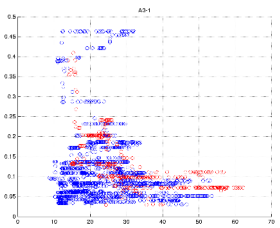

(k) $\mathscr{R}_3$covar

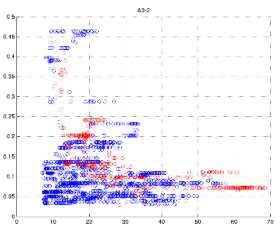

(l) $\mathscr{R}_3$correl

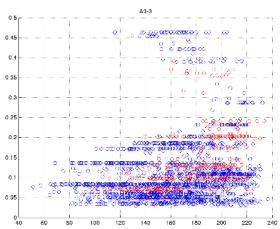

(m) $\mathscr{R}_3$correl-volume

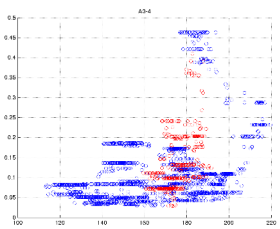

(n) $\mathscr{R}_3$correl-mcap

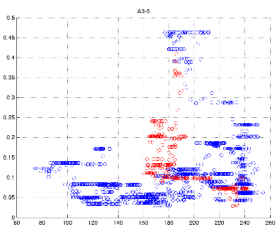

(o) $\mathscr{R}_3$correl-leverage

NASDAQ: Indicators of the α-series. Red: in-sample ; Blue: out-of-sample

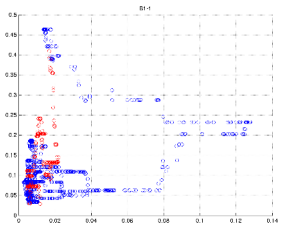

(a) rspec-covar

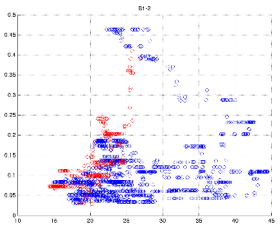

(b) rspec-correl

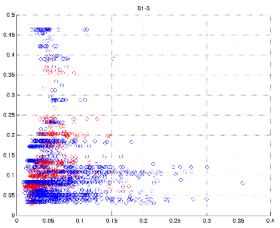

(c) rspec-correl-volume

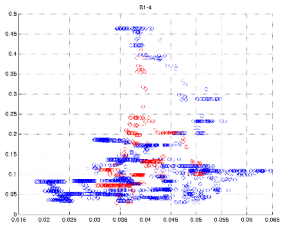

(d) rspec-correl-mcap

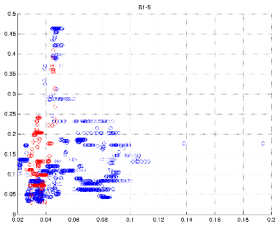

(e) rspec-correl-leverage

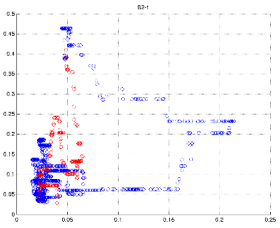

(f) trace-covar

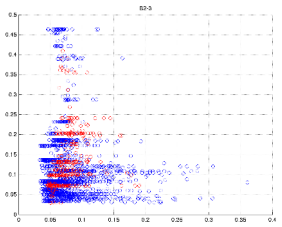

(g) trace-correl-volume

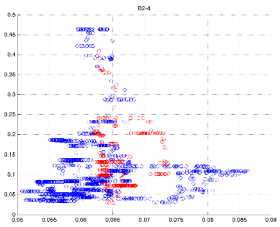

(h) trace-correl-mcap

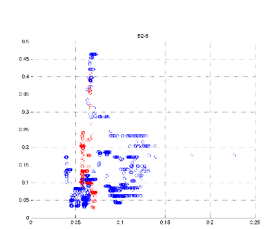

(i) trace-correl-leverage

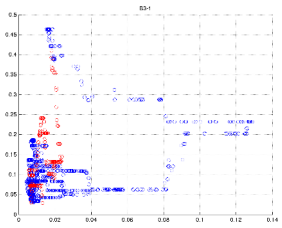

(j) froben-covar

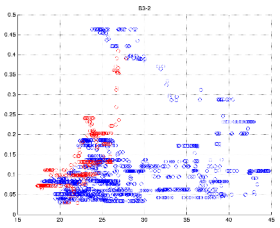

(k) froben-correl

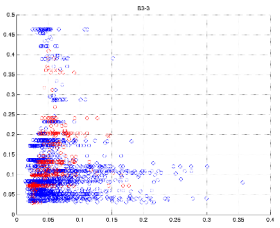

(l) froben-correl-volume

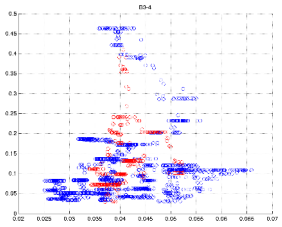

(m) froben-correl-mcap

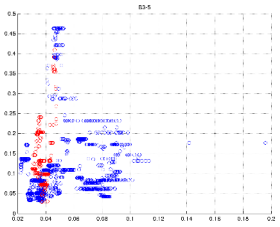

(n) froben-correl-leverage

NASDAQ: Indicators of the β-series. Red: in-sample ; Blue: out-of-sample

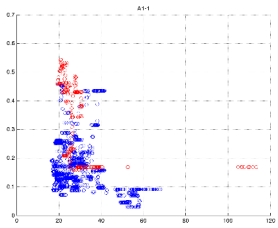

(a) $\mathscr{R}_1$covar

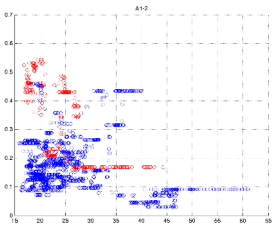

(b) $\mathscr{R}_1$correl

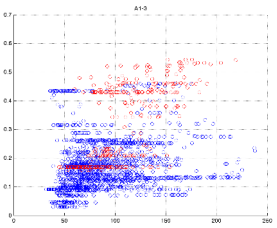

(c) $\mathscr{R}_1$correl-volume

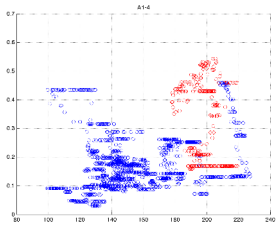

(d) $\mathscr{R}_1$correl-mcap

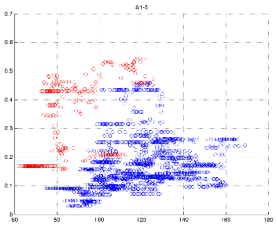

(e) $\mathscr{R}_1$correl-leverage

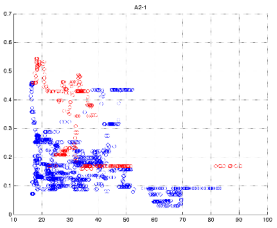

(f) $\mathscr{R}_2$covar

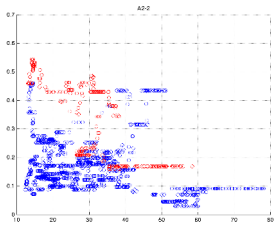

(g) $\mathscr{R}_2$correl

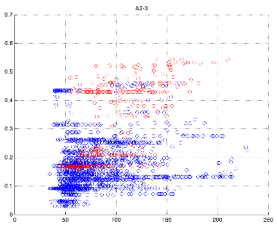

(h) $\mathscr{R}_2$correl-volume

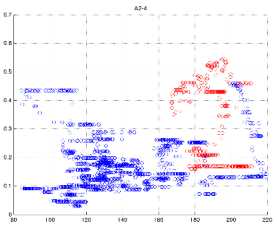

(i) $\mathscr{R}_2$correl-mcap

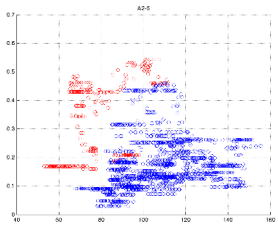

(j) $\mathscr{R}_2$correl-leverage

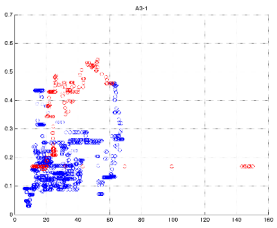

(k) $\mathscr{R}_3$covar

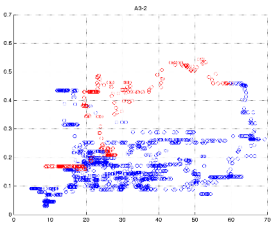

(l) $\mathscr{R}_3$correl

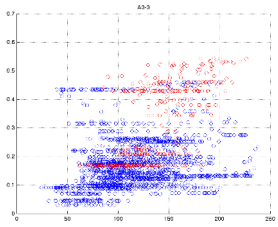

(m) $\mathscr{R}_3$correl-volume

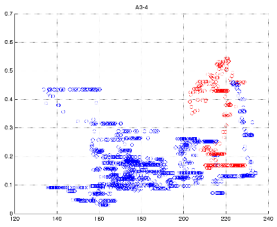

(n) $\mathscr{R}_3$correl-mcap

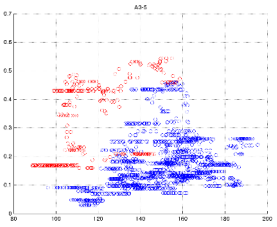

(o) $\mathscr{R}_3$correl-leverage

SHSZ300: Indicators of the α-series. Red: in-sample ; Blue: out-of-sample

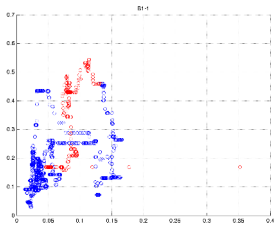

(a) rspec-covar

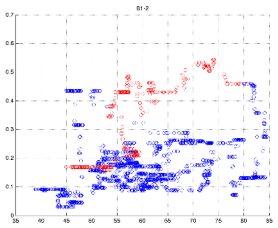

(b) rspec-correl

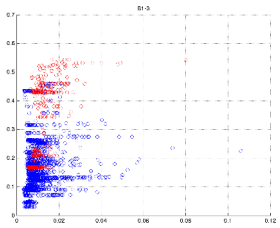

(c) rspec-correl-volume

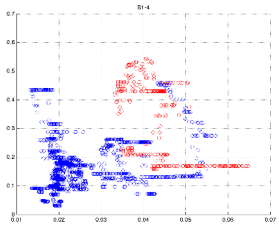

(d) rspec-correl-mcap

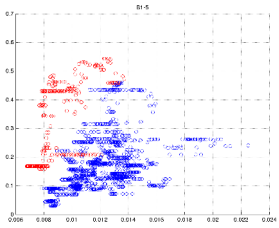

(e) rspec-correl-leverage

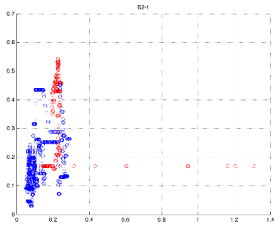

(f) trace-covar

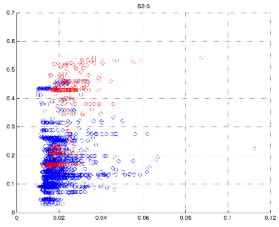

(g) trace-correl-volume

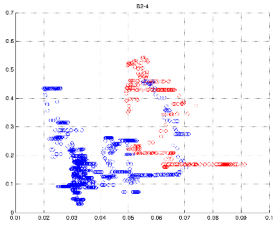

(h) trace-correl-mcap

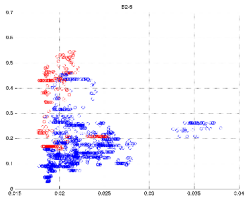

(i) trace-correl-leverage

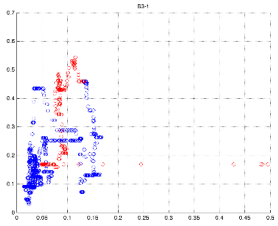

(j) froben-covar

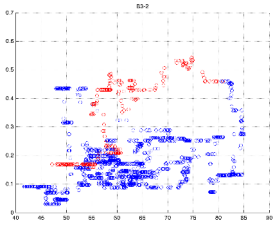

(k) froben-correl

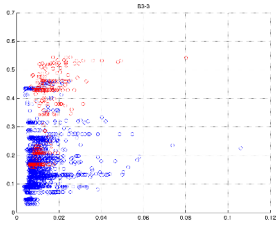

(l) froben-correl-volume

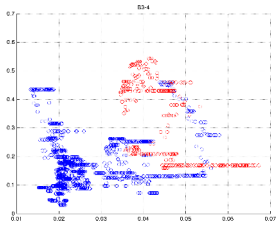

(m) froben-correl-mcap

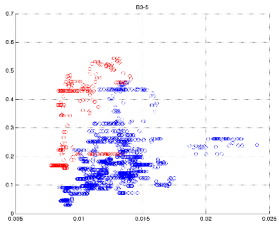

(n) froben-correl-leverage

SHSZ300: Indicators of the β-series. Red: in-sample ; Blue: out-of-sample

Funding

This work was achieved through the Laboratory of Excellence on Financial Regulation (Labex RéFi) supported by PRES heSam under the reference ANR10LABX0095. It benefited from a French government support managed by the National Research Agency (ANR) within the project Investissements d'Avenir Paris Nouveaux Mondes (Investments for the Future Paris New Worlds) under the reference ANR11IDEX000602.

Chapter 3

Stochastic Evolution of Distributions and Application to CDS Indices

Stochastic Evolution of Distributions - Applications to CDS indices

Guillaume Bernis*, Nicolas Brunel†, Antoine Kornprobst‡and Simone Scotti§

September 4, 2017

Abstract: We use mixture of percentile function to model credit spread evolution, which allows to obtain a flexible description of credit index and their components at the same time. We show regularity results in order to extend mixture percentile to the dynamic case. We characterise the stochastic differential equation of the flow of cumulative distribution function and we link it with the ordered list of the components of the credit index. The main application is to introduce a functional version of Bollinger bands. The crossing of bands by the spread is associated with a trading signal. Finally, we show the richness of the signals produced by functional Bollinger bands compared with standard one with a practical example.

1 Introduction

The modelling of both market indices and their components is an open question in finance. Notably, there have appeared many relevant papers (e.g. [15], [16]) focusing on the global evolution of a market and the assets composing it. However, this analysis is generally applied to the class of stock assets but that cannot be extended directly to other classes and mainly to credit risk market. The aim of

*Natixis Asset Management, Fixed Income. eMail: guillaume.bernis@am.natixis.com. The opinions and views expressed in this document are those of the authors and do not necessarily reflect those of Natixis Asset Management.

†Laboratoire de Mathématiques et Modélisation d'Evry - UMR CNRS 8071. Université d'Evry Val d'Essonne and ENSIIE

‡Université Paris 1 Panthéon Sorbonne, Labex RéFi

§LPMA, Université Paris Diderot. eMail: scotti@math.univ-paris-diderot.fr

this paper is to fill this gap proposing a model to describe the evolution of a credit default swap (CDS) index and their components in a parsimonious but flexible way. One of the most traded CDS index is the iTraxx Europe index composed of the most liquid 125 CDS referencing European investment grade credits. A CDS is an agreement that the seller of the CDS insures the buyer against a loan default, the word swap indicates that the buyer pays regular premium payments, called spread, to the seller. These spreads are the underlying in credit risk market, since market quotes are usually expressed in terms of spread rather than bond price, in order to ease the comparison of products. As a consequence the index is a synthetic asset, in the sense that it cannot be reproduced using a static portfolio, for more details see e.g. section 2.1 in [5]. Moreover, the spreads exhibit special features due to their construction and the rules used to select the issuers.

Motivated by those issues we introduce a new, flexible and parsimonious representation of the evolution of credit indices and their components. The basic idea is to seize some of the features of credit risk market transforming them from drawback to advantage. Mainly, the specific rules used to select the issuers of the CDS composing the index leads us to assume the interchangeability of the CDS. As a consequence, we will set the issuers aside and rearrange at all time the CDS list by increasing spread. Moreover, the very large number of components (i.e. 125) of CDS indices justifies to consider, for all fixed times, the list of the CDS as a measure on $\mathbb{R}^+$. Assuming moreover that the measure is renormalised, that is considering probability measures, the mean is linked to the index. Of course, many approaches are possible and studied in literature, in particular we can use the chaos decomposition as in [12] and [7]. The main drawback comes from the fact that the extreme flexibility of the chaos decomposition leads up to a time consuming and less manageable for one of the practical application of our model, that is anticipation of movements extending Bollinger bands.

The problem of optimal investment in financial markets has been widely studied in literature. Moreover, the techniques applied span a large class of mathematical tools for instance by restricting to recent years (but without any claim to being exhaustive), optimal switching [28], optimal investment with trend detection [10], [5] and [6], adding jumps and over/under-reaction to information [9] or using techniques from neural network [13]. The significant innovation of the present paper is to deal with the whole components and not the only index. To the best of our knowledge, this is the first paper dealing with the problem of trend detection in an infinite dimensional framework.

We then decide to link the problem of market index and their components evolution to the transport of measures. Several references on the question of deterministic

or stochastic evolution of densities can be found across various fields of mathematics. The scope of applications encompasses statistics, biology, physics and finance. Bellomo and Pistone [4] study the action of an abstract dynamical system on a probability density. From a statistical point of view, some authors analyse the density as the outcome of a Dirichlet law: Ferguson [14] or Shao [23]. This question is also at the core of the optimal transport, see for instance Villani [26], Alfonsi et al [2] and the references therein. In this vein, Bass [3] studies the deformation of a parameter-based family of densities. Another approach is based on the mixture of percentiles. This method introduced by Sillitto [24] has been used, more recently, by Karvanen [19] and Gouriéroux and Jasiak [17] to fit distributions of stock returns. This is the approach that we will adopt in this paper.

Let us consider some integrable probability distribution on the positive half-line, represented by its percentile function. Assume that we have a breakdown the percentile as a sum of percentile functions of distributions on the positive half-line. Then, we can construct deformations of the initial distribution by considering weighted sums of the percentile function with positive coefficients. Then, we replace the mixing coefficients by correlated diffusion processes.

This method construct a process with values in a space of probability distributions, represented by their percentiles: hence a random measure on the positive half-line. We show that, under mild assumptions on the underlying diffusion, regularity results hold for the distribution-valued process. First, the process is continuous in time with respect to the expected Wasserstein distance, see Bass [3], which is a natural metric in this context. Second, the stochastic differential equation which drives the cumulated distribution function is explicit. We also provide results on the average and the variance of the cumulated distribution function.

Using this framework, at each date, we can calculate a confidence interval for the percentile at a given (short) time horizon. We show that the upper and lower boundaries of this interval are also percentile functions. We study trading signals triggered when the realised percentile function crosses either the upper or the lower band of this confidence interval. This method can be seen as a extension of the widely used Bollinger bands, see for instance Kaufman [20], where the bands are not only functions of the time, but functions of the time and of the level of the percentile. Hence, it defines functional lower and upper bands. We also analyse the link between the crossing of one of the bands and the measure of risk according to the second order stochastic dominance.

In the first section, we introduce the mixture of percentiles method in a static setting and analyse its properties. Topological aspects as well as differentiability of the cumulated distribution functions are studied. Insights on the notion of stochastic

dominance, in relation with the possible deformations of the initial distribution, are given. Then, in section 3, we use Markov diffusion processes as mixing coefficients and provide the dynamics of the distribution. Thus, we obtain a model where both percentile and cumulative distribution functions have some explicit diffusion equation, and satisfies some regularity results. Last section is dedicated to a case study for CDS indices.

2 Decomposition of probability distributions

This section is dedicated to the analysis of the mixture of percentiles, as defined in Sillitto [24], in a static context. We prove regularity results that will be useful for the dynamic case, detailed in section 3. After setting our framework, we present the mixture method and study its properties. Then, we derive results on the derivatives of the cumulative distribution function. Finally, we investigate the deformation of the distribution in term of stochastic dominance.

First, let us define the setting under which we will work throughout the paper. Consider the measured space $\big([0,+\infty), \mathcal{B}([0,+\infty)), dx\big)$, where $\mathcal{B}\big([0,+\infty)\big)$ is the Borelian sigma-field over $[0,+\infty)$ and dx the Lebesgue measure. Let f be a probability distribution function (hereafter p.d.f.) on this space, F the cumulative distribution function (c.d.f.) of f, and q the percentile function, i.e. the inverse[1] of F. We denote by $\mathcal{D}$ the set of all probability distributions on $\big([0,+\infty), \mathcal{B}([0,+\infty)), dx\big)$ and by (f, F, q) an element of $\mathcal{D}$. Where there is no ambiguity, we will indicate only one element among the p.d.f, the c.d.f or the percentile function. The next straightforward Lemma highlights some properties of $\mathcal{D}$.

Lemma 1 (Properties of percentile function) *The set $\mathcal{D}$ is a convex cone i.e. $\forall (q_1, q_2) \in \mathcal{D}^2$ and $(\lambda_1, \lambda_2) \in (\mathbb{R}_*^+)^2$, $\lambda_1 q_1 + \lambda_2 q_2 \in \mathcal{D}$. Moreover, it can be endowed with a partial order relation on the set $\mathcal{D}$, equivalent to the stochastic dominance of first order, as defined by Quirk and Saposnik [22], see also Levy [21]: $q_1 \succeq q_2$ if, for any $\varepsilon \in [0,1)$, $q_1(\varepsilon) \geq q_2(\varepsilon)$, which is equivalent to, $\forall\, x \geq 0$, $F_1(x) \leq F_2(x)$, in terms of c.d.f. For any $q_1 \succeq q_2$ and q, $q_1 + q \succeq q_2$.*

Throughout the paper, we consider the set $\mathcal{D}_0 \subset \mathcal{D}$ of probability distributions satisfying the following assumption:

Assumption 1 *A probability distribution $(f, F, q) \in \mathcal{D}$ is said to belong to $\mathcal{D}_0$ if:*

[1] The notion of generalized inverse should be used at this stage, but, hereafter, we will restrict our attention to distributions for which the c.d.f is actually invertible.

1. *Its p.d.f. is positive, almost everywhere (a.e.).*
2. *Its c.d.f. is a diffeomorphism from* $[0, +\infty)$ *onto* $[0, 1)$ *and is twice continuously derivable with right-derivatives at* 0*. Moreover,* $F(0) = q(0) = 0$*.*
3. *Its probability distribution has finite first two moments.*

We can extend the previous Lemma 1 to show:

Proposition 1 *The set* $\mathcal{D}_0$ *is a convex cone.*

Proof: Let $q_1, q_2 \in \mathcal{D}_0$, since $\mathcal{D}_0 \subset \mathcal{D}$, applying the results of Lemma 1 we have that $q := \lambda_1 q_1 + \lambda_2 q_2 \in \mathcal{D}$ for all $\lambda_1, \lambda_2 \in \mathbb{R}_*^+$. Then we need to show the three properties in Assumption 1:

1. The mapping q is strictly increasing, with $q(0) = 0$, and tends to $+\infty$ in 1^-. Thus, it defines a bijection from $[0, 1)$ onto $[0, +\infty)$. It is, therefore, invertible, with an inverse denoted by F and strictly increasing. This implies that the p.d.f is well defined and positive a.e.
2. By implied function theorem, the derivative of F exists. Moreover, as q_1 and q_2 have derivatives of order up to two, so q has the same property and F too.
3. The existence of the moments of first and second orders stems from the following identity, obtained by the variable change $x = q(\varepsilon)$, i.e. $\varepsilon = F(x)$: for $k = 1, 2$
$$\int_0^\infty x^k f(x) dx = \int_0^1 (q(\varepsilon))^k d\varepsilon$$
Thus, if (f, F, q) has a second order moment so has $\left(\frac{1}{\lambda} f\left(\frac{\cdot}{\lambda}\right),\ F\left(\frac{\cdot}{\lambda}\right),\ \lambda q\right)$, for any $\lambda > 0$: $\int_0^1 (\lambda q(\varepsilon))^k d\varepsilon = \lambda^k \int_0^1 (q(\varepsilon))^k d\varepsilon$, $k \in \{1, 2\}$. Therefore, it is sufficient to show that, for $q_1, q_2 \in \mathcal{D}_0$, $q_1 + q_2$ and $(q_1 + q_2)^2$ are integrable. The integrability of $q_1 + q_2$ is a consequence of the linearity of the integral. In order to show the integrability of $(q_1 + q_2)^2 = q_1^2 + q_2^2 + 2q_1 q_2$, it is sufficient to show that $q_1 q_2$ is integrable. This is a consequence of the Cauchy-Schwarz inequality. □

In the following, we endow the space $\mathcal{D}_0$ with the second-order Wasserstein distance, see for instance Vallander [25], which is defined, for any $(q_1, q_2) \in \mathcal{D}_0$ by

$$\mathcal{W}_2(q_1, q_2) := \sqrt{\int_0^1 [q_1(\varepsilon) - q_2(\varepsilon)]^2 d\varepsilon}$$

This distance is well suited to the analysis of deformation of probability distributions, and can be adapted in a dynamic setting. See, for instance, Bass [3] and Alfonsi et al. [2].

2.1 Mixture of percentile functions

In this section, following Sillitto [24], we introduce the method to construct various percentiles functions from an initial one. We provide results on the regularity of the functions obtained by this method. In particular, we prove that they belong to $\mathcal{D}_0$. In this section, we set out $(f, F, q) \in \mathcal{D}_0$.

Definition 1 (Basis of percentile function associated to (f, F, q)) *A n-uple of mappings $\psi := (\psi_i)_{1 \leq i \leq n}$, is called a n-basis of percentile functions associated to (f, F, q) if*

1. *The family is linearly independent;*
2. *For all $i \in \{1, \dots, n\}$ ψ_i is non-decreasing, taking non-negative values, twice continuously derivable on $[0, 1)$ and*
3. *The total sum of the percentile functions ψ_i reconstruct the percentile function q, i.e. $\sum_{i=1}^{n} \psi_i = q$.*

The set of all n-basis of percentile function associated to (f, F, q) will be denoted by $\mathcal{P}_n(q)$.

The following Lemma summarizes some properties of the basis representation:

Lemma 2 *Let ψ be a n-basis of percentile functions associated to (f, F, q) satisfying Assumption 1. Then, we have*

1. **Initial value***: For all $i \in \{1, \dots, n\}$ $\psi_i(0) = 0$*
2. **Existence of a diverging term***: There exists $i^* \in \{1, \dots, n\}$ such that $\lim_{\varepsilon \to 1^-} \psi_{i^*}(\varepsilon) = \infty$.*

Proof: The first property is a direct consequence of $q(0) = 0$ and the fact that the functions ψ_i take non-negative values. If the second property does not hold, the limit of q, as ε goes to $1-$, would be finite. Hence a contradiction with point 1 in Assumption 1. □

Now, let us introduce a method to generate a large class of probability distribution based on a basis of percentile functions.

Definition 2 (Mixture Method) *Let $y := (y_i)_{1\leq i\leq n} \in (\mathbb{R}_*^+)^n$, and $\psi \in \mathcal{P}_n(q)$. The mixing of ψ with coefficients y is defined by*

$$\forall \varepsilon \in [0,1),\ \ q(\varepsilon, y) = q(x, y_1, \ldots, y_n) := \langle y, \psi(\varepsilon)\rangle = \sum_{i=1}^{n} y_i \psi_i(\varepsilon). \tag{1}$$

where $\langle \cdot, \cdot \rangle$ stands for the Euclidean scalar product on $\mathbb{R}^n$.

Note that $q(\varepsilon) = \langle e, \psi(\varepsilon)\rangle = q(\varepsilon, e)$, where $e := (1, \ldots, 1)^T \in \mathbb{R}^n$. In order to maintain consistent notations throughout the paper, the first variable ε will always denote the level of probability used in the percentile function and x and element of $[0, +\infty)$, i.e. the variable of the p.d.f. and c.d.f., whereas the element y of $(\mathbb{R}_*^+)^n$ will represent a vector of mixing coefficients. The function $\varepsilon \mapsto q(\varepsilon, y)$ will be denoted, for short, $q(\cdot, y)$. Accordingly, we denote by $f(\cdot, y)$ the p.d.f. and by $F(\cdot, y)$ the c.d.f. associated to $q(\cdot, y)$. Both functions are defined on $[0, +\infty)$. It is clear that the mixing method defines an element of $\mathcal{D}$. As we will see in Corollary 1, it also defines an element of $\mathcal{D}_0$, this is a direct consequence of Proposition 1.

Corollary 1 *Let y and ψ as in Definition 2. Then, the p.d.f associated to $q(\cdot, y)$, given by Equation (1), satisfies Assumption 1. Moreover, if $y_{min} = \min\{y_i | 1 \leq i \leq n\}$, we have, for $1 \leq k \leq 2$,*

$$y_{min}^k \int_0^{+\infty} x^k f(x) dx \leq \int_0^{+\infty} x^k f(x, y) dx \leq \langle y, e\rangle^k \int_0^{+\infty} x^k f(x) dx \tag{2}$$

Proof: The first part of the proof is a direct consequence of Lemma 2. For the integrability condition, let us write $\forall \varepsilon \in [0,1),\ \ q(\varepsilon) y_{min} \leq q(\varepsilon, y) \leq q(\varepsilon) \times \langle y, e\rangle$.

Therefore, we have boundaries on $q(\cdot, y)$ for the first order stochastic dominance. This can be translated into the inverse order for integral of any increasing mapping, see Levy [21]. Taking $x \mapsto x^k$, $k \in \{1, 2\}$ yields Equation (2). □

Another result on the influence of the mixture method on the distribution is given in Proposition 2. To this purpose, let us denote by $|\cdot|$ the Euclidean norm on $\mathbb{R}^n$, and by $||\cdot||_2$ the L^2-norm on $\mathcal{D}_0$.

Proposition 2 *The mapping $y \mapsto f(\cdot, y)$, form $(\mathbb{R}_*^+)^n$ into $\mathcal{D}_0$, endowed with the Wasserstein distance $\mathcal{W}_2$, is Lipschitz with coefficient $||q||_2$.*

Proof: For any $y, z \in (\mathbb{R}_*^+)^n$, the Wasserstein distance satisfies the following inequality, which is a consequence of Schwarz inequality in $\mathbb{R}^n$:

$$\mathcal{W}_2\big(q(\cdot,y),q(\cdot,z)\big) = \left[\int_0^1 < y-z, \psi(\varepsilon) >^2 d\varepsilon\right]^{\frac{1}{2}} \leq \left[\sum_{i=1}^n \int_0^1 |\psi(\varepsilon)|^2 \times |y-z|^2 d\varepsilon\right]^{\frac{1}{2}}.$$

But, we have $|\psi(\cdot)| \leq q(\cdot)$ due to the non-negativity of ψ, and, thus, the following inequality holds: $\mathcal{W}_2(q(\cdot,y),q(\cdot,z)) \leq ||q||_2 \times |y-z|$. □

With these result in hand, we can investigate the topological properties of the set of all possible mixtures given a basis of percentile functions.

Lemma 3 *Let $\psi_i \in \mathcal{D}_0$, for $i \in \{1,\dots,n\}$ and assume that the family $\psi := (\psi)_{1\leq i\leq n}$ is linearly independent. Let $A := \big\{q(\cdot,y) \mid y \in (\mathbb{R}_*^+)^n\big\}$ be the set of mixtures associated to the family $(\psi_i)_{1\leq i\leq n}$. Then, the closure of A for $\mathcal{W}_2$ is the convex cone spanned by the ψ_i, $i \in \{1,\dots,n\}$ and an element of the closure is either 0 or an element of $\mathcal{D}_0$.*

Proof: Let $(q_k)_{k\geq 0} \in A^{\mathbb{N}}$ converging toward q^*. For each q_k, there exists $y_k \in (\mathbb{R}_*^+)^n$. On the one hand, a converging sequence is also a Cauchy sequence, hence, for any $k \geq 0$, $\mathcal{W}_2(q_k, q_{k+p})$ tends to 0 as p goes to infinity. On the other hand, $\mathcal{W}_2^2(q_k,q_{k+p}) = (y_{k+p}-y_k)^T\Psi(y_{k+p}-y_k)$ where Ψ is the $n\times n$-matrix, the elements of which are given by $\Psi_{k,i} := \int_0^1 \psi_k(\varepsilon)\psi_i(\varepsilon)d\varepsilon$ for $(i,k) \in \{1,\dots,n\}^2$. As the family ψ is free, matrix Ψ is definite positive: it is the matrix of the quadratic form associated to the L^2-norm, with respect to the basis ψ. Thus, it implies that $(y_{k+p}-y_k)$ tends to 0 (for any norm on $\mathbb{R}^n$) as p tends to infinity. As $\mathbb{R}^n$ is complete, the sequence $(y_k)_{k\geq 0}$ is converging towards $y \in (\mathbb{R}^+)^n$. It remains to show that $q^*(\cdot) = q(\cdot,y)$, which is a direct consequence of the triangular inequality for $\mathcal{W}_2$. Hence, any limit of a sequence of elements of A can be written as $q(\cdot,y)$ with $y \in (\mathbb{R}^+)^n$. This is exactly the convex cone spanned by the ψ_i for $i \in \{1,\dots,n\}$. □

A direct consequence of the previous lemma is the following:

Corollary 2 *Let the assumptions of Lemma 3 prevail. Set, for $U \subseteq (\mathbb{R}_*^+)^n$, $B := \{q(\cdot,y) \mid y \in U\}$. Then, if U is closed (respectively, compact) the set B is closed (respectively, compact) for $\mathcal{W}_2$.*

We now turn our attention to investigate the form of the derivatives of the c.d.f. that will be used to define the dynamics of the c.d.f. in Section 3.

2.2 Derivatives of the c.d.f

Our purpose is to express the derivatives of the c.d.f. $F(\cdot, y)$, as given in Definition 2, in terms of y, ψ and F. These results will be at the core of the expression of the stochastic evolution of the c.d.f. in Section 3. Indeed, in order to apply Itō calculus, we need to obtain the expression of the first and second order derivatives.

Corollary 1 provides the differentiability of F. In order to clarify the notations of partial derivatives F, we set, $\dot{F}_x(x,y) := \frac{\partial F}{\partial x}(x,y)$, the partial derivative with respect to x and for $y = (y_i)_{1\leq i\leq n}$, $\dot{F}_i(x,y) := \frac{\partial F}{\partial y_i}(x,y)$, the partial derivative with respect to the i^{th} component of the vector y, with $i \in \{1,\dots,n\}$. Accordingly, we set $\ddot{F}_{x,j}(x)$, with $j \in \{1,\dots,n\}$ and $\ddot{F}_{i,j}(x)$, with $(i,j) \in \{1,\dots,n\}^2$, the second order derivatives. Concerning functions on the real line, such as the ψ_i, $i \in \{1,\dots,n\}$, the successive derivatives will be denoted by ψ_i' and ψ_i''.

Proposition 3 *We have the two following derivatives.*

$$\dot{F}_x(x,y) = \frac{1}{\langle y, \psi'(F(x,y))\rangle} \tag{3}$$

$$\dot{F}_i(x,y) = -\frac{\psi_i(F(x,y))}{\langle y,\ \psi'(F(x,y))\rangle} \tag{4}$$

Proof: As seen in the proof of Proposition 1, the mapping $F(\cdot, y)$ is the inverse of $q(\cdot, y)$ and this relation writes, for any $\varepsilon \in [0,1)$,

$$F(q(\varepsilon, y), y) = \varepsilon \tag{5}$$

By derivation of (5) with respect to y_i, $i \in \{1,\dots,n\}$, we find out

$$\psi_i(\varepsilon)\dot{F}_x(q(\varepsilon,y),y) + \dot{F}_i(q(\varepsilon,y),y) = 0 \tag{6}$$

By derivation of (5) with respect to ε, we find out

$$\langle y, \psi'(\varepsilon)\rangle \dot{F}_x(q(\varepsilon,y),y) = 1 \tag{7}$$

Substituting (7) in (6) yields, for any $i \in \{1,\dots,n\}$,

$$\dot{F}_i(q(\varepsilon,y),y) = \frac{-\psi_i(\varepsilon)}{\langle y, \psi'(\varepsilon)\rangle} \tag{8}$$

We recall that, if $x = q(\varepsilon, y)$, then $\varepsilon = F(x,y)$. Thus, Equation (8) gives us a formulation of the first order derivatives of F with respect to y_i, $i \in \{1,\dots,n\}$, as a function of $F(x,y)$, ψ and y. □

Now, let us turn to the second order derivatives with similar arguments used in Proposition 3.

Proposition 4 *We have the following second derivatives.*

$$\ddot{F}_{xx}(x,y) = -\frac{\langle y, \psi''(F(x,y))\rangle}{\left(\langle y,\, \psi'(F(x,y))\rangle\right)^3} \tag{9}$$

$$\ddot{F}_{x,i}(x,y) = \psi_i((F(x,y))\frac{\langle y, \psi''(F(x,y))\rangle}{\left(\langle y,\, \psi'(F(x,y))\rangle\right)^3} - \frac{\psi_i'((F(x,y))}{\left(\langle y,\, \psi'(F(x,y))\rangle\right)^2} \tag{10}$$

$$\begin{aligned}\ddot{F}_{i,j}(x,y) = {} & \frac{\psi_i'((F(x,y))\,\psi_j((F(x,y)) + \psi_j'((F(x,y))\,\psi_i((F(x,y))}{\left(\langle y,\, \psi'(F(x,y))\rangle\right)^2} \\ & -\psi_i((F(x,y))\,\psi_j((F(x,y))\frac{\langle y, \psi''((F(x,y))\rangle}{\left(\langle y,\, \psi'(F(x,y))\rangle\right)^3}\end{aligned} \tag{11}$$

Now, let us state a result that will prove itself useful to describe the form of the volatility in Section 3.

Lemma 4 *For any $y \in (\mathbb{R}_*^+)^n$, we have the following limit*

$$\lim_{x\to+\infty} \dot{F}_i(x,y) = 0$$

for $i \in \{1,\dots,n\}$ and this convergence is uniform with respect to y on any compact set.

Proof: The existence of such a c.d.f and its differentiability has been proved in Proposition 1. As q is increasing in y_i, $i \in \{1,\dots,n\}$, F is decreasing in this variable. This implies that the convergence of $F(x,y_1,\dots,y_n)$ towards 1, when x tends to $+\infty$, is uniform in y_i, on interval of the form $(0,\overline{y}_i]$. Without loss of generality, let us consider the case $i=1$ for some given $(y_2,\dots,y_n)$. For any $y_1 \in (\eta, \overline{y}_1 - \eta]$, and for any $0 < |h| \leq \eta$, set

$$g(x,h) := \frac{1}{h}\Big[F(x,y_1+h,y_2,\dots,y_n) - F(x,y_1,\dots,y_n)\Big]$$

The function g converges to 0 when x tends to $+\infty$, uniformly in h. It also converges to $\dot{F}_{i+1}(x,y_1,\dots,y_n)$ when h tends to 0. Therefore, we can permute the limits over x and h to obtain the result. □

Before turning to the study of dynamic distributions, i.e. stochastic processes with values in $\mathcal{D}_0$, let us analyse the effect of the mixture of percentiles on the risk of the underlying distribution.

2.3 Mixture and stochastic order

Let us consider a basis of percentiles $(\psi_i)_{1\leq i\leq n}$. Let $\left(y^{(1)}\right)$ and $\left(y^{(2)}\right)$ be in $(\mathbb{R}_*^+)^n$. If, for any $i \in \{1,\ldots,n\}$, $y_i^{(1)} \geq y_i^{(2)}$, then $q\left(\cdot, y^{(1)}\right) \succeq q\left(\cdot, y^{(2)}\right)$, i.e. the distribution associated to $y^{(1)}$ dominates the distribution associated to $y^{(2)}$ for the first order stochastic dominance. Now, let us investigate the case of the second order stochastic dominance and answer the question: can we characterize a mixture which dominates the initial distribution with respect to this order? First, let us recall that $(f_1, F_1, q_1) \in \mathcal{D}_0$ dominates (f_2, F_2, q_2) for the second order stochastic dominance if, for any $x \geq 0$,

$$\int_0^x F_1(x)dx \leq \int_0^x F_2(x)dx,$$

with a strict inequality for at least one value of x.

Lemma 5 *Let $q \in \mathcal{D}_0$ and $\psi \in \mathcal{P}_n(q)$. There exists $h \in \mathbb{R}^n$ and $\widehat{\delta} > 0$, such that, for any $\delta \in \left(0, \widehat{\delta}\right]$, $q(\cdot, e+\delta h) \succeq q(\cdot)$, if, and only if,*

$$\forall \varepsilon \in [0,1], \quad \sum_{i=1}^n h_i \int_0^\varepsilon \psi_i(u)du \geq 0, \tag{12}$$

and the inequality is strict for one ε.

Proof: If $q(\cdot, e+\delta h) \succeq q(\cdot)$ for any $\delta \in \left(0, \widehat{\delta}\right]$, we have

$$\forall x \geq 0, \ \int_0^x \Big[F(u, e+\delta h) - F(u)\Big]du \leq 0\,.$$

If we divide the two members of the previous inequality by $\delta > 0$, and let it goes to 0, we obtain

$$\forall x \geq 0, \ \int_0^x \sum_{i=1}^n \dot{F}_i(u,e)h_i\, du \leq 0.$$

By Equations (3) and (4), it yields

$$\forall x \geq 0, \ \sum_{i=1}^n h_i \int_0^x \psi_i(F(u,e))f(u,e)du = \sum_{i=1}^n h_i \int_0^{F(x)} \psi_i(v)dv \geq 0.$$

Hence, the sufficient condition. For the necessary condition, we write a second order Taylor expansion: for any $u \in [0, x]$, there exists $\theta(u) \in [0, \delta]$, such that

$$\frac{1}{\delta}\int_0^x [F(u, e+\delta h) - F(u)]\, du = \int_0^x \sum_{i=1}^n \dot{F}_i(u, e) h_i \, du + \delta \int_0^x \sum_{i,j} \ddot{F}_{i,i}(u, e+\theta(u)h) h_i h_j \, du$$

As F is twice continuously derivable, its second order derivatives are uniformly bounded on $[0, 1] \times [e, e + \delta h]$. Therefore, there exists $K(h) > 0$ such that

$$\frac{1}{\delta}\int_0^x [F(u, e+\delta h) - F(u)]\, du \leq \int_0^x \sum_{i=1}^n \dot{F}_i(u, e) h_i du + \delta\, K(h)$$

This implies that, for δ small enough $\int_0^x [F(u, e+\delta h) - F(u)]\, du \leq 0$ and the inequality is strict if $x \neq 0$. □

According, to Lemma 5, a deviation from the initial distribution q, with increasing second order stochastic dominance, can decrease some mixture coefficients as long as condition (12) prevails. Let us consider an example:

Example 1 *Let us consider a basis of two log-normal percentiles, i.e.* $\psi_i(\varepsilon) = e^{\sigma_i \Phi^{-1}(\varepsilon)}$, $i \in \{1, \ldots, n\}$, *where* Φ *is the c.d.f. of the standard normal law,* $0 < \sigma_1 < \sigma_2$. *We have* $\int_0^\varepsilon \psi_i(u) du = \Phi\left(\Phi^{-1}(\varepsilon) - \sigma_i\right) \times e^{\frac{\sigma_i^2}{2}}$. *Assuming* $h_2 < 0 < h_1$, *condition (12) writes, for any* $\varepsilon \in (0, 1)$,

$$\frac{h_1}{|h_2|} \geq \frac{\Phi\left(\Phi^{-1}(\varepsilon) - \sigma_2\right)}{\Phi\left(\Phi^{-1}(\varepsilon) - \sigma_1\right)}\, e^{\frac{\sigma_2^2 - \sigma_1^2}{2}}$$

The right hand side of the inequality is uniformly bounded by $e^{\frac{\sigma_2^2 - \sigma_1^2}{2}}$ *on* $[0, 1)$ *since the numerator and denominator are equivalent in* 0^+. *Hence, the existence of* h_1 *and* h_2. *Besides, set* $h_1 = 1$ *and* $h_2 = -\exp\left(\frac{(\sigma_1^2 - \sigma_2^2)}{2}\right)$. *Condition* (12) *is satisfied and the distributions* $f(\cdot, e+h)$ *and* $f(\cdot)$ *have the same expectation. In this case, the two percentile functions do cross each over. The modified percentile function,* $q(\cdot, e+h)$ *is above* $q(\cdot)$ *on* $[0, \varepsilon_0)$ *and below* $q(\cdot)$ *on* $(\varepsilon_0, 1)$, *for a unique* $\varepsilon_0 > 0$. *It means that, although* $q(\cdot, e+h)$ *has the same expectation than* $q(\cdot)$, *it puts more weight on both low and large values: it is a so called mean-preserving spread, see Levy* [21].

3 Dynamic distributions

We now turn to the dynamic extension of the previous analysis in order to model the evolution of distributions.

Consider some $f \in \mathcal{D}_0$, with c.d.f F and percentile function q. We also set-out some $\psi \in \mathcal{P}_n(q)$. Let $(\Omega, \mathcal{F}, \mathbb{P})$ a probability space. The operator $\mathbb{E}[\cdot]$ denotes the expectation under $\mathbb{P}$. We consider a n-dimensional Brownian motion $\{W(t) := (W_i(t))_{1\leq i\leq n}\}_{t\geq 0}$, centred, with reduced volatilities, but a non-degenerated correlation matrix $C = [c_{i,j}]_{1\leq i,j\leq n}$ on $(\Omega, \mathcal{F}, \mathbb{P})$. The natural filtration of W will be denoted by $\mathbb{F} := \{\mathcal{F}_t\}_{t\geq 0}$. We shall deal with a $\mathbb{F}$-adapted diffusion process, denoted by $\left\{Y(t) := (Y_i(t))_{1\leq i\leq n}\right\}_{t\geq 0}$, with values in $(\mathbb{R}_*^+)^n$. More precisely, set, for $i \in \{1, \ldots, n\}$, $Y_i(0) = 1$ and

$$dY_i(t) = \mu_i(Y_i)dt + \sigma_i(Y_i)dW_i(t)$$

where μ_i and σ_i are Borelian mappings. We will work in the remaining of the paper under the following assumption.

Assumption 2 *For any $t \geq 0$, the process $\{Y(t)\}_{t\geq 0}$ is a Markov diffusion, square integrable, with positive values $\mathbb{P}$-a.s. Moreover, there exists $K > 0$ such that, for any $y > 0$ and $i \in \{1, \ldots, n\}$, we have $\mu_i(y)^2 + \sigma_i(y)^2 \leq K \times (1 + y^2)$.*

Let us provide two examples of stochastic processes satisfying Assumption 2.

Example 2 (Log-normal diffusion) *Set, for any $i \in \{1, \ldots, n\}$, $\sigma_i(x) = \overline{\sigma}_i \times x$, with $\overline{\sigma}_i > 0$ and $\mu_i(x) = \overline{\mu}_i \times x$. We have*

$$Y_i(t) = \exp\left[\left(\overline{\mu}_i - \frac{\overline{\sigma}_i^2}{2}\right)t + \overline{\sigma}_i W_i(t)\right]$$

The process Y_i is positive and square integrable.

Example 3 (Jacobi process) *Let $0 < m < \overline{\mu}_i < M$, $\overline{\sigma}_i > 0$, $\lambda_i > 0$, for any $i \in \{1, \ldots, n\}$, with*

$$\frac{\overline{\sigma}_i^2}{2\lambda_i} \leq \frac{\overline{\mu}_i - m}{M - m} \leq 1 - \frac{\overline{\sigma}_i^2}{2\lambda_i}$$

We set out

$$dY_i(t) = \lambda_i(\overline{\mu}_i - Y_i(t))dt + \overline{\sigma}_i\sqrt{(M - Y_i(t))(Y_i(t) - m)}\, dW_i(t)$$

The process Y_i is a Jacobi process with values in (m, M),hence positive. It is also square integrable. See, e.g., Delbaen and Shirakawa [11] or Ackerer et al. [1]. The condition on drift and volatility functions in Assumption 2 is clearly satisfied because the drift is linear and the volatility bounded.

Let us define the distribution-valued process.

Definition 3 *We set, for any $\varepsilon \in [0,1)$, and $t \geq 0$, $\widetilde{q}(t,\varepsilon) = q(\varepsilon, Y(t))$, with $q(\cdot, y)$ defined by Equation (1). The p.d.f, respectively, c.d.f., associated to $\widetilde{q}(t,\cdot)$ is denoted by $\widetilde{f}(t,\cdot)$, respectively $\widetilde{F}(t,\cdot)$.*

The following lemma provides some boundaries on the expected Wasserstein distance between the distributions at time s and t, with $0 \leq t \leq T$. In particular, it provides the continuity with respect to time, in terms on the expected Wasserstein distance, which is a natural tool to control the stochastic evolution of probability densities. The reader can refer to Alfonsi et al. [2], for applications in the convergence of Euler schemes.

Lemma 6 *For any $T \geq 0$, with K as in Assumption 2, there exist a constant, $C_{n,T,K}$ such that, for any $0 \leq s < t \leq T$,*

$$\mathbb{E}\left[\mathcal{W}_2\big(\widetilde{q}(t,\varepsilon), \widetilde{q}(s,\varepsilon)\big)\right] \leq ||q||_2 C_{n,T,K}\sqrt{1+n}\sqrt{t-s}$$

Proof: We use Jensen inequality and Proposition 2 to state

$$\mathbb{E}\left[\mathcal{W}_2\big(\widetilde{q}(t,\varepsilon), \widetilde{q}(s,\varepsilon)\big)\right]^2 \leq \mathbb{E}\left[\mathcal{W}_2^2\big(\widetilde{q}(t,\varepsilon), \widetilde{q}(s,\varepsilon)\big)\right] \leq ||q||_2^2 \times |Y(t) - Y(s)|^2$$

Then, by Problem 3.15, p. 306, in Karatzas and Shreve [18], under Assumption 2, we have the existence of a constant $L_{n,K,T}$ such that $\mathbb{E}\left[|Y(t) - Y(s)|^2\right] \leq L_{K,T}\big(1 + |Y(0)|^2\big)(t-s)$. But $|Y(0)|^2 = n$, which yield the result. □

Now, let us turn to the explicit dynamics of the c.d.f.

Proposition 5 *For any $x > 0$, the process $\big(\widetilde{F}(t,x), Y(t)\big)_{t\geq 0}$ is a Markov diffusion, with values on $[0,1] \times (\mathbb{R}_*^+)^n$, with $\widetilde{F}(t,0) = 0$. The dynamics of $\big(\widetilde{F}(t,x)\big)_{t\geq 0}$ is given by*

$$d\widetilde{F}(t,x) = \sum_{i=1}^{n} A_i(x, Y(t))dt + \sum_{i=1}^{n} B_i(x, Y(t))dW_i(t) \tag{13}$$

where the mappings A_i and B_i from $(\mathbb{R}_*^+)^{n+1}$ into $\mathbb{R}$ are given by

$$\begin{aligned} B_i(x,y) &= \frac{-\psi_i(F(x,y))}{\langle y, \psi'(F(x,y))\rangle}\sigma_i(y_i) \\ A_i(x,y) &= \frac{-\psi_i(F(x,y))}{\langle y, \psi'(F(x,y))\rangle}\mu_i(y_i) + \frac{1}{2}(\sigma_i(y_i))^2 V_{i,i}(F(x,y),y) \\ &\quad +\sigma_i(y_i)\sum_{j>i}^{n} c_{i,j}\sigma_j(y_j)y_j V_{i,j}(F(x,y),y) \end{aligned}$$

with, for $F \in [0,1]$ and $y \in (\mathbb{R}_*^+)^n$,

$$V_{i,j}(F,y) := \left[\frac{\psi_i'(F)\psi_j(F) + \psi_j'(F)\psi_i(F)}{\langle y, \psi'(F)\rangle)^2} - \psi_i(F)\psi_j(F)\frac{\langle y, \psi''(F)\rangle}{(\langle y, \psi'(F)\rangle)^3}\right] \tag{14}$$

Proof: By applying Itō calculus, we have

$$\begin{aligned} d\widetilde{F}(t,x) = &\sum_{i=1}^{n} \dot{F}_i\big(x, Y(t)\big)\left[\mu_i(Y_i(t))dt + \sigma_i(Y_i(t))dW_i(t)\right] \\ &+ \frac{1}{2}\sum_{i=1}^{n}\sum_{j=1}^{n} \ddot{F}_{i,j}\big(x, Y(t)\big)\sigma_i(Y_i(t))\sigma_j(Y_j(t))c_{i,j}dt \end{aligned} \tag{15}$$

Using Equations (8) and (9), we obtain, for $i \in \{1,\ldots,n\}$, the mappings A_i and B_i. □

The fact that $x \mapsto \widetilde{F}(x,t)$ is a c.d.f has some implication on its volatility (as a random variable on $(\Omega, \mathcal{F}, \mathbb{P})$), in particular, when x goes to to infinity. This property is declined into two results, depending on the type of behaviour of the volatility of Y.

Corollary 3 *Assume that*

(i) For $i \in \{1,\ldots,n\}$, $\sigma_i(x) \leq \overline{\sigma}_i x$

(ii) There exists $L > 0$ such that, for all $x \in \mathbb{R}^+$ and $y \in (\mathbb{R}_*^+)^n$, $0 \leq xf(x,y) \leq L$

Then, for any $T > 0$ and $i \in \{1,\ldots,n\}$, $\lim_{x\to+\infty} \mathbb{E}\left[\int_0^T B_i^2\big(x, Y(s)\big)ds\right] = 0$.

Proof: By Problem 315 p. 306 in Karatzas and Shreve [18], we know that, under Assumption 2, the random variable $U^*_{i,T} := \max_{0\leq s\leq T} Y_i^2(s)$ is integrable. We write

$$\mathbb{E}\left[\int_0^T B_i^2\big(x,Y(s)\big)ds\right] \leq \overline{\sigma}_i^2 N^2\, \mathbb{E}\left[\mathbb{I}_{\{U^*_{i,T}\leq N\}}\ \int_0^T \dot{F}_i^2(x,Y(s))ds\right] + \overline{\sigma}_i^2 L^2 T\, \mathbb{P}\left[U^*_{i,T}\geq N\right]$$

Now, set $\eta > 0$ and choose N such that $\mathbb{P}\left[U^*_{i,T}\geq N\right] \leq \frac{\eta}{2\overline{\sigma}_i^2 T L^2}$. As a consequence of Lemma 4, there exists X_N such that, for all $x \geq X_N$, for any $y \in ([0,N])^n$,

$$\left|\dot{F}_i(x,Y(s))\right| \leq \frac{\eta}{2\overline{\sigma}_i^2 T}$$

Hence, $\mathbb{E}\left[\int_0^T B_i^2\big(x,Y(s)\big)ds\right] \leq \eta$, for $x \geq X_N$. □

Remark 1 *Point (ii) of Lemma 3 is satisfied, for instance, for log-normal distributions as can be seen in the proof of Proposition 6.*

Corollary 4 *Assume that, for $i \in \{1,\ldots,n\}$, the process Y_i takes its values in the finite interval (m,M). Then, for any $T>0$ and $i \in \{1,\ldots,n\}$,*

$$\lim_{x\to+\infty} \mathbb{E}\left[\int_0^T B_i^2\big(x,Y(s)\big)ds\right] = 0$$

Proof: By Assumption 2, we have the straightforward inequality

$$\mathbb{E}\left[\int_0^T B_i^2\big(x,Y(s)\big)ds\right] \leq K(1+M^2)T\left[\sup_{y\in[m,M]^n}\{\dot{F}_i(x,y)\}\right]^2$$

As a consequence of Lemma 4, the right-hand side converges to 0 as x goes to infinity. □

We can provide a result on the regularity of the expected value of $\widetilde{F}(t,\cdot)$ and its link with the expected value of $\widetilde{f}(t,\cdot)$. For technical reasons, we will work with a basis of log-normal percentile functions. Indeed, in this setting, we can show that the derivation with respect to x and the integration with respect to $\mathbb{P}$ do permute.

Proposition 6 *Assume that, for all $i \in \{1,\ldots,n\}$, $\psi_i : \varepsilon \mapsto e^{\gamma_i \Phi^{-1}(\varepsilon)}$, with $\gamma_i > 0$, with the notations set out in Example 1. Assume that $[\langle Y(t), e\rangle]^{-1}$ is square-integrable. Then, $M(t,\cdot) := \mathbb{E}\{F(\cdot,Y(t))\}$ is the c.d.f of an element of $\mathcal{D}_0$, with p.d.f $m(t,\cdot) = \mathbb{E}\{f(\cdot,Y(t))\}$.*

Proof: First of all, it is clear that $M(t,\cdot)$ is increasing and $M(t,0) = 0$. By Lebesgue monotone convergence theorem, we also have $M(t,x) \to 1$, when $x \to +\infty$. Therefore, it defines an element of $\mathcal{D}$. In order to show that is is, actually, in $\mathcal{D}_0$, we need to show that the derivatives of $F(\cdot, Y(t))$ of order 1 and 2 are uniformly bounded. Let us start with some facts deduced from the log-normal distribution. Set $\phi := \Phi'$. We have

$$\psi_i'(\varepsilon) = \frac{\gamma_i \psi_i(\varepsilon)}{\phi\left(\Phi^{-1}(\varepsilon)\right)} \text{ and } \psi_i''(\varepsilon) = \frac{\gamma_i^2 \psi_i(\varepsilon) + \gamma_i \psi_i(\varepsilon)\Phi^{-1}(\varepsilon)}{\left[\phi\left(\Phi^{-1}(\varepsilon)\right)\right]^2}$$

We also notice that $q(\frac{1}{2}, y) = \langle y, e\rangle$. We define $\gamma_{min} := \min\{\gamma_i \mid 1 \le i \le n\}$ and $\gamma_{max} := \max\{\gamma_i \mid 1 \le i \le n\}$ and set out, for any $z > 0$,

$$K(x,z) := \begin{cases} \Phi\left(\frac{1}{\gamma_{min}} \ln\left(\frac{x}{z}\right)\right) & \text{if } x \ge z \\ \Phi\left(\frac{1}{\gamma_{max}} \ln\left(\frac{x}{z}\right)\right) & \text{if } x < z \end{cases}$$

We obtain the following inequality $0 \le F(x,y) \le K(x, \langle y, e\rangle)$. This shows that, basically, the c.d.f. $F(\cdot, y)$ is below the log-normal c.d.f with the smallest volatility if $F(x,y) \ge \frac{1}{2}$ and below the log-normal c.d.f with the largest volatility if $F(x,y) < \frac{1}{2}$.

Equations (7) and (9) and the calculations above yield the following inequality:

$$0 \le f(x,y) \le \frac{\phi\left(\Phi^{-1}(F(x,y))\right)}{\gamma_{min} x}$$

Using the boundary $K(x, \langle y, e\rangle)$, we obtain

$$0 \le f(x,y) \le \frac{1}{\gamma_{min} x} \begin{cases} \phi\left(\frac{1}{\gamma_{min}} \ln\left(\frac{x}{\langle y,e\rangle}\right)\right) & \text{if } x \ge \langle y, e\rangle \\ \phi\left(\frac{1}{\gamma_{max}} \ln\left(\frac{x}{\langle y,e\rangle}\right)\right) & \text{if } x < \langle y, e\rangle \end{cases}$$

In the left hand side we recognize the log-normal densities with mean $\ln(\langle y, e\rangle)$ and volatility γ_{min} and γ_{max}, respectively. By using the mode of these densities, we obtain the following inequality:

$$0 \le f(x,y) \le H(y) := \frac{e^{\frac{\gamma_{max}^2}{2}}}{\gamma_{min}\sqrt{2\pi}\langle y, e\rangle}$$

Hence, $f(x, Y(t)) = \dot{F}_x(x, Y(t))$ is uniformly bounded in x by some $\mathbb{P}$-integrable random variable $H(Y(t))$. Hence, $M(t,\cdot)$ is derivable and its derivative is $m(t,\cdot)$.

We can go one step further and compute the second order derivative. For $x < \langle y, e\rangle$, we have, for some constant $c_1 > 0$,

$$|\ddot{F}_{xx}(x,y)| \leq \frac{1}{\gamma_{min}^3}\phi\left(\frac{1}{\gamma_{max}}\ln\left(\frac{x}{\langle y,e\rangle}\right)\right) \times \frac{\gamma_{max}x - x\ln\left(\frac{x}{\langle y,e\rangle}\right)}{x^3}$$

The maximum of the function in right hand side is achieved at

$$\langle y,e\rangle \exp\left[-\gamma_{max}^2 + \frac{\gamma_{max}}{2} - \sqrt{\gamma_{max}^4 + \frac{3}{2}\gamma_{max}^3 + \frac{5}{4}\gamma_{max}^2}\right] < \langle y,e\rangle$$

At this point, the maximum is of the form $v(\gamma)(\langle y,e\rangle)^{-2}$, hence $\mathbb{P}$-integrable, by assumption. The same argument applies to the case $x > \langle y,e\rangle$. This provides the second order derivative as the expectation of $\ddot{F}_{xx}(x, Y(t))$. □

Now, we can characterize the form of the probability density of $\widetilde{q}(t,\cdot)$ and $\widetilde{F}(t,\cdot)$. Let us introduce the following replacing function $\mathcal{R} : \mathbb{R}^n \times \{1,\dots,n\} \times \mathbb{R} \to \mathbb{R}^n$: for any $r \in \mathbb{R}^n$, $i \in \{1,\dots,n\}$, and $u \in \mathbb{R}$, $\mathcal{R}(r;i,u) = z$ where $z_j = r_j\mathbb{I}_{j\neq i} + u\mathbb{I}_{j=i}$. That is the replacing function $\mathcal{R}$ transform the original vector r in the one in which coordinate i has been replaced by u.

Proposition 7 *Let $\mathcal{K}_t : (\mathbb{R}_*^+)^n \to \mathbb{R}^+$ be the density $Y(t)$. Let $\eta(t,\varepsilon,x)$ and $\rho(t,\varepsilon,x)$ denote, respectively, the derivative of the percentile and the p.d.f., at fixed time t. Assume also that there exists $i^\star \in \{1,\dots,n\}$ such that $\psi_{i^\star} \in \mathcal{D}_0$.*

Then, the derivative function satisfies, for any $x \geq 0$ and $\varepsilon > 0$,

$$\eta(t,\varepsilon,x) = \int_{(\mathbb{R}_*^+)^{n-1}} \mathcal{K}_t\left[\mathcal{R}\left(z; i^\star, \frac{x - \sum_{i\neq i^\star}\psi_i(\varepsilon)z_i}{\psi_{i^\star}(\varepsilon)}\right)\right]\prod_{i\neq i^\star} dz_i$$

Proof: The result is obtained by a change of variable $z_{i^\star} = \langle\psi(\varepsilon), y\rangle$, $z_i = y_i$, $i \neq i^\star$, and the fact that $\psi_{i^\star}(\varepsilon) > 0$ as soon as $\varepsilon > 0$. □

In order to construct the functional Bollinger bands, we need to be able to define a confidence interval for $F(t,x)$, seen as a random variable on $(\Omega,\mathcal{F},\mathbb{P})$. For this purpose, we use the following functions:

Definition 4 *For any $\eta \in (0,1)$, $t > 0$ and $x > 0$, $H_\eta(t,x)$ is the solution (in $H \geq 0$) of $\mathbb{P}\left[\widetilde{F}(t,x) \leq H\right] = \eta$. For any $\eta \in (0,1)$, $t > 0$ and $\varepsilon \in (0,1)$, $I_\eta(t,x)$ is the solution in $\in (0,1)$ of $\mathbb{P}\left[\widetilde{q}(t,\varepsilon) \leq I\right] = \eta$*

The functions $x \mapsto H_\eta(t,x)$ and $\varepsilon \mapsto I_{1-\eta}(t,\varepsilon)$ are, respectively, a (non random) c.d.f and a (non-random) percentile function, associated to the same probability distribution. This is, basically, what is proved in next proposition. These functions can be used to define the confidence interval on $\widetilde{F}(t,x)$ or $\widetilde{q}(t,\varepsilon)$, respectively.

Proposition 8 *Let the assumption of Theorem 7 prevails. Assume that Y takes its values in a open (possibly not bounded) subset of $(\mathbb{R}_*^+)^n$, with unattainable boundaries, and, for every non empty ball B in this subset $\mathbb{P}[Y \in B] > 0$. Then, the mapping $\varepsilon \mapsto I_\eta(t,\varepsilon)$ is derivable, increasing, with $\lim_{\varepsilon\to 0+} I_\eta(t,\varepsilon) = 0$ and $\lim_{\varepsilon\to 1-} I_\eta(t,\varepsilon) = +\infty$*

Proof: First, let us denote by $\mathcal{K}_t(y)$ the density of $Y(t)$. Set, for any $\varepsilon \in [0,1)$, $h \geq 0$,

$$Q(\varepsilon,h) := \mathbb{P}\left[q(\varepsilon,Y(t)) \leq h\right] = \int_{y\in(\mathbb{R}_*^+)^d} \mathbb{I}_{\{q(\varepsilon,y)\leq h\}} \mathcal{K}_t(y)dy$$

First, if $\varepsilon > 0$, the mapping $h \mapsto Q(\varepsilon,h)$ is increasing, with $Q(\varepsilon,0) = 0$ and $\lim_{h\to+\infty} Q(\varepsilon,h) = 1$. The fact that $Q(\varepsilon,0) = 0$ is clear, because $q(\varepsilon,y) > 0$ if and only if $\varepsilon > 0$. It is increasing because, if $0 \leq h_1 < h_2$, $\{q(\varepsilon,y) \leq h_1\} \neq \{q(\varepsilon,y) \leq h_2\}$. Indeed, as at least one of the ψ_i is not equal to 0 (because $q(\varepsilon) > 0$), it is always possible to increase $q(\varepsilon,y)$ by increasing the corresponding component of y. Therefore, there is an open ball included in the second interval and not in the first. By assumption of this proposition, it is given a positive weight by $K(t,\cdot)$. The limit when h goes to infinity is a consequence of the Beppo-Levi monotone convergence theorem. Besides, the mapping $(\varepsilon,h) \mapsto Q(\varepsilon,h)$ is also derivable. This is a consequence of theorem 7.

The mapping $Q(\varepsilon,\cdot)$ defines a (continuous) bijection form $[0,+\infty)$ onto $[0,1)$. Hence, $\eta \mapsto I_\eta(t,\varepsilon)$ is well defined and continuous with respect to both variable. It is increasing because $q(\cdot,y)$ is increasing. Set $Q_{max}(h) := \mathbb{P}(\langle Y(t),e\rangle \leq h)$ and $Q_{min}(h) := \mathbb{P}\big[\min_i\{Y_i(t)\} \leq h\big]$. From the inequality $\min_i\{Y_i(t)\}\times q(\varepsilon) \leq q(\varepsilon,Y(t)) \leq \langle Y(t),e\rangle \times q(\varepsilon)$, we deduce that

$$Q_{max}\left(\frac{I_\eta(t,\varepsilon)}{q(\varepsilon)}\right) \leq \eta \leq Q_{min}\left(\frac{I_\eta(t,\varepsilon)}{q(\varepsilon)}\right)$$

The first inequality yields the limit when ε goes to 0^+ and the second the limit when ε goes to 1^-. By definition of $F(x,y)$, we have $q(\varepsilon,y) \leq h \Rightarrow \varepsilon \leq F(h,y)$. Hence, the inverse of $I_\eta(t,\cdot)$ is $H_{1-\delta}(t,\cdot)$. □

At this stage, we can define the functional Bollinger bands by

Definition 5 *Set $\eta \in \left(0, \frac{1}{2}\right)$, the functional Bollinger bands, for the percentile, at horizon t are defined by the mappings $\varepsilon \mapsto I_\eta(t,\varepsilon)$ (the lower band) and $\varepsilon \mapsto I_{1-\eta}(t,\varepsilon)$ (the upper band). The functional Bollinger bands, for the c.d.f., at horizon t are defined by the mappings $x \mapsto H_\eta(t,x)$ (the lower band) and $x \mapsto H_{1-\eta}(t,x)$ (the upper band). These mappings are elements of $\mathcal{D}$, as proved in Proposition 8.*

An interesting property of this approach is that the lower and upper bands for the percentile (respectively, the c.d.f) are percentiles (resp., c.d.f). Moreover, the percentile upper band is the inverse of the c.d.f lower band (and symmetrically for the other bands). Hence, the percentile $\widetilde{F}(t,\cdot)$ can be compared to the lower and upper bands $H_\eta(t,\cdot)$ and $H_{1-\eta}(t,\cdot)$ through the concept of second order stochastic dominance. If $\widetilde{F}(t,\cdot)$ dominates $H_\eta(t,\cdot)$ for the second order stochastic dominance, it implies that the distribution at time t involves more risk than what was expected at time 0, with a confidence level of $2\,\eta$. This situation can occur even if the averages of the two distributions are the same. Such a situation could be a good trading signal. This is what we want to illustrate in the following subsection.

4 Application to Credit Indices

In this section, we consider the evolution of the spreads of all the 125 components of a the iTraxx Europe (with maturity 5 years). Although this index is rolled every 6 months, we will consider - for a purely illustrative purpose - a fixed composition, corresponding to one given series of this index.

Given these samples, we can calculate, at each date t_j, with $t_1 = 0 < \cdots < t_m$, the empirical percentiles function, denoted by $\overline{q}(t_j,\cdot)$.

Consider n elements of $\mathcal{D}$, represented by their percentile functions $v := (v_k)_{1\leq k\leq n}$, assuming that one of those is in $\mathcal{D}_0$. We also assume that these elements are linearly independent. As a typical example, we consider $v_k(\varepsilon) := \exp(\gamma_k \Phi^{-1}(\varepsilon))$, where Φ is the c.d.f of the standard normal law and the γ_k are positive, two by two distinct real numbers. In this case, each v_k is the percentile of a log-normal law.

A each date t_j, we will perform a constrained regression of $\overline{q}(t_j,\cdot)$ on v, using the Wasserstein distance. A short calculation shows that it amounts solving the following (constrained) quadratic program in $\mathbb{R}^n$:

$$(\mathcal{R})_j \; : \begin{cases} \min_{z\in\mathbb{R}^n} \left[z^T \cdot \Psi \cdot z - 2Q(j)^T \cdot z\right] \\ \text{s.t. } \forall k \in \{1,\ldots,p\} \;\; z_k \geq \delta > 0 \end{cases}$$

where Ψ is defined in the proof of Lemma 3, and $Q(j)$ is a vector of $\mathbb{R}^n$ with $Q_k(j) = \int_0^1 \psi_k(\varepsilon)\overline{q}(t_j, \varepsilon)d\varepsilon$. As in Lemma 3, the matrix is invertible because the family of log-normal percentiles is free as soon as the volatilities are distinct.

In many practical cases that we will analyse in this section, the constraints of program $(\mathcal{R})_j$ are not binding and this program amounts to a classic least-square method.

Let us denote by $\widehat{z}^{(j)}$ the solution of program $(\mathcal{R})_j$, and set $\widehat{Y}_k(t_j) := \widehat{z}_k^{(j)} \times (\widehat{z}_k^{(0)})^{-1}$ and $\psi_k(\cdot) = \widehat{z}_k^{(0)} \times v_k(\cdot)$, $k \in \{1, \ldots, n\}$. By definition, ψ is an element of $\mathcal{P}_p(\widehat{q}_0)$ where $\widehat{q}_0 := \langle \widehat{z}^{(0)}, v(\cdot) \rangle \in \mathcal{D}_0$. Hence, we are in the framework developed above, and we have obtained a sample path for Y, on the basis of which we can calibrate the parameters defined in Section 3. For each date t_j, we have $\widehat{q}_j(\cdot) = \langle v(\cdot), \widehat{z}^{(j)} \rangle$.

Once the parameters of the diffusion Y are calibrated, according to Definition 3, we have the full dynamics of $\widetilde{q}(t, \cdot)$.

In the following examples, we shall develop our method based on the function Bollinger bands, defined in 5. Let us emphasize the analogy with the standard, one dimensional case. For a single valued process, in the trading strategies area, the Bollinger bands method consists, basically, to look at a confidence interval on the price of a financial instrument, based on historical trailing volatility and average. Hence, implicitly a Gaussian case. Trading signals are triggered when the price crosses the bands. See Kaufman [20], for definition and use in trading strategies, or Bernis and Scotti [6] for applications to credit indices in the context of non-linear filtering. In our setting, the equivalent of crossing the upper (respectively, lower) band will be the case where the current distribution $F(t, \cdot)$ dominates the upper (resp., lower) functional band $H_\eta(t, \cdot)$ (resp. $H_{1-\eta}(t, \cdot)$) for the second order stochastic dominance. More precisely, we denote by $F(t_j, \cdot)$ the c.d.f. at time t_j, stemming from the fit of the empirical percentiles at this date. Given the calibration of the diffusion parameters for Y on the sample $0 \leq t_i \leq t_m$, we calculate at time t_m, the lower and upper functional bands, at horizon t_{m+l}, $H_\eta(t_{m+l} - t_m, \cdot)$, $H_{1-\eta}(t_{m+l} - t_m, \cdot)$, with $l > 0$ some fixed horizon. Then, we can compare $\overline{F}(t_{m+l} - t_m, \cdot)$ to the bands. This formulation can be transposed to the lower and upper functional bands on the percentiles.

As an example, we display in Figure 1 the upper and lower bands on July the 13^{th} 2015 (t_{m+l}), as well as the c.d.f at this date. We take $n = 2$, $\gamma_1 = 25\%$ and $\gamma_2 = 85\%$. The dynamics of Y_1, Y_2 is assumed to be log-normal, with no drift. Calibration on market data (1 year) yields $\overline{\sigma}_1 = 29\%$, $\overline{\sigma_2} = 80\%$ and a correlation of some 23%. The lower and upper bands are computed using a normal approximation over the last 5 business days, according to formula (13). It can be interesting to observe that

the drift has a second order effect in this example. At this date, the c.d.f dominates the upper band, for the SOSD, which means that the distribution is significantly less risky than expected. In the same time, the average spread on July the 13^{th} 2015 (t_m) is around 75 bps (a rather high level over the last weeks) and is about 68 bps at t_{m+l}. We can reasonably expect that the index average spread will keep on tightening over the next few days: 5 business days later, it is around 63 bps.

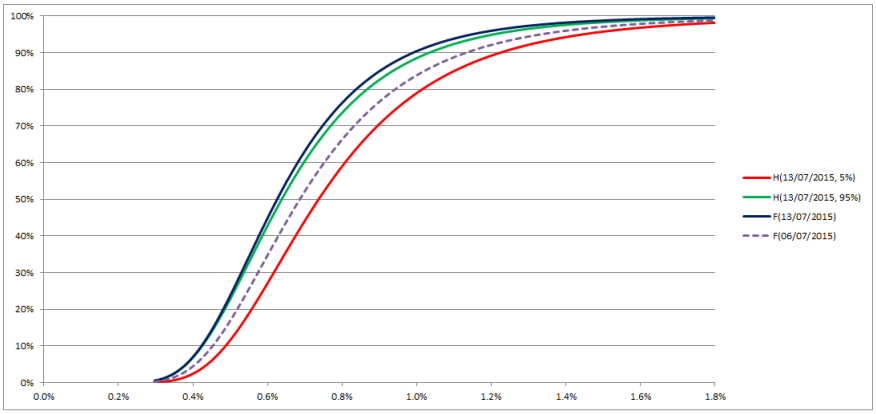

Figure 1: **Lower (5%) and upper (95%) bands, c.d.f on July the 13^{th} 2015 and July the 6^{th} 2015**.

We propose, for a deeper understanding of this example, to have a look at the form of the volatility functions $B_i(\cdot, Y(t_m))$, $1 \leq i \leq 2$. The two mappings are represented in Figure 2, in the context of Figure 1. The volatility function $B_1(\cdot, Y(t_m))$ is smaller than $B_2(\cdot, Y(t_m))$ for average and large values of x. This is due to the fact that the mapping ψ_2, associated to a large value of γ_2, mainly controls the extreme percentiles values. This basis function requires more volatility stemming from Y_2, in order to fit the percentiles in case of turmoil. In these periods, the extreme percentiles tend to increase sharply, showing some decorrelation from the lower percentiles. The same effect is captured by B_2, which remains larger than B_1 for large values of x. However, as given by Corollary 3, both functions tends to 0 as x goes to $+\infty$.

It may be interesting to investigate a criterion less restrictive than SOSD. For instance, as displayed in Figure 3, on February the 1^{st} 2016 the c.d.f began to cross the lower band (even if not dominating it for SOSD). The average spread at t_m is close to its level at t_{m+l}: respectively, 111 and 112 bps. However, the band crossing detects the increase of the risk in the index distribution: 5 days later the average spread is around 130 bps. The c.d.f. dominates the lower band in terms of SOSD shortly after this date, but when it occurs most part of the spread widening has already occurred.

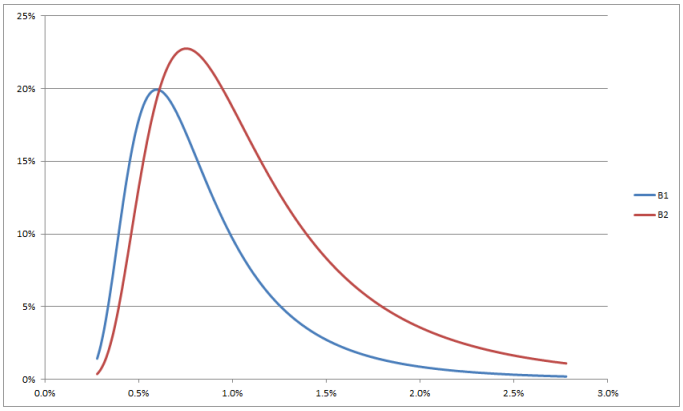

Figure 2: **Volatility functions** $B_i(\cdot, Y(t_m))$**,** $1 \leq i \leq 2$, where t_m is July the 13^{th} 2015.

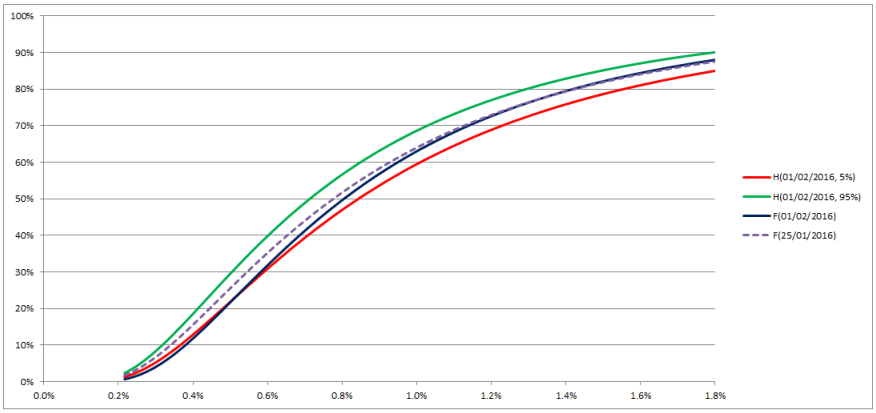

Figure 3: **Lower** (5%) **and upper** (95%) **bands, c.d.f on July the** 13^{th} **2015 and July the** 6^{th} **2015**.

References

[1] Ackerer, D., Filipović, D. and Pulido, S. (2016) The Jacobi stochastic volatility model *Swiss Finance Institute Research Paper* pp. 16-35.

[2] Alfonsi, A., Jourdain, B. and Kohatsu-Higa, A. (2014) Pathwise Optimal Transport Bounds between a One-Dimensional Diffusion and its Euler Scheme *The Annals of Applied Probability*, vol. 24(3), pp. 1049-1080.

[3] Pass, P. (2013) Optimal transportation with infinitely many marginals. *J. Funct. Anal.*, vol. 264(4), pp.947-963.

[4] Bellomo, N. and Pistone, G. (1980), Time-Evolution of the Probability Density Under the Action of a Deterministic Dynamical System. *Journal of Mathematical Analysis and Applications*, vol. 77, pp. 215-224.

[5] Bernis, G., Carassus, L., Docq, G., and Scotti, S. (2015), Optimal credit allocation under regime uncertainty with sensitivity analysis. *International Journal of Theoretical and Applied Finance*, 18(01), 1550002.

[6] Bernis, G. and Scotti, S. (2015), Trend Detection under Erroneous Observations: Application to Quantitative Finance Strategies. *Journal of Investment Strategies*, vol. 4(3), pp. 83-104.

[7] Bernis, G. and Scotti, S. (2016), Alternative to beta coefficients in the context of diffusions. *Alternative to beta coefficients in the context of diffusions*, http://dx.doi.org/10.1080/14697688.2016.1188214, pp. 1-14.

[8] Bondesson, L. (1981), Classes of Infinitely Divisible Distributions and Densities. *Z. Wahrscheinlichkeitstheorie verw. Gebiete*, vol. 57, pp. 39-71.

[9] Callegaro, G.; Gaigi, M.; Scotti, S. and Sgarra C. (2016), Optimal Investment in Markets with Over and Under-Reaction to Information, *Mathematics and Financial Economics*, forthcoming.

[10] Dai, M.; Yang, Z.; Zhang, Q. and Zhu Q.J. (2016), Optimal Trend Following Trading Rules, *Mathematics of Operations Research*, vol. 41-2, pp. 626-642.

[11] Delbaen, F. and Shirakawa, H. (2002) An Interest Rate Model with Upper and Lower Bounds, *Asia-Pacific Financial Markets*, vol. 9, pp. 191-209.

[12] Di Persio, L.; Pellegrini, G. and Bonollo, M. (2015), Polynomial Chaos Expansion Approach to Interest Rate Models, *J. Probability and Statistics*, vol. 2015, Article ID 369053.

[13] Di Persio, L. and Honchar, O. (2016), Artificial Neural Networks Architectures for Stock Price Prediction: Comparisons and Applications, working paper.

[14] Ferguson, T.S. (1973), A Bayesian analysis of some non-parametric problems. *Annals of Statistics*, vol. 1, pp. 209-230.

[15] Fernholz, E.R. (2001) Equity portfolios generated by ranked market weights. *Finance and Stochastics*. 5, pp. 469-486.

[16] Fernholz, E.R.; Kardaras C. and Karatzas I. (2005), Diversity and arbitrage in models of equity markets. *Finance and Stochastics*, volume 9, pp. 1-27.

[17] Gouriéroux, C. and Jasiak, J. (2008) Dynamic quantile models. *Journal of Econometrics*, vol. 147, pp. 198-205.

[18] Karatzas, I. and Shreve, S.E. (1991) Brownian Motion and Stochastic Calculus. 2nd ed. Springer-Verlag, Berlin.

[19] Karvanen, J. (2006) Estimation of quantile mixtures via L-moments and trimmed L- moments. *Computational Statistics and Data Analysis*, vol. 51, pp. 947-959.

[20] Kaufman, P.J. (2004): *New Trading Systems and Methods.*Fourth Edition, John Wiley & Sons, Inc.

[21] Levy, H. (1992), Stochastic dominance and expected utility: survey and analysis. *Management Science*, vol. 38, pp. 555–593.

[22] Quirk J.P. and Saposnik, R. (1962). Admissibility and measurable utility functions. *Review of Economic Studies*, vol. 29, pp. 140-146.

[23] Shao, J. (2011) A new probability measure-valued stochastic process with Ferguson-Dirichlet process as reversible measure. Electronic Journal Of Probability, vol. 16, pp. 271-292.

[24] Sillitto, G. (1969) Derivation of approximants to the inverse distribution function of a continuous univariate population from the order statistics of the sample. *Biometrika*, vol. 56, pp. 641-650.

[25] Vallander, S.S. (1973), Calculation of the Wasserstein distance between probability distributions on the line. *Teor. Veroyatnost. i Primenen.*, vol. 18(4), pp. 824-827.

[26] Villani, C. (2003), Topics in Optimal Transportation. *Graduate Studies in Mathematics.*, vol. 58, American Society, Providence.

[27] Wagner, N. (2008) Credit Risk, Models, Derivatives and Management. Chapman & Hall Financial Mathematics Series.

[28] Zervos, M.; Johnson, T.C. and Alazemi, F. (2013) Buy-low and sell-high investment strategies. *Mathematical Finance*, vol. 23, pp. 560-578.